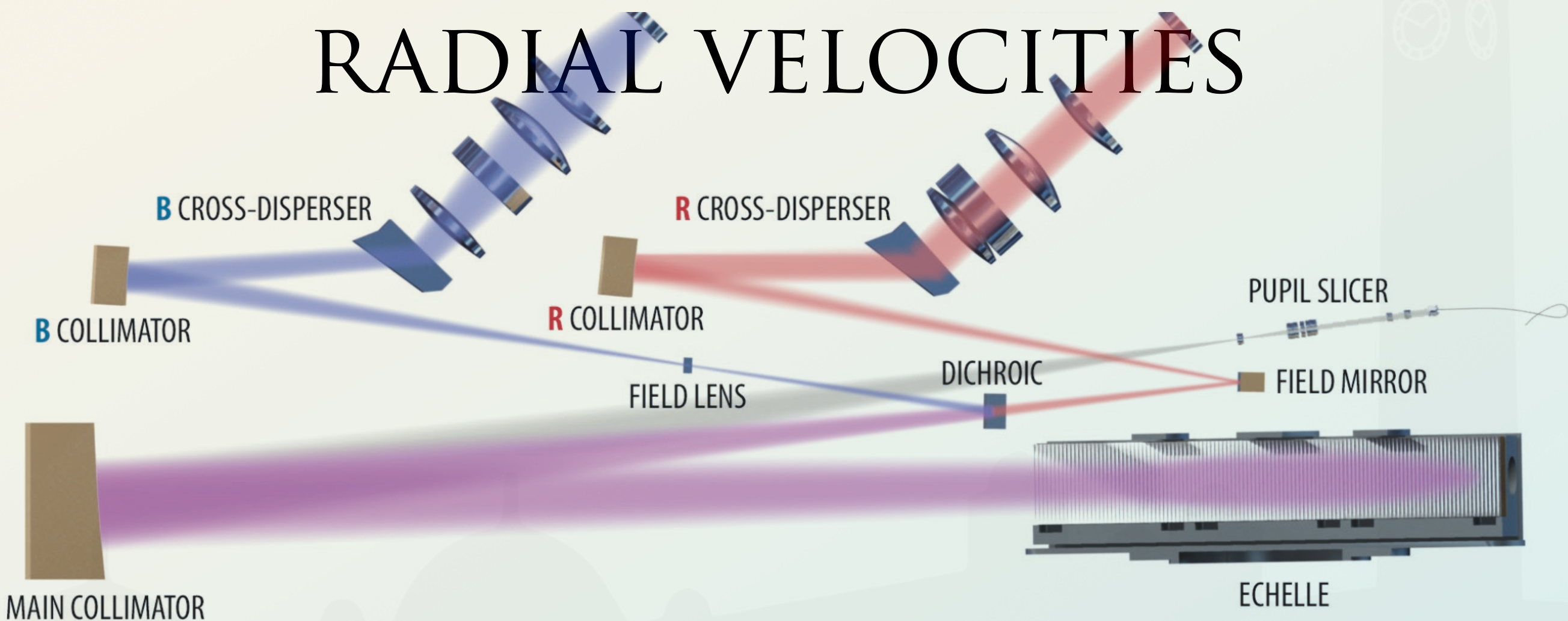




DETECTION METHODS



KEY CONCEPTS

- First detection method: radial-velocities
- Orbital motion around a barycentre
- Binary stars
- Exoplanet detection
- How radial velocities are measured
- Results from the radial velocity method

INDIRECT METHODS OF PLANET DETECTION

Directly observing exoplanets is difficult (we will see that later). This is why many indirect methods of detection were devised.

The planet's existence is **deduced** from the way it affects the light from its host star.

For the radial-velocity method, a planet affects the position of absorption lines in a star's spectrum. As the planet orbits, it gently pulls on its host star, with both objects orbiting a common centre of mass.

As the star orbits, its emerging spectrum is affected by the Doppler effect. The radial-velocity method is also called the Doppler method. Radial-velocity measurements are sometimes called velocimetric measurements.

THE DOPPLER EFFECT

The Doppler effect happens when an object producing a wave is moving. It can be sound. For stars it is light.

$$\Delta\lambda = \lambda_{\text{obs}} - \lambda_0$$
$$\lambda_{\text{obs}} = \lambda_0 \frac{1 + \frac{v}{c}}{\left(1 - \frac{v^2}{c^2}\right)^{1/2}}$$

3.1

which for $v \ll c$

$$v = \frac{\Delta\lambda}{\lambda_0} c \rightarrow V_{\text{rad}} = v \sin i = \frac{\Delta\lambda}{\lambda_0} c$$

3.2

where i is the inclination angle compared the plane of the sky

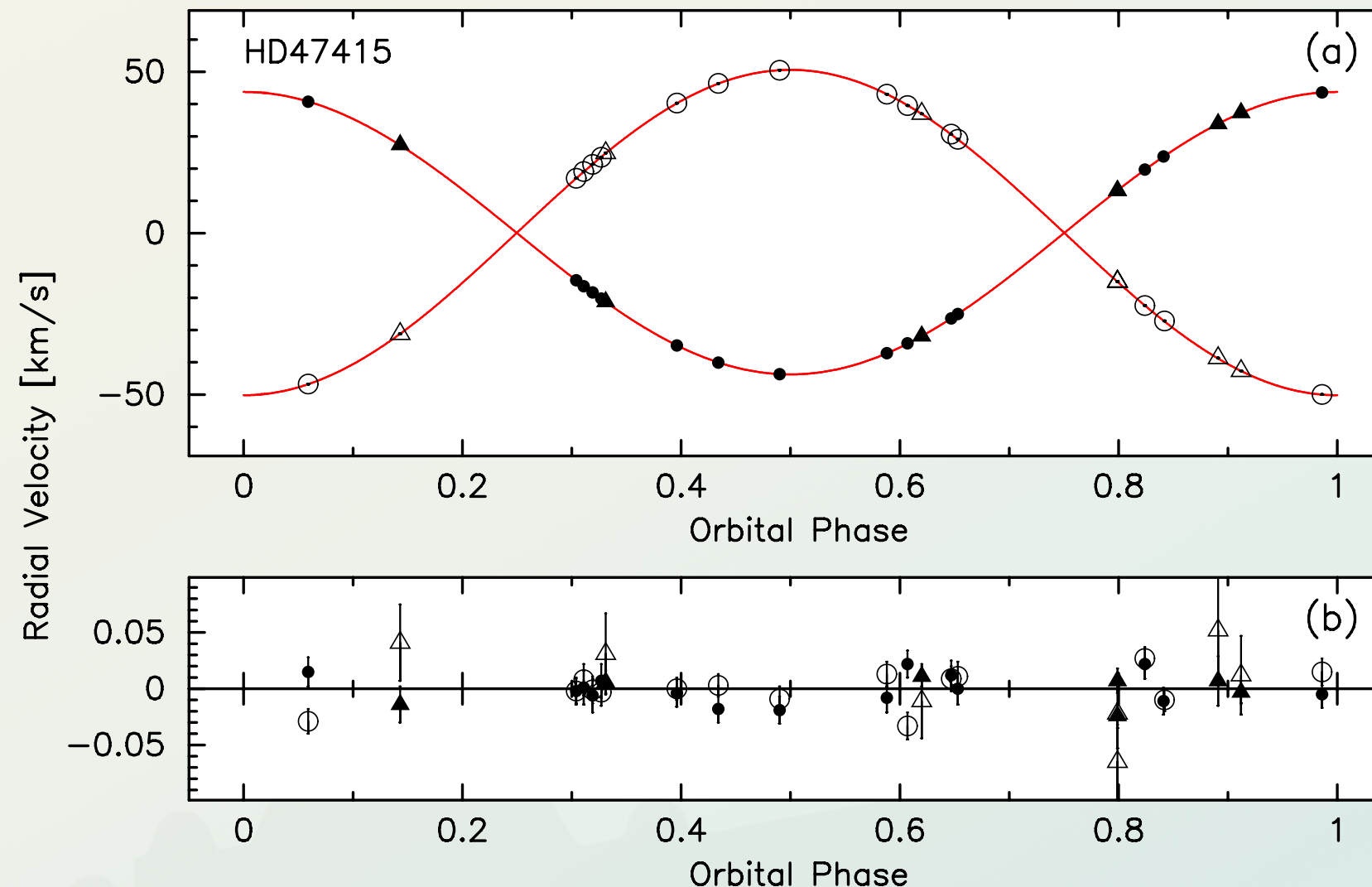
face-on: $i = 90^\circ$; side-on, $i = 0^\circ$

by convention, red-shifted, a receding velocity, is a positive V_{rad}

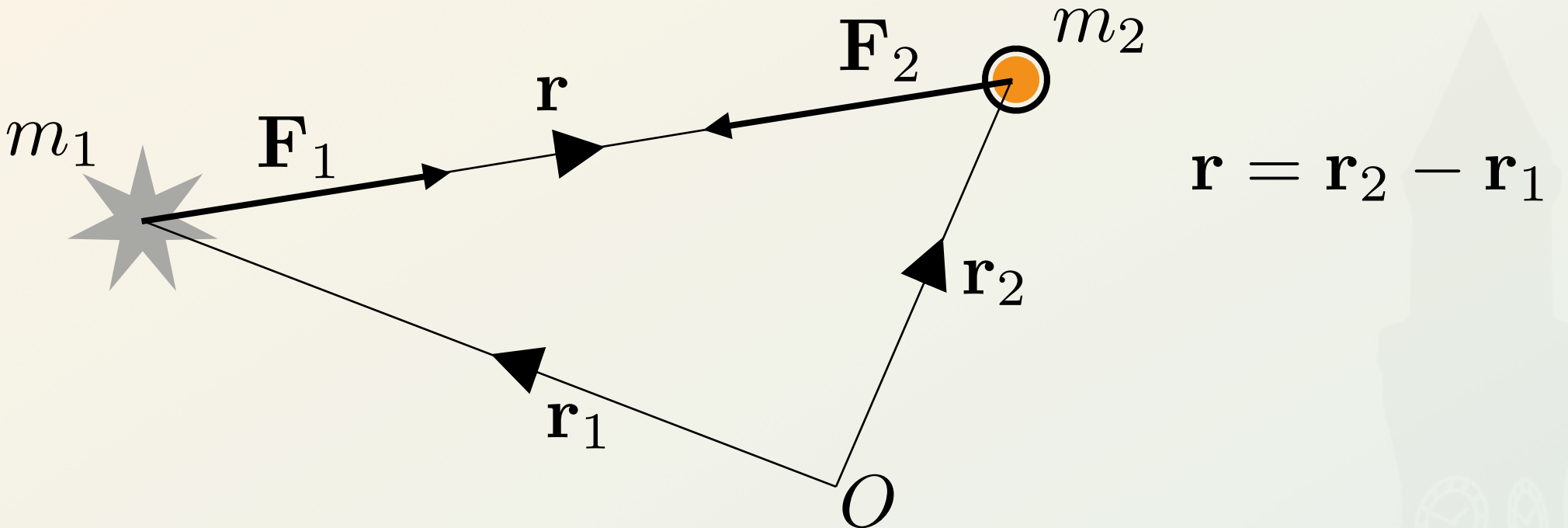
RADIAL-VELOCITY IN ACTION

Let's take a binary star at short orbital period. The two stars are not resolved on sky, but they produce two sets of absorption lines on the combined spectrum. Both sets move with respect to one another, and we can measure their radial-velocities.

What we will do now is find how to calculate the red lines.

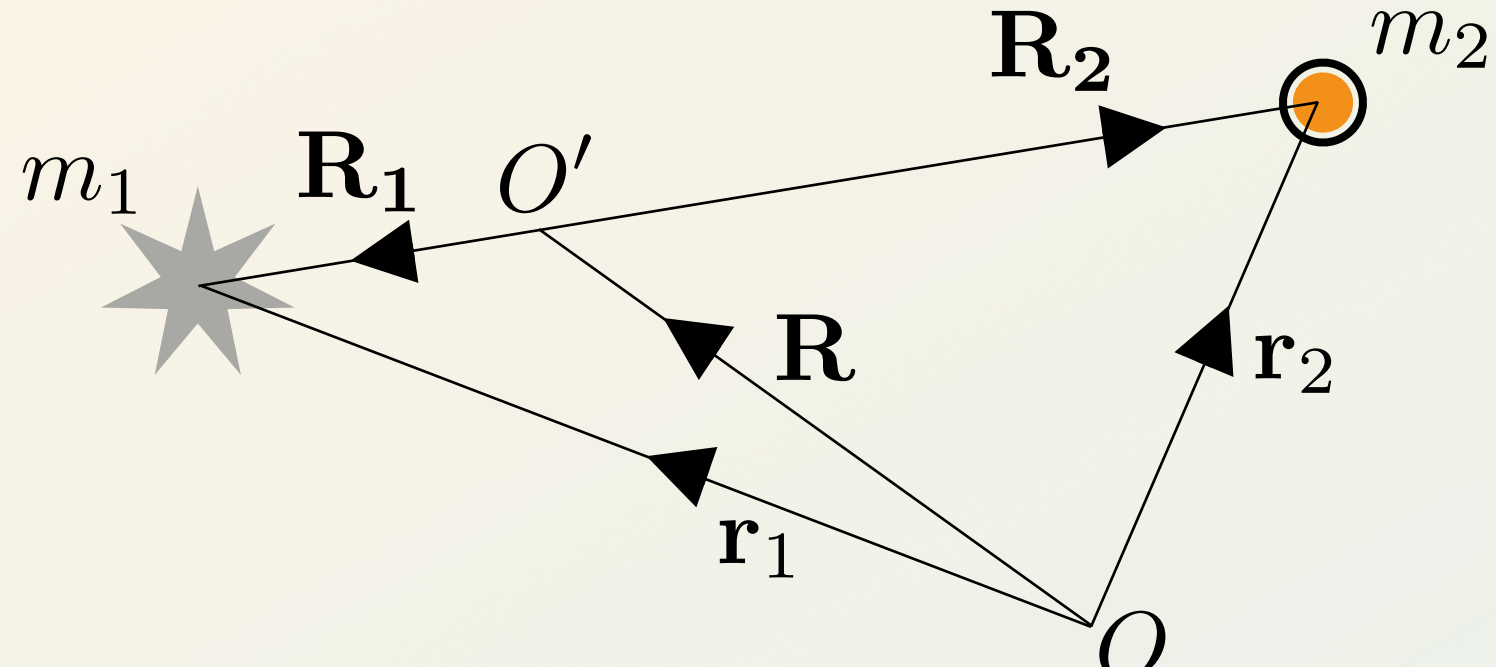


MOVING THE ORIGIN



The Two-Body problem was with respect to an external origin. To detect planets using the radial velocity method, we need to see how the two masses move with respect to one another around their common centre of mass, which we call: the **barycentre**.

INTRODUCING A BARYCENTRE



$$\mathbf{R} = \frac{m_1 \mathbf{r}_1 + m_2 \mathbf{r}_2}{m_1 + m_2}$$

$$\ddot{\mathbf{R}} = \frac{m_1 \ddot{\mathbf{r}}_1 + m_2 \ddot{\mathbf{r}}_2}{m_1 + m_2} = 0$$

Using 2.1 & 2.2,

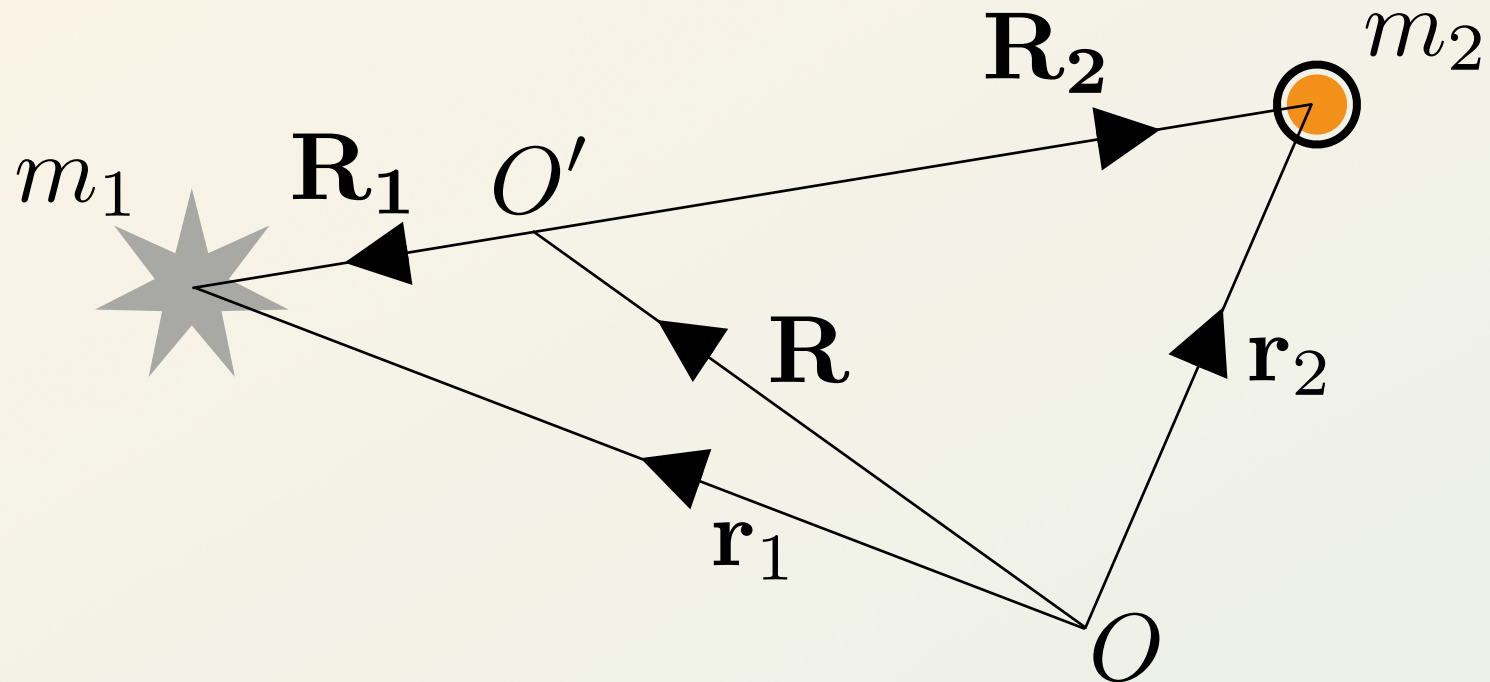
the systemic velocity γ

3.3

3.4

proper motion

MOTION ABOUT A BARYCENTRE



then we find,

$$m_1 \mathbf{R}_1 + m_2 \mathbf{R}_2 = 0$$

and because

$$\mathbf{R}_1 + \mathbf{R}_2 = \mathbf{R}$$

we have

$$R_2 = \frac{m_1}{M} a = a_2$$

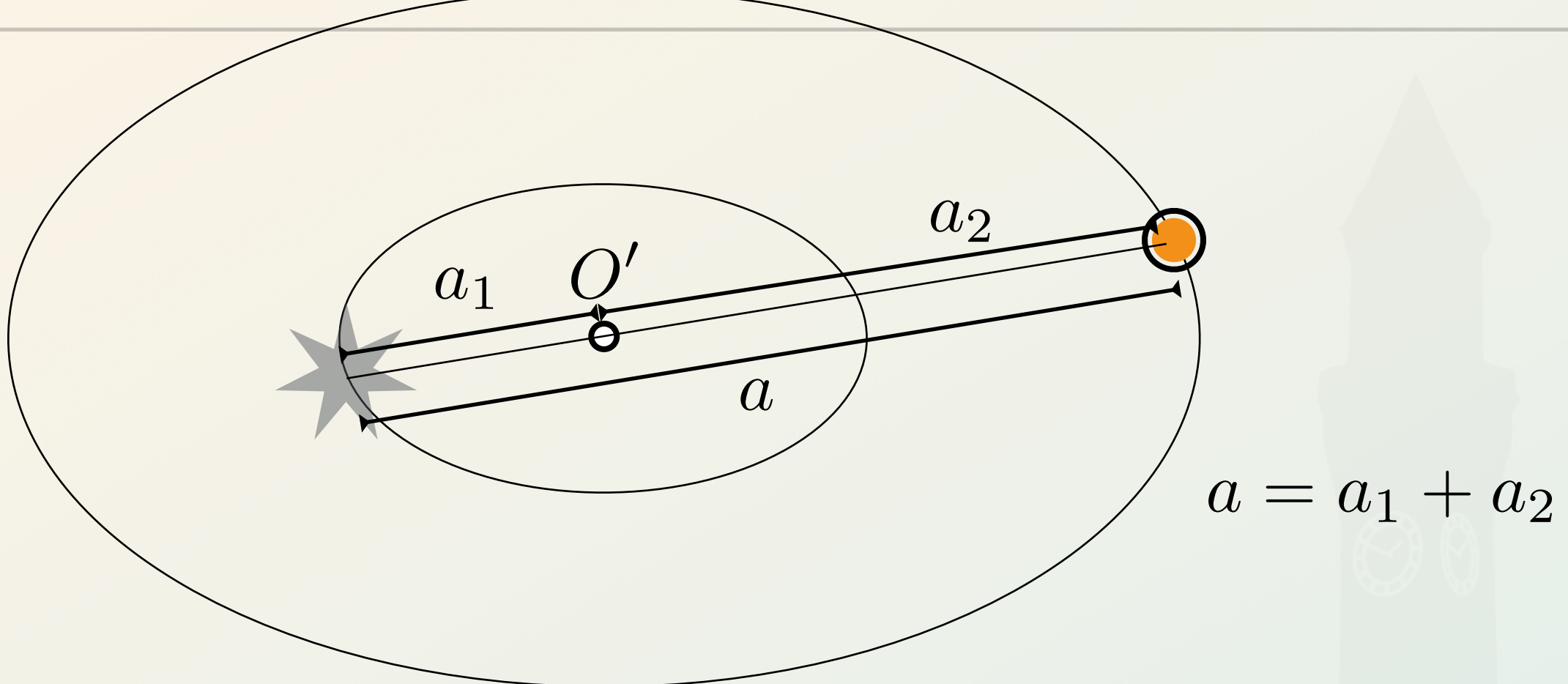
$$R_1 = \frac{m_2}{M} a = a_1$$

$$M = m_1 + m_2$$

3.5

3.6

MOTION ABOUT A BARYCENTRE



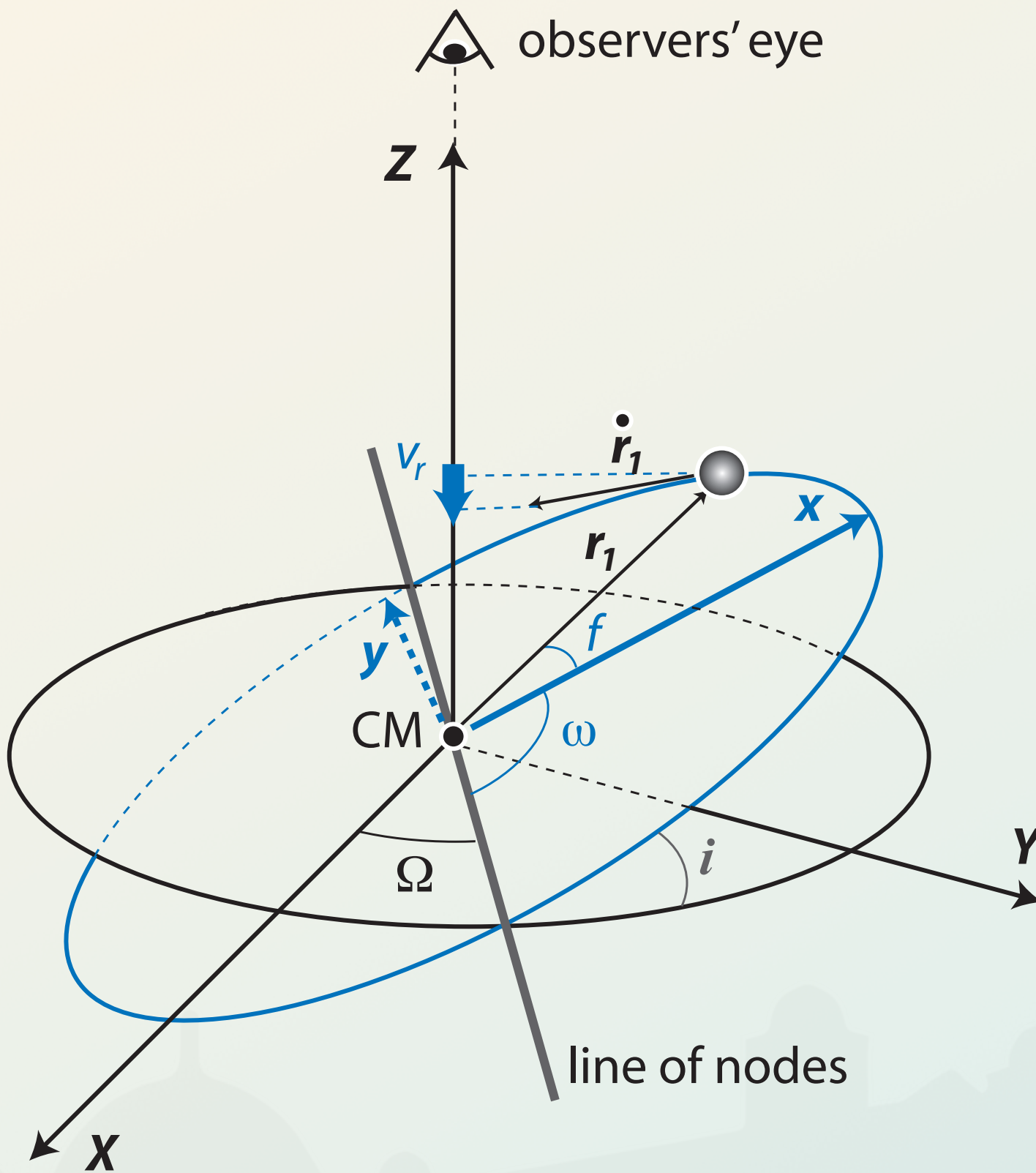
Let's introduce equalities imposed by the orbital motion:

$$T_1 = T_2 = T \quad e_1 = e_2 = e \quad a_1 : a_2 : a = m_2 : m_1 : M$$

Kepler's law, 2.14 is

$$\frac{4\pi^2}{GT^2} = \frac{M}{a^3} = \frac{m_2^3/M^2}{a_1^3} = \frac{m_1^3/M^2}{a_2^3}$$

ORBITS IN 3D



RADIAL VELOCITY

$$\begin{aligned} x &= r \cos(f + \omega) \\ y &= r \sin(f + \omega) \\ z &= r \sin(f + \omega) \sin i \end{aligned} \quad \begin{array}{l} \text{in plane of the sky} \\ \text{line of sight} \end{array}$$

$$V_{\text{rad}} = \dot{z} = \sin i \left[\dot{r} \sin(f + \omega) + r \dot{f} \cos(f + \omega) \right] \quad 3.7$$

from 2.12, differentiate:

$$\dot{r} = \frac{r e \dot{f} \sin f}{1 + e \cos f} \quad 3.8$$

because ϖ is constant, $\dot{\theta} = \dot{f}$

re-arrange 2.12 and 3.8, and insert in 3.7, do some trigonometry:

$$\begin{aligned} V_{\text{rad}} &= \frac{2\pi a}{T} \frac{\sin i}{\sqrt{1 - e^2}} [\cos(f + \omega) + e \cos \omega] \\ &= K [\cos(f + \omega) + e \cos \omega] + \gamma \end{aligned} \quad 3.9$$

RADIAL VELOCITY

$$\begin{aligned} V_{\text{rad}} &= \frac{2\pi a}{T} \frac{\sin i}{\sqrt{1-e^2}} [\cos(f+\omega) + e \cos \omega] \\ &= K [\cos(f+\omega) + e \cos \omega] + \gamma \end{aligned}$$

3.9

where the semi-amplitude K is

$$K = \frac{2\pi a}{T} \frac{\sin i}{\sqrt{1-e^2}}$$

3.10

In the case of binary stars (or any orbiting pair where both objects emit light:

$$V_{\text{rad},1} \propto K_1 \propto a_1 \sin i \quad V_{\text{rad},2} \propto K_2 \propto a_2 \sin i$$

RADIAL VELOCITY

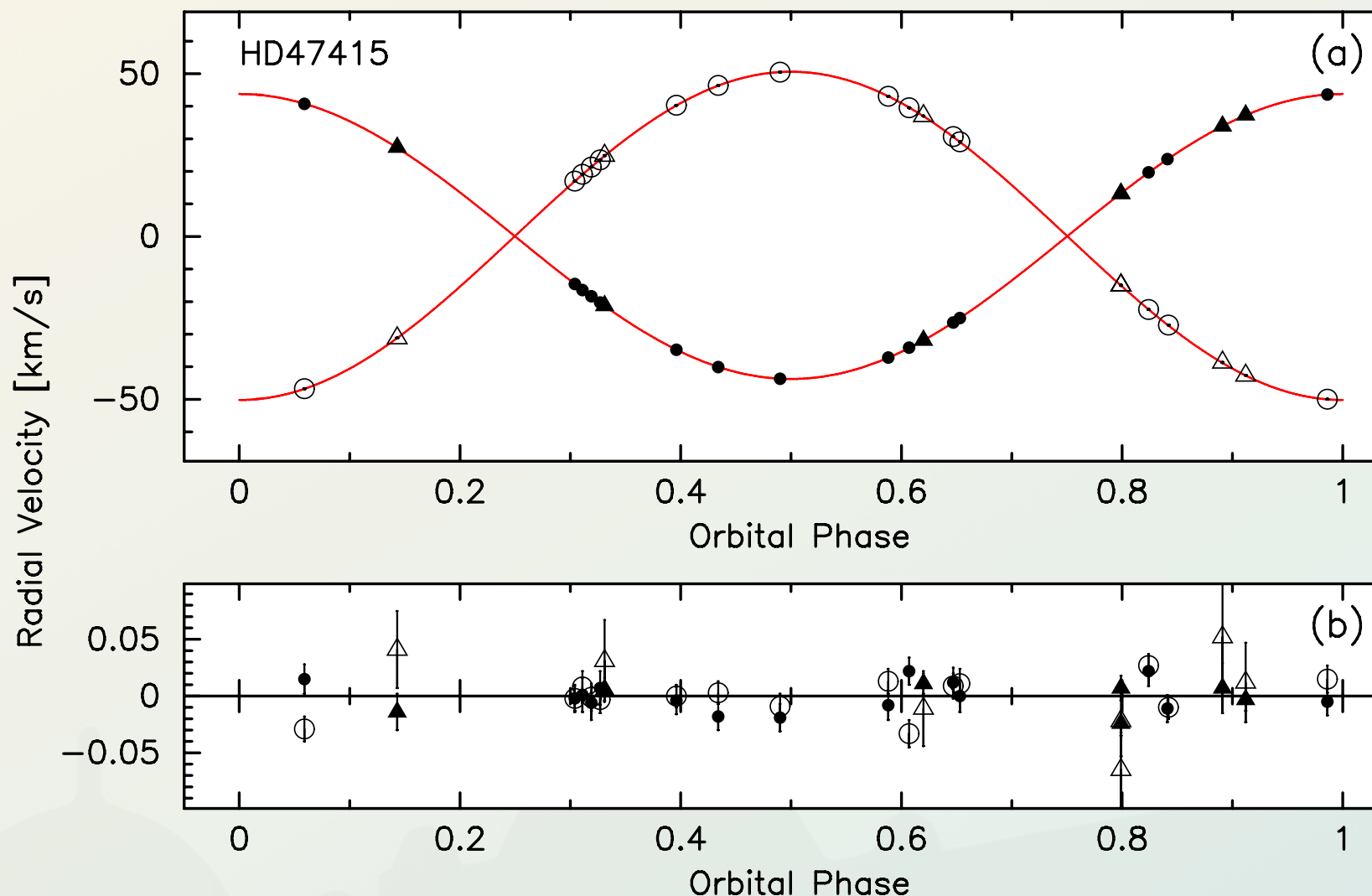
$$V_{\text{rad},1} \propto K_1 \propto a_1 \sin i$$

$$V_{\text{rad},2} \propto K_2 \propto a_2 \sin i$$

thus, we write

3.11 $K_1 = \frac{m_2}{m_1 + m_2} \frac{2\pi}{T} \frac{a \sin i}{\sqrt{1 - e^2}}$

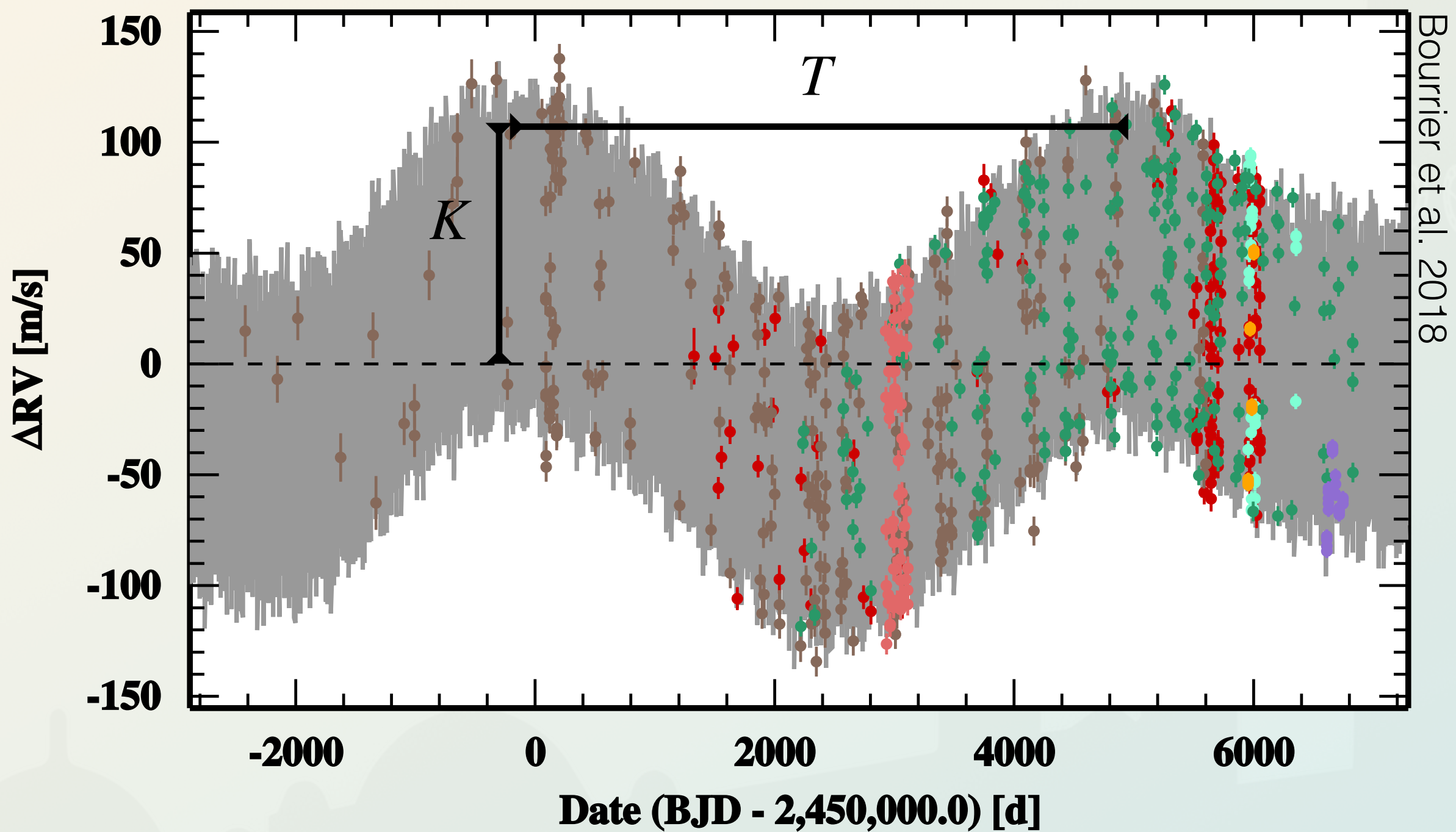
3.12 $K_2 = \frac{m_1}{m_1 + m_2} \frac{2\pi}{T} \frac{a \sin i}{\sqrt{1 - e^2}}$



$$\frac{K_1}{K_2} \rightarrow \frac{m_2}{m_1}$$

55 CANCRI

Keplerian signals add linearly on top of one another. If there are multiple planets, there are simply multiple sinusoidal curves each with an independent set of orbital elements, and a common γ

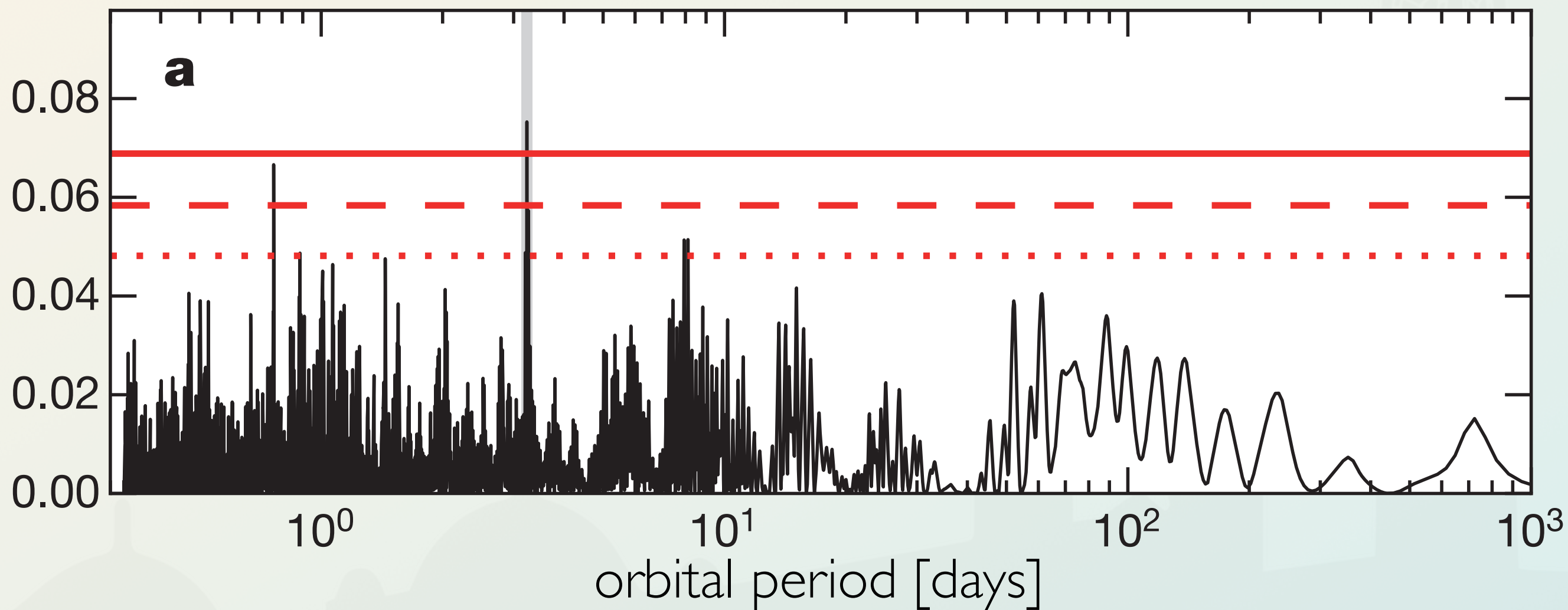


FINDING A SIGNAL WITH A PERIODOGRAM

Doing a Lomb-Scargle periodogram is doing a Fourier decomposition of the data, revealing various sinusoidal signals in the RV data. Those that pass a False Alarm Probability threshold are typically kept as “detected signals”.

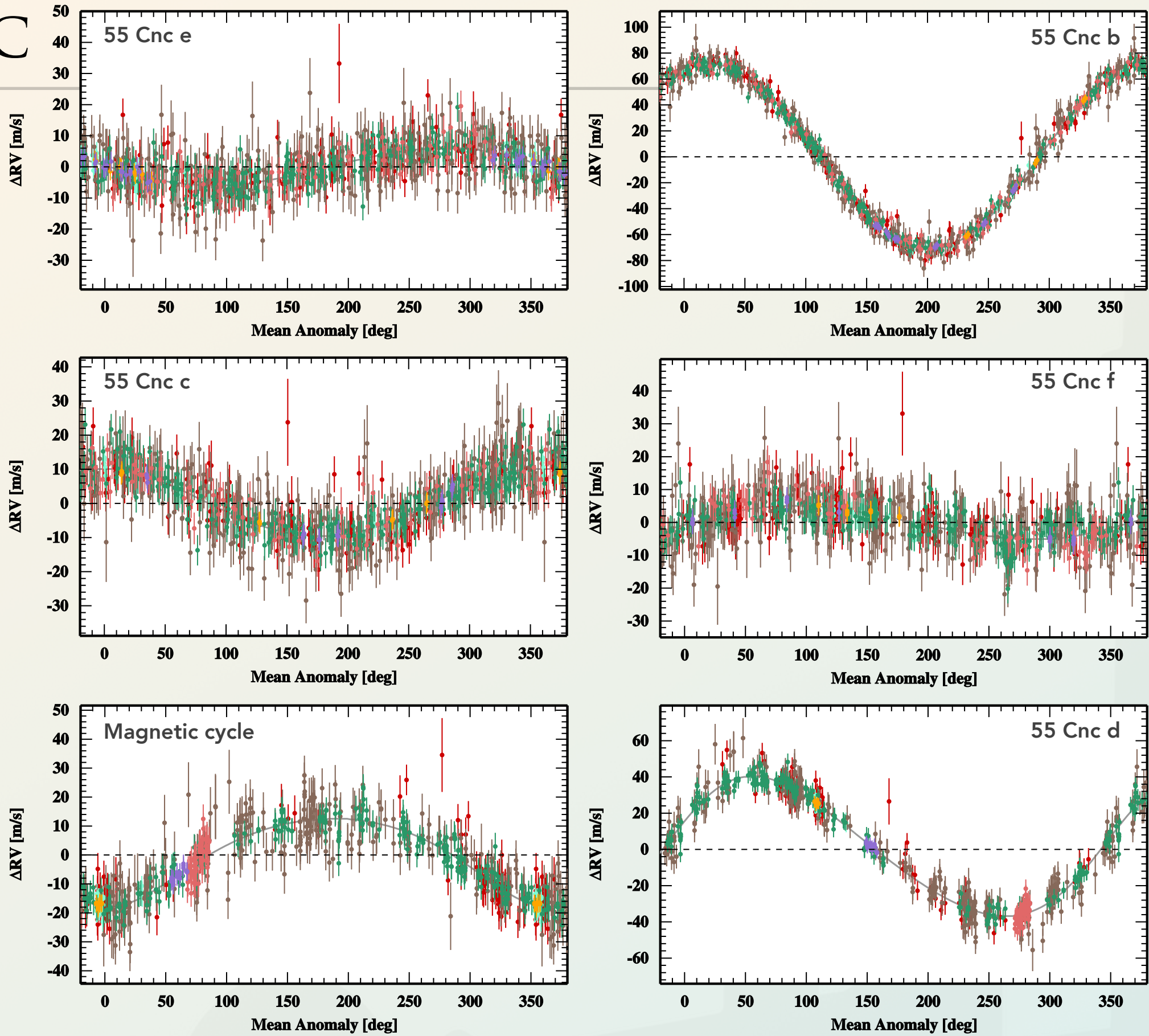
Periodograms can detect signals that are not planetary.

Periodograms assume $e = 0$ by design.



55 CNC

Bourrier et al. 2018



Smooth Model
HRS
TULL

Drift
KECK

HARPN
LICK

HARPS
SOPHIE

RADIAL VELOCITY MOTION OF A STAR

for a planet, we only measure K_1 or K_\star

$$K_\star = \frac{m_p}{M_\star + m_p} \frac{2\pi}{T} \frac{a \sin i}{\sqrt{1 - e^2}}$$

3.11

use Kepler's law (2.14), and solve, to reach

$$K_1 = 28.4 \text{ m/s} \left(\frac{1 \text{ yr}}{T} \right)^{1/3} \left(\frac{m_p \sin i}{M_{\text{Jup}}} \right) \left(\frac{M_\odot}{m_\star} \right)^{2/3} \frac{1}{\sqrt{1 - e^2}}$$

$m_p \sin i$ is referred to as the *minimum mass*

rearranging 3.11, we can also get to the *mass function*

$$f(m_2) = \frac{m_2^3 \sin^3 i}{(m_1 + m_2)^2} = (1 - e^2)^{3/2} \frac{T K_1^3}{2\pi G}$$

3.13

RADIAL VELOCITY MOTION OF A STAR

$$K_{\star} = \frac{m_p}{M_{\star} + m_p} \frac{2\pi}{T} \frac{a \sin i}{\sqrt{1 - e^2}}$$

3.11

$$K_1 = 28.4 \text{ m/s} \left(\frac{1 \text{ yr}}{T} \right)^{1/3} \left(\frac{m_p \sin i}{M_{\text{Jup}}} \right) \left(\frac{M_{\odot}}{m_{\star}} \right)^{2/3} \frac{1}{\sqrt{1 - e^2}}$$

Poll

$$f(m_2) = \frac{m_2^3 \sin^3 i}{(m_1 + m_2)^2} = (1 - e^2)^{3/2} \frac{T K_1^3}{2 \pi G}$$

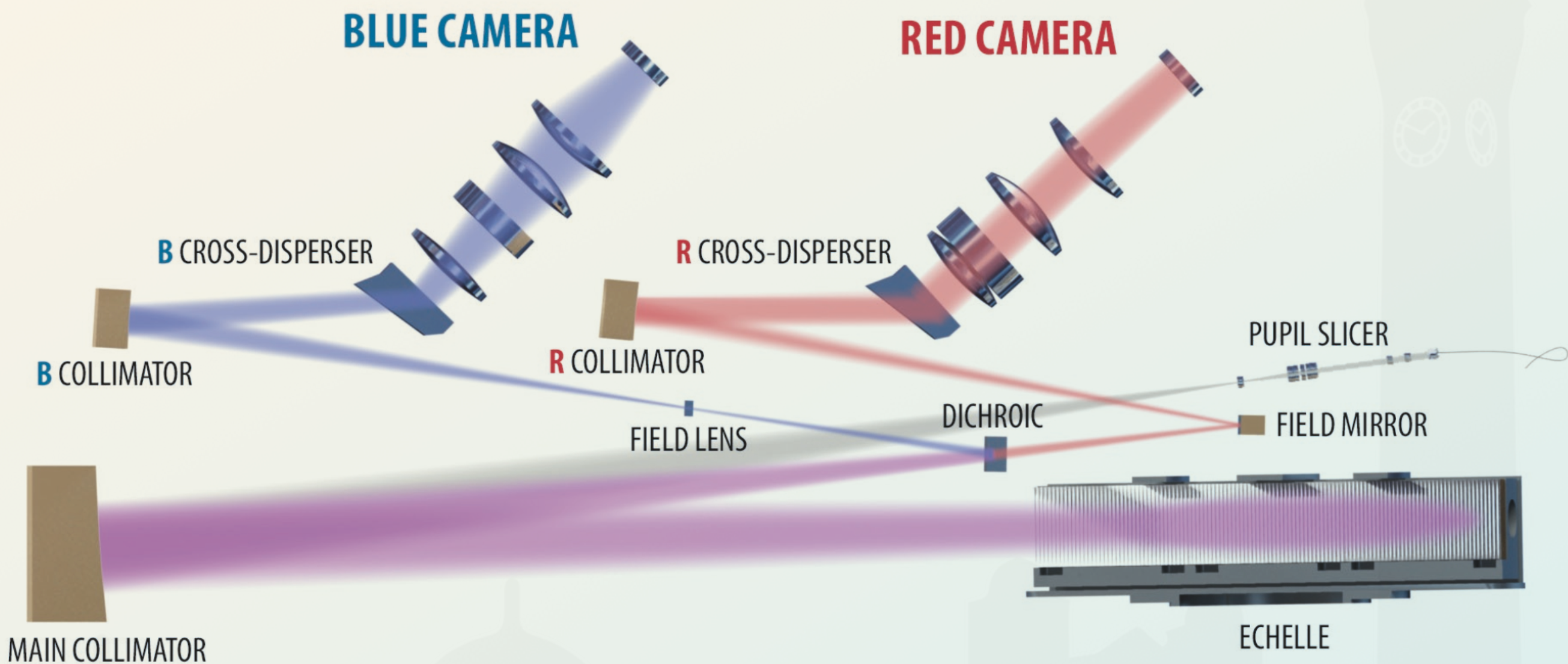
3.13

The planet mass can only be determined in relation to the stellar mass. If the stellar mass is unknown the planet mass is not known.

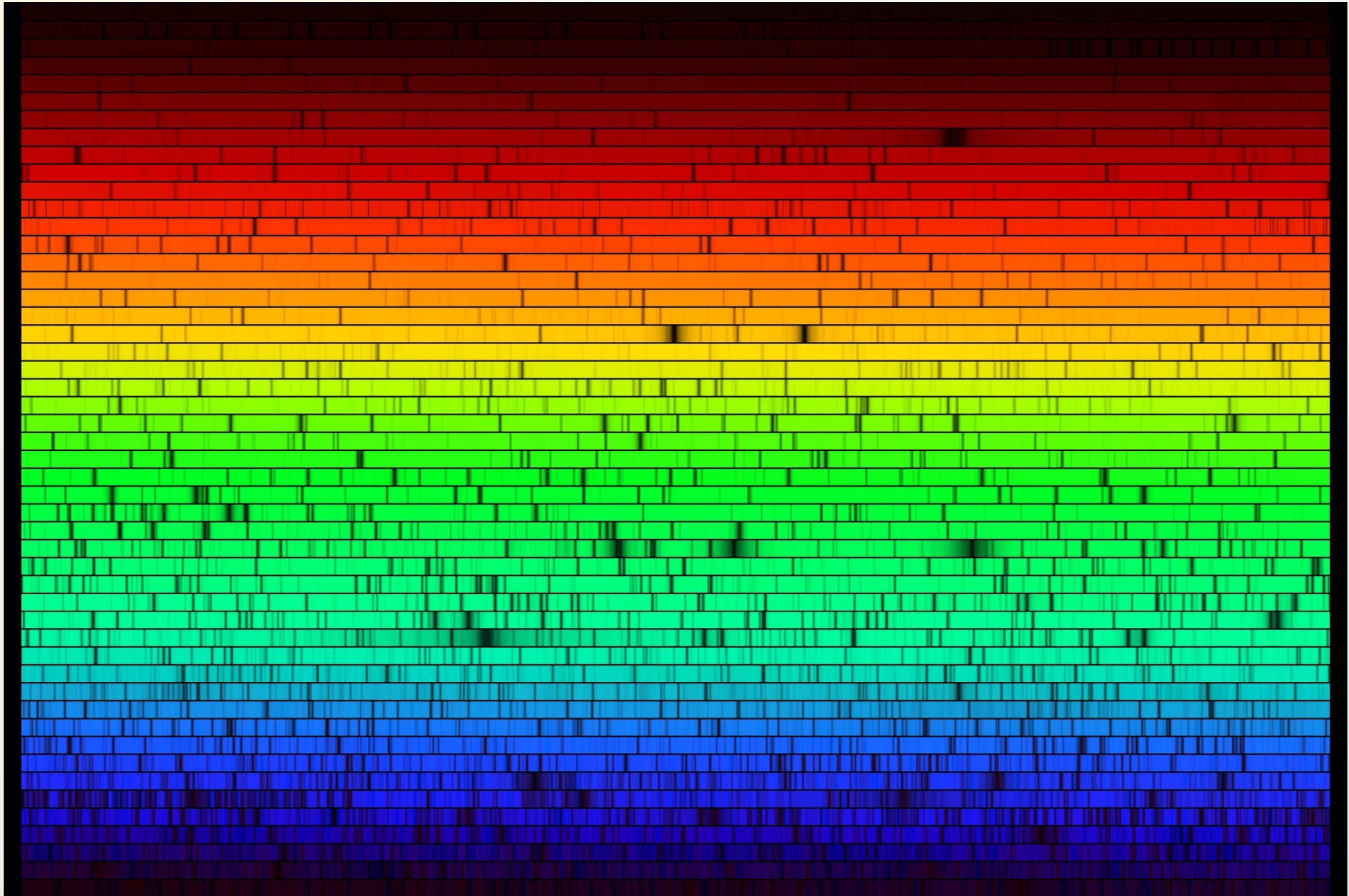
The mass function comes in hand for that it is a sort of mass ratio, which tells us that the unseen orbiting object is likely substellar in mass. It has the advantage to solely dependent on **observables**.

THE ESPRESSO SPECTROGRAPH

ESPRESSO is on the VLT in Chile, and is the most modern of the high-resolution, stable spectrographs used to detect planets with the radial-velocity method.

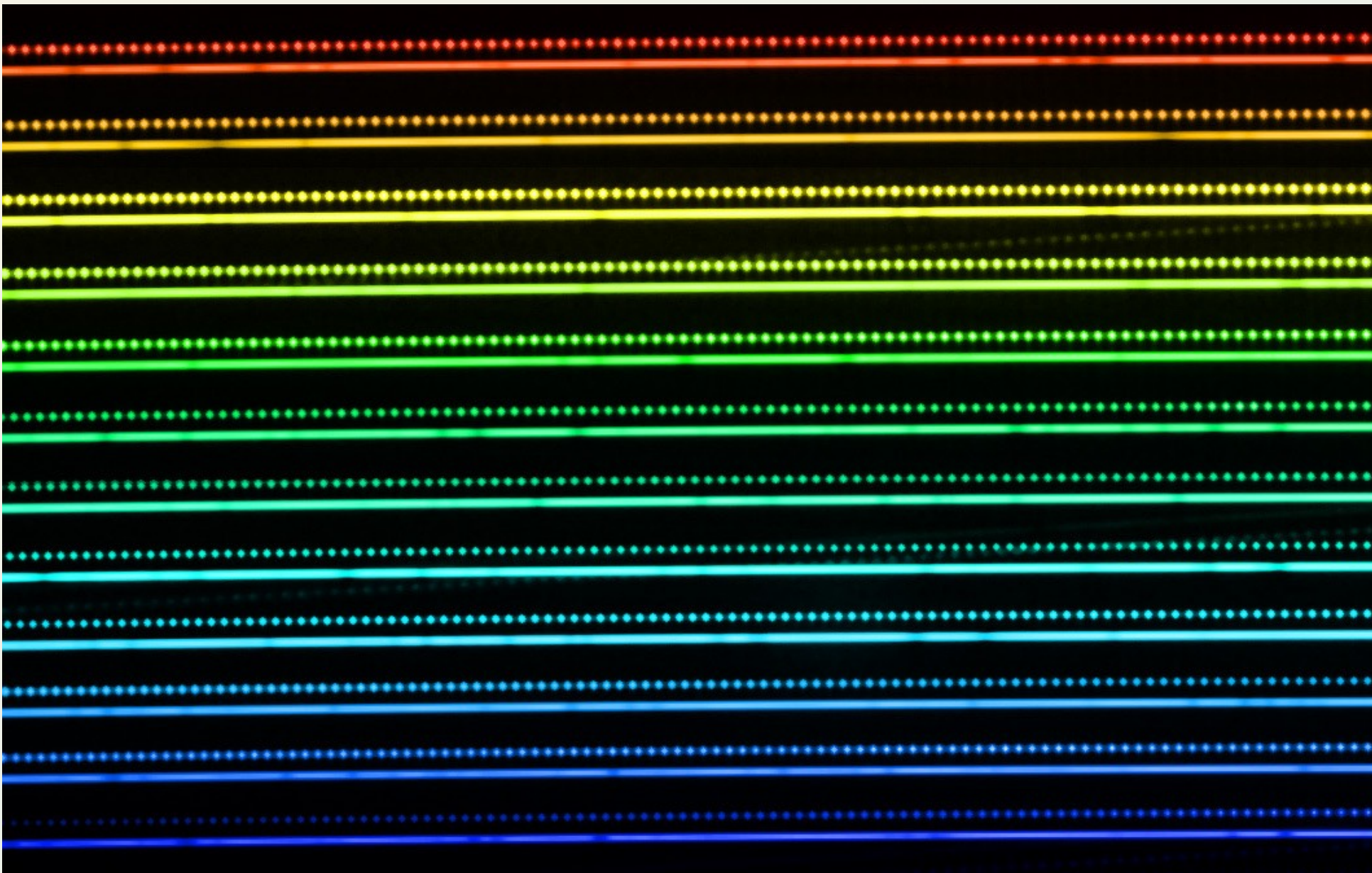


EXTRACTING RADIAL-VELOCITIES



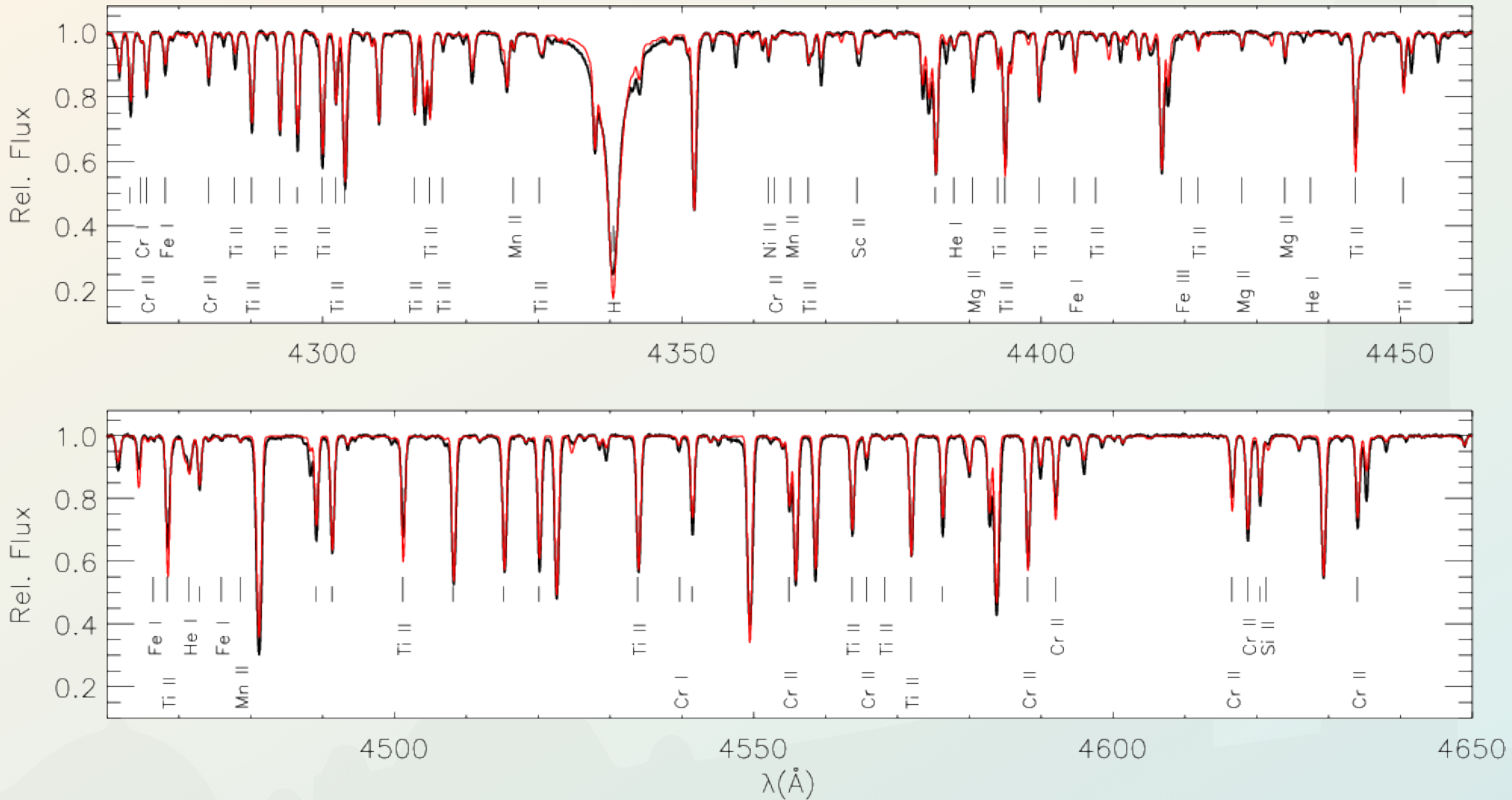
WHAT A SPECTRUM LOOKS LIKE

This is what the spectrum looks like inside of HARPS one of the chief planet-hunting spectrographs. The dots are an etalon, a calibration, which here uses a Fabry-Pérot system. This etalon has a known λ_0 , which is used to measure $\Delta\lambda$ and get V_{rad}



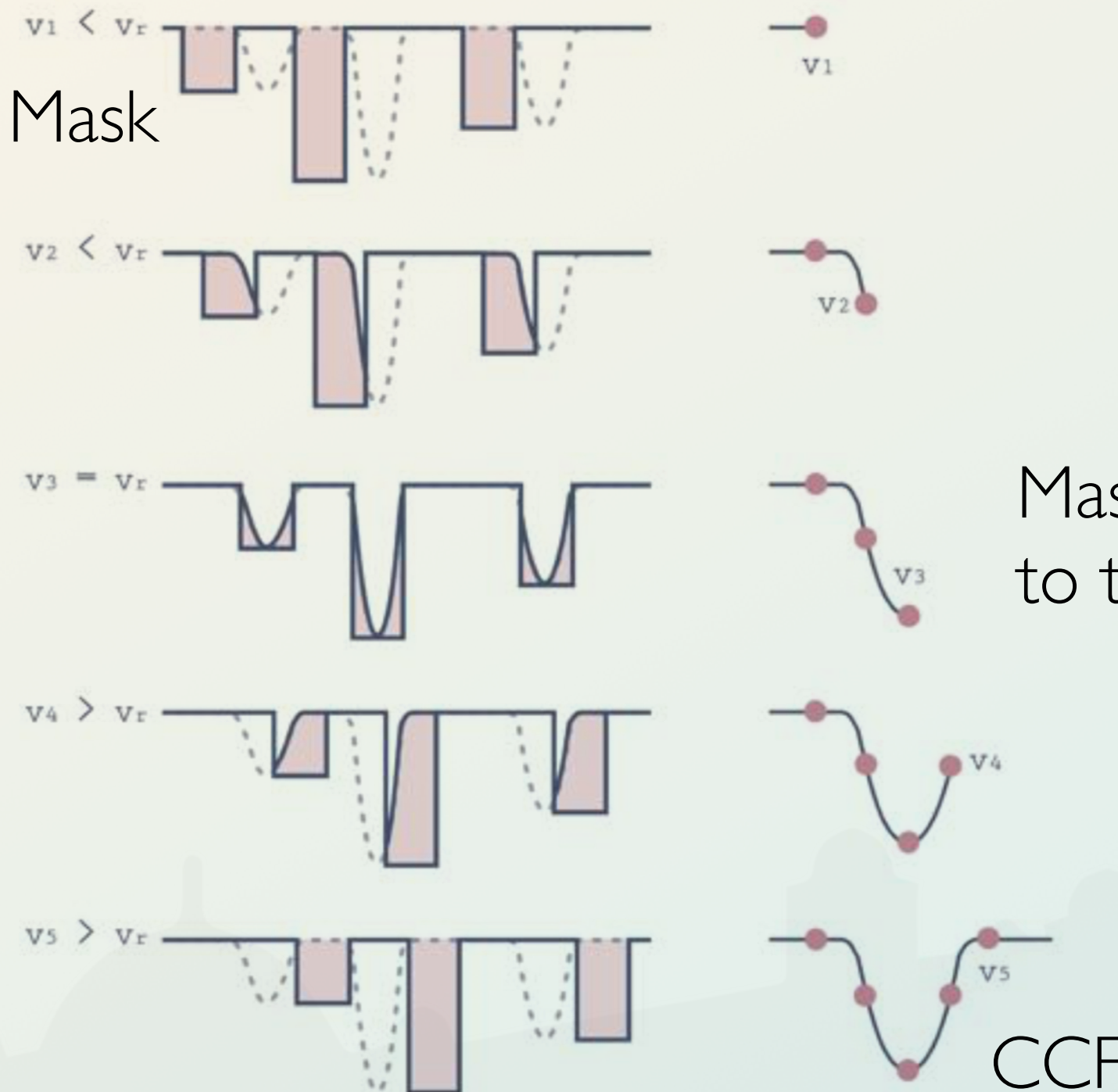
EXTRACTING RADIAL-VELOCITIES

Each order is transformed into a 1D spectrum. Thousands of lines exist. Rather than measure the radial-velocity for each of them individually, a cross-correlation is instead used.



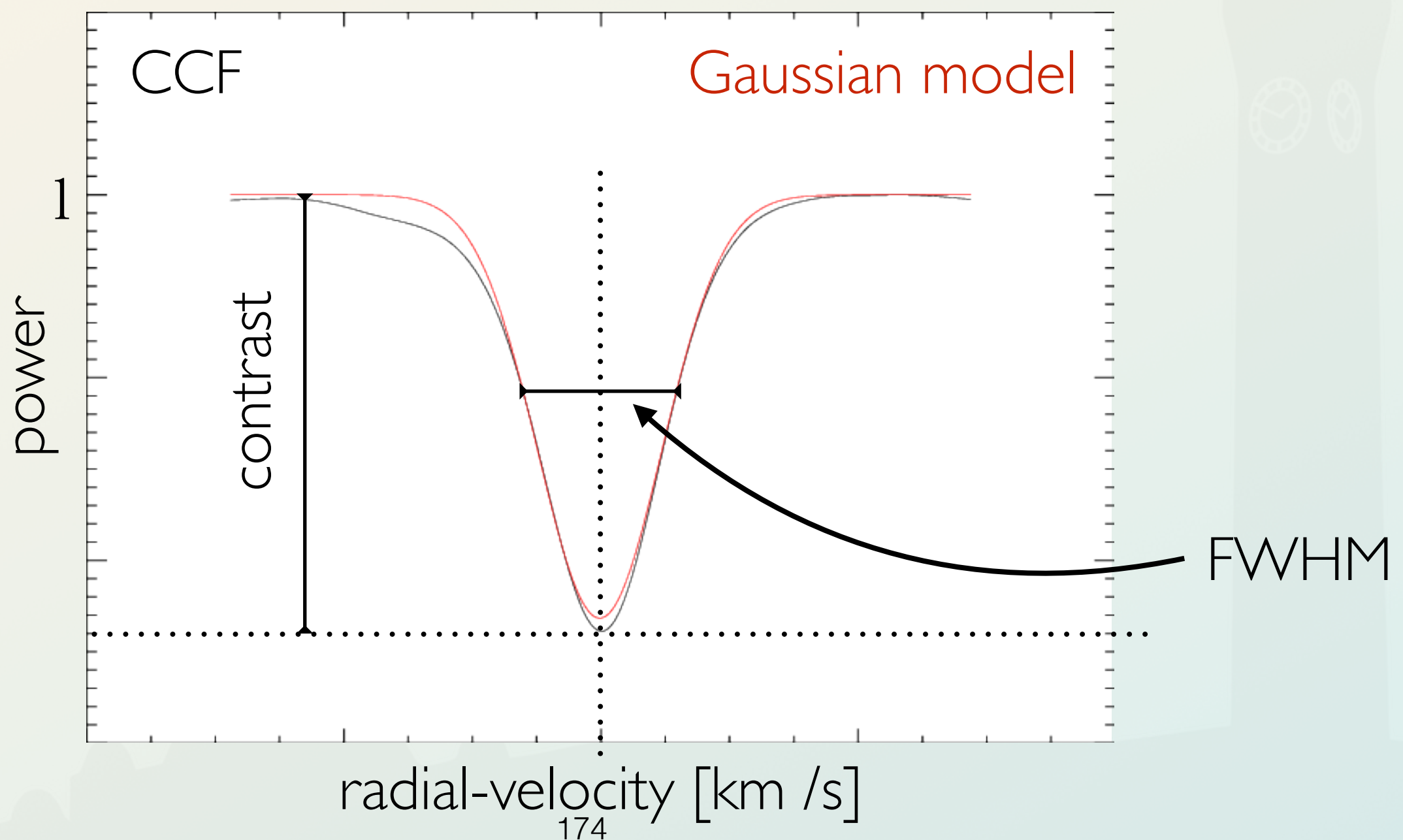
CROSS CORRELATION FUNCTION

The cross-correlation is done either with a template spectrum, or with a mask corresponding to an absorption line list. In the case of mask the procedure is the following:



CROSS CORRELATION FUNCTION

Using a mask the cross-correlation function (CCF) is approximately Gaussian in shape. The Full Width at Half Maximum (FWHM) is a key measure of the CCF. A FWHM gets wider if the star rotates faster ($v \sin i_\star$), and because of granulation (macro turbulence), and instrumental resolution.



RADIAL-VELOCITY PRECISION

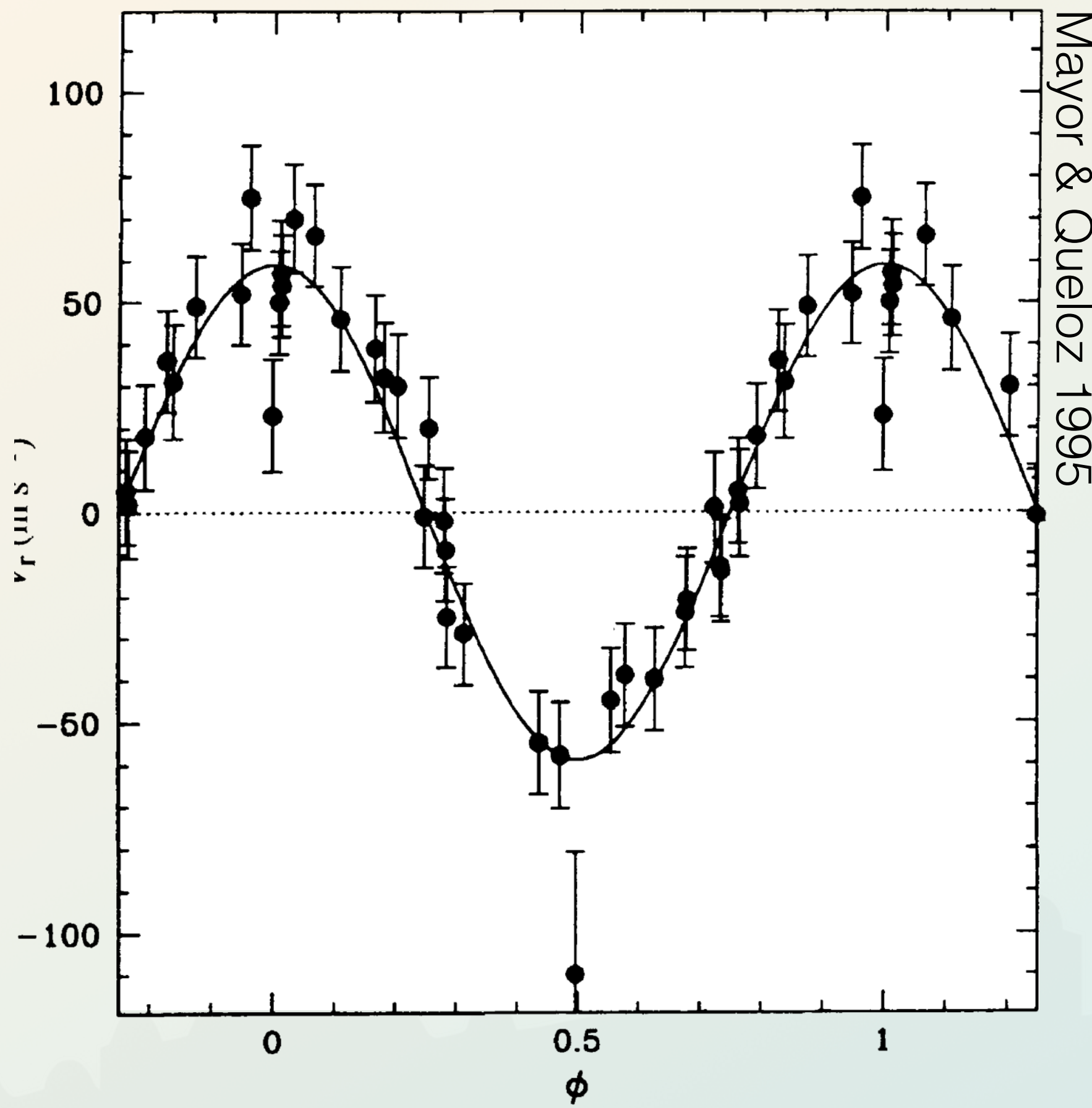
Several elements improve precision. Obviously more photons (a longer exposure, a brighter star helps). Importantly, the width of the line is important and, preferably it needs to be resolved. The thinner the lines, the thinner the CCF, and the radial-velocity is better determined. This is why the instrumental resolution R is important. The more resolving power, weaker $\Delta\lambda$ can be measured.

$$R = \frac{\lambda}{\Delta\lambda} \quad R = \frac{c}{\delta V_{\text{rad}}}$$

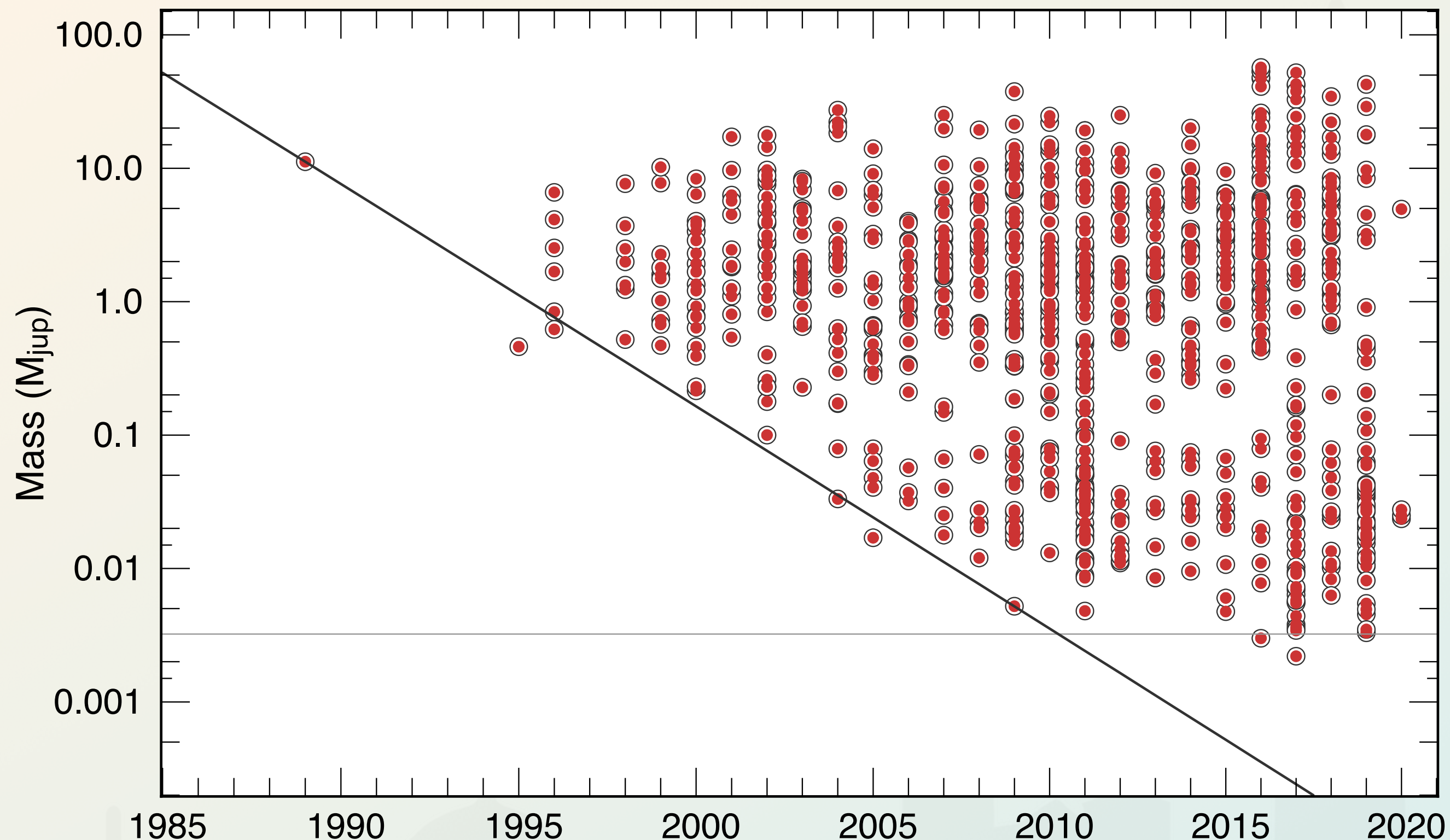
HARPS has $R \sim 115,000$, which means its velocity resolution is approximately 2.5 km/s. HARPS has a precision of 70 m/s on the mean of a single absorption line (V_{rad}).

The number of absorption lines is also extremely relevant. Precision approximately scales as $1/\sqrt{N}$, where N is the number of lines. Thanks to its wavelength range, HARPS observes $N \sim 5,000$ lines, which brings its precision below 1 m/s on the entire spectrum.

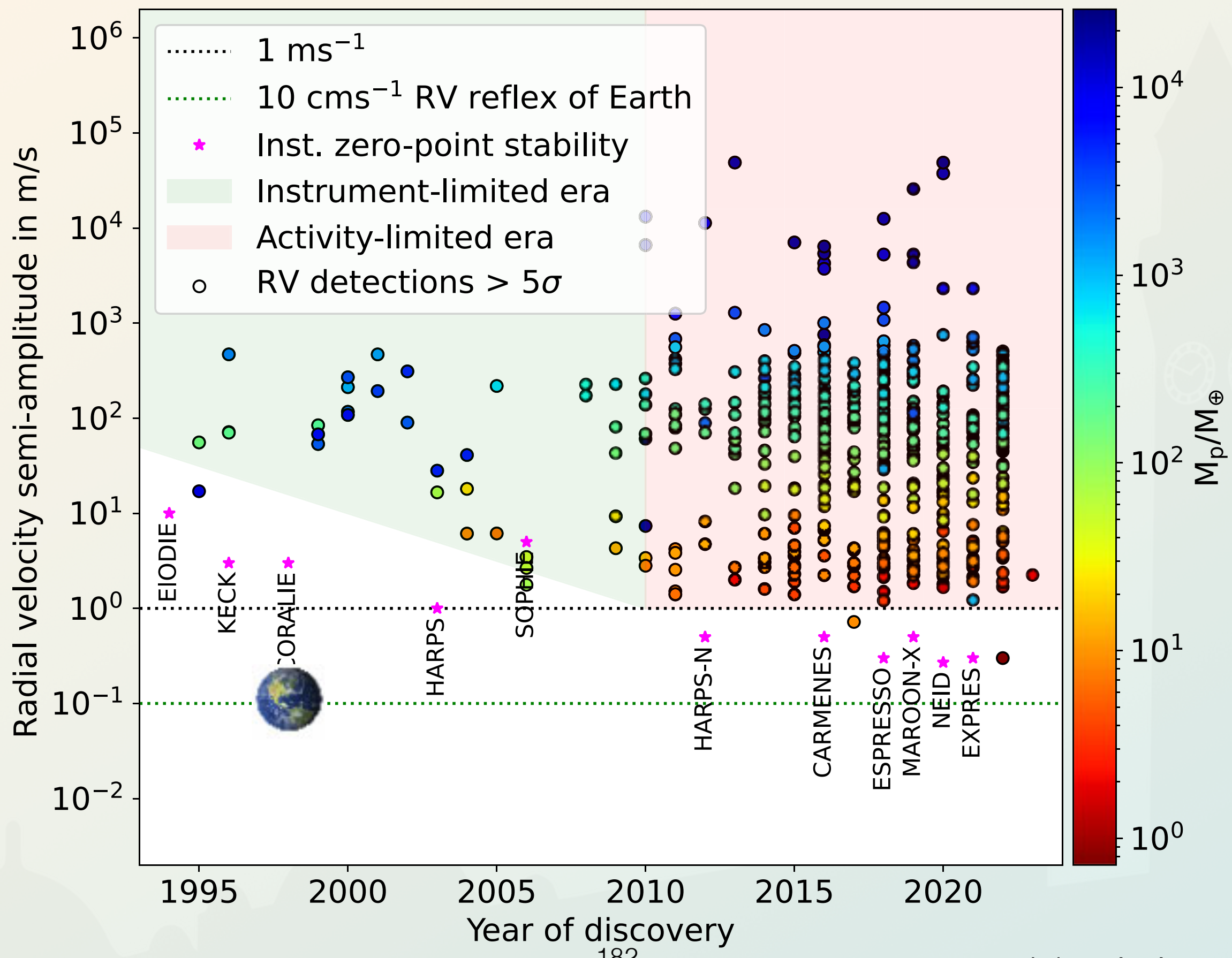
51 PEGASI B



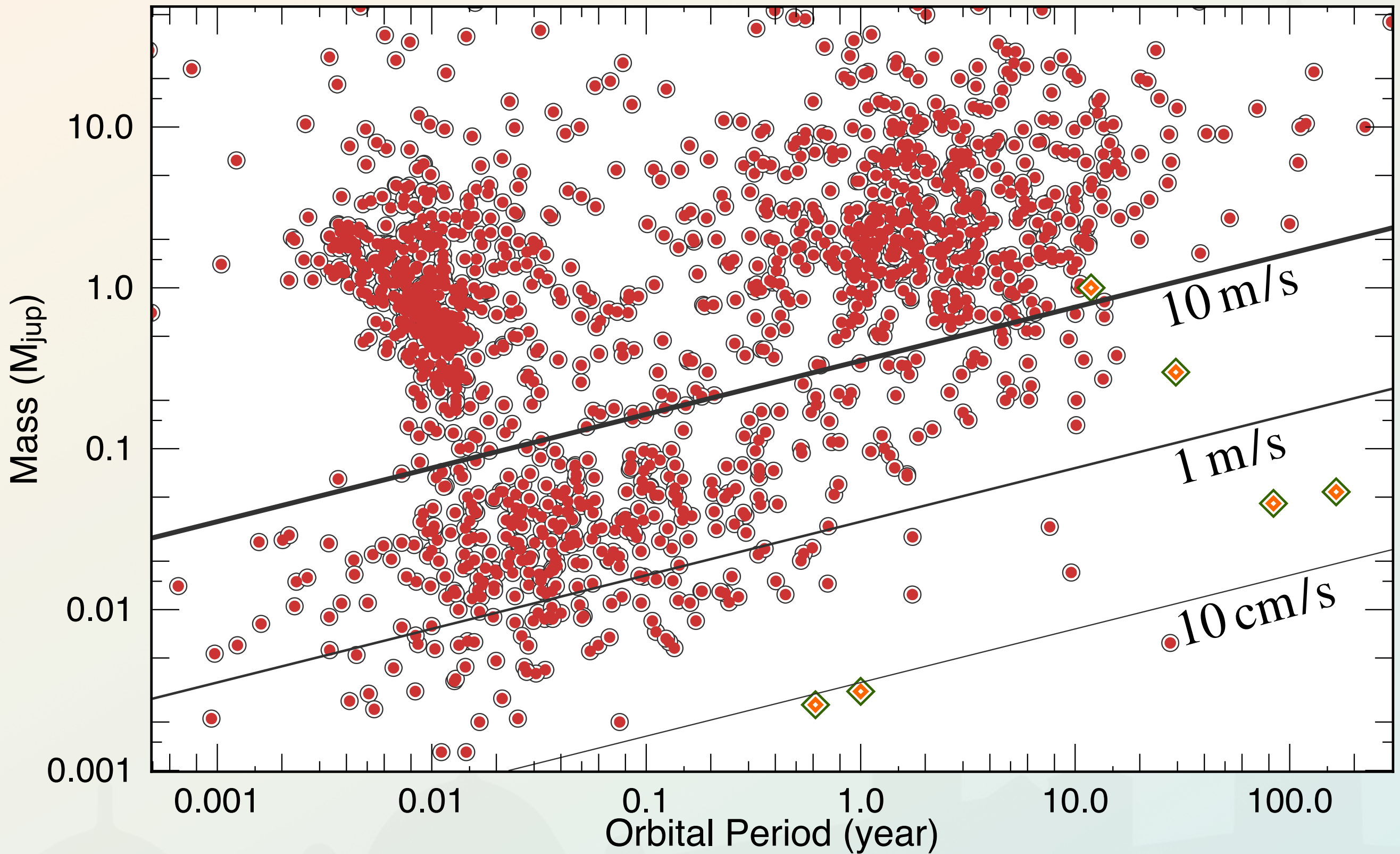
DECades of Research



DECades of Research



THE RESULTS



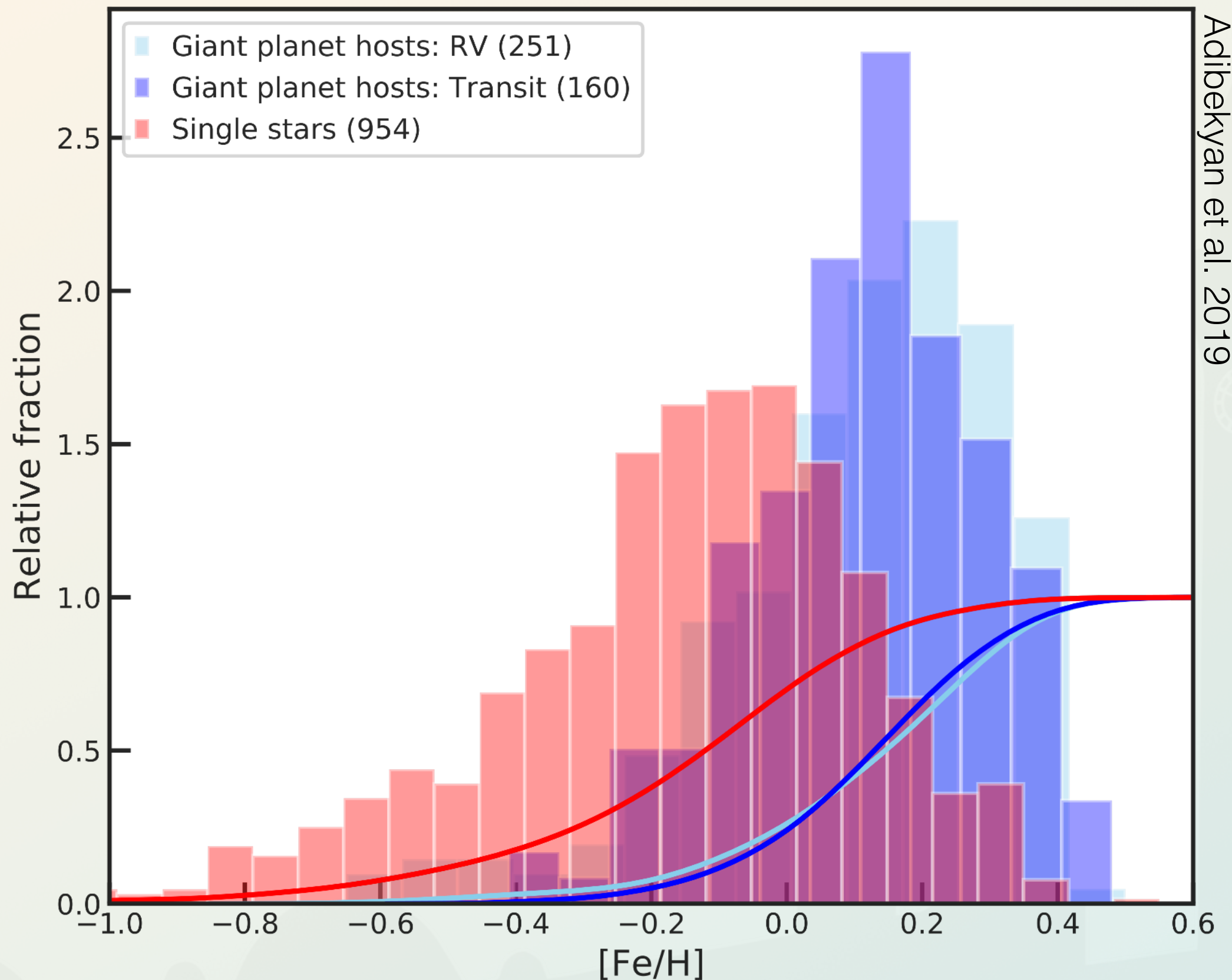
This is equation 3.13 plotted for different precisions.

CURRENT HIGH-RESOLUTION SPECTROGRAPHS

List of the more important instruments currently in use.

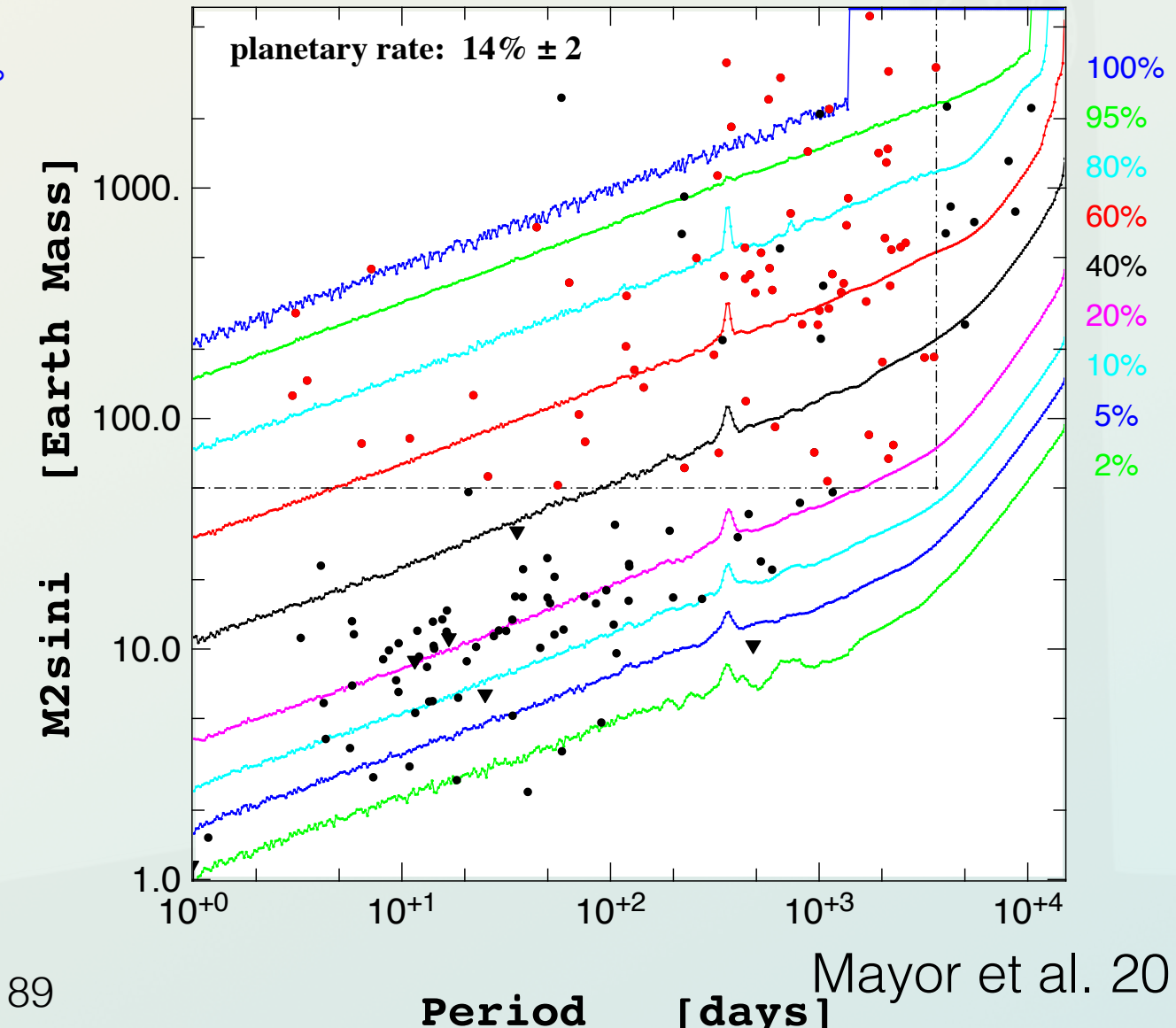
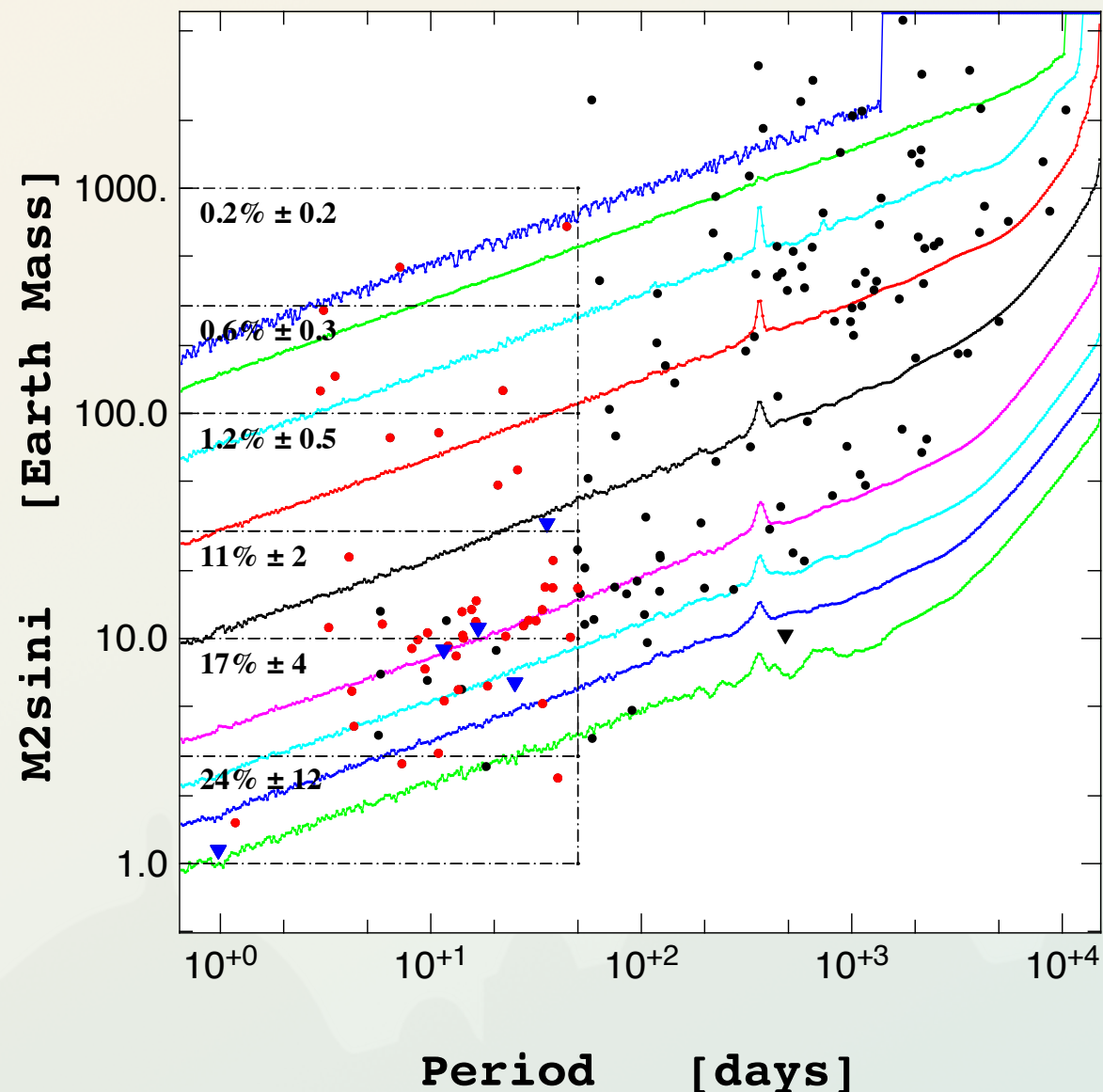
- HARPS (3.6m tel, Chile): 1 m/s stability, 0.5 m/s precision
- HIRES (10m tel, Hawai'i): 2 m/s stability, 1 m/s precision
- ESPRESSO (8m tel, Chile), 0.3 m/s stability, 0.2 m/s precision
- SOPHIE (2m tel, France), 2 m/s stability, 1 m/s precision
- CARMENES (4m tel, Spain), 1 m/s stability, 1 m/s precision

METALLICITY CORRELATION

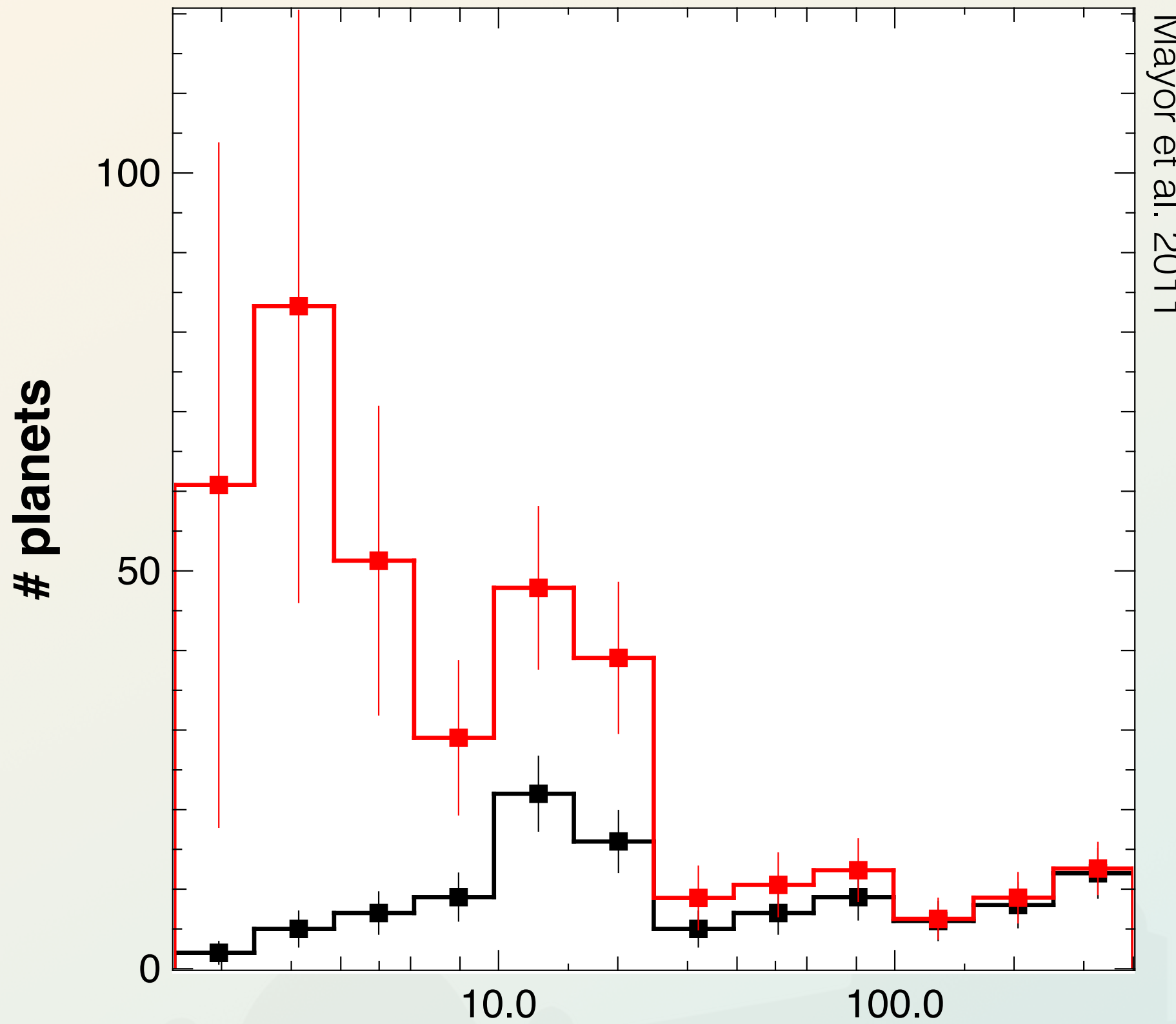


OCCURENCE RATES

Mass limits	Period limit	Planetary rate based on published planets	Planetary rate including candidates	Comments
$> 50 M_{\oplus}$	< 10 years	13.9 ± 1.7 %	13.9 ± 1.7 %	Gaseous giant planets
$> 100 M_{\oplus}$	< 10 years	9.7 ± 1.3 %	9.7 ± 1.3 %	Gaseous giant planets
$> 50 M_{\oplus}$	< 11 days	0.89 ± 0.36 %	0.89 ± 0.36 %	Hot gaseous giant planets
Any masses	< 10 years	65.2 ± 6.6 %	75.1 ± 7.4 %	All "detectable" planets with $P < 10$ years
Any masses	< 100 days	50.6 ± 7.4 %	57.1 ± 8.0 %	At least 1 planet with $P < 100$ days
Any masses	< 100 days	68.0 ± 11.7 %	68.9 ± 11.6 %	F and G stars only
Any masses	< 100 days	41.1 ± 11.4 %	52.7 ± 13.2 %	K stars only
$< 30 M_{\oplus}$	< 100 days	47.9 ± 8.5 %	54.1 ± 9.1 %	Super-Earths and Neptune-mass planets on tight orbits
$< 30 M_{\oplus}$	< 50 days	38.8 ± 7.1 %	45.0 ± 7.8 %	As defined in Lovis et al. (2009)



OCCURENCE RATES



Mayor et al. 2011



UNIVERSITY OF
BIRMINGHAM

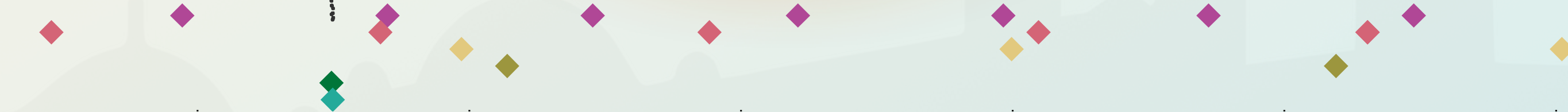
AMAURY TRIAUD
PHYSIC WEST G32
A.TRIAUD@BHAM.AC.UK
OFFICE HOURS: MON 1-2PM
VEVOX.APP 137-795-664

DETECTION METHODS

PHOTOMETRY

space ground

1b 1c 1d 1e 1f 1g 1h



RADIAL VELOCITY

We have a problem with $\sin i$:

$$\begin{aligned} V_{\text{rad}} &= \frac{2\pi a}{T} \frac{\sin i}{\sqrt{1-e^2}} [\cos(f+\omega) + e \cos \omega] \\ &= K [\cos(f+\omega) + e \cos \omega] + \gamma \end{aligned}$$

3.9

$$K_1 = \frac{m_2}{m_1 + m_2} \frac{2\pi}{T} \frac{a \sin i}{\sqrt{1-e^2}}$$

3.11

$$K_2 = \frac{m_1}{m_1 + m_2} \frac{2\pi}{T} \frac{a \sin i}{\sqrt{1-e^2}}$$

3.13

$$f(m_2) = \frac{m_2^3 \sin^3 i}{(m_1 + m_2)^2} = (1 - e^2)^{3/2} \frac{T K_1^3}{2\pi G}$$

RADIAL VELOCITY

We have a problem with $\sin i$:

This means that only the minimum mass of a planet can be measured.

For binary stars, only the mass ratio can be determined.

If both orbiting object eclipse one another, then i can be determined, and all the radial-velocity equations can be solved to obtain **true masses**. In the case of an eclipsing binary the **absolute masses** are obtained (or dynamical masses). In the case of a transiting planet, the mass is still relative to the stellar mass, unless the planet itself is resolved and K_p is measured which is very rare.

THE TRANSIT METHOD

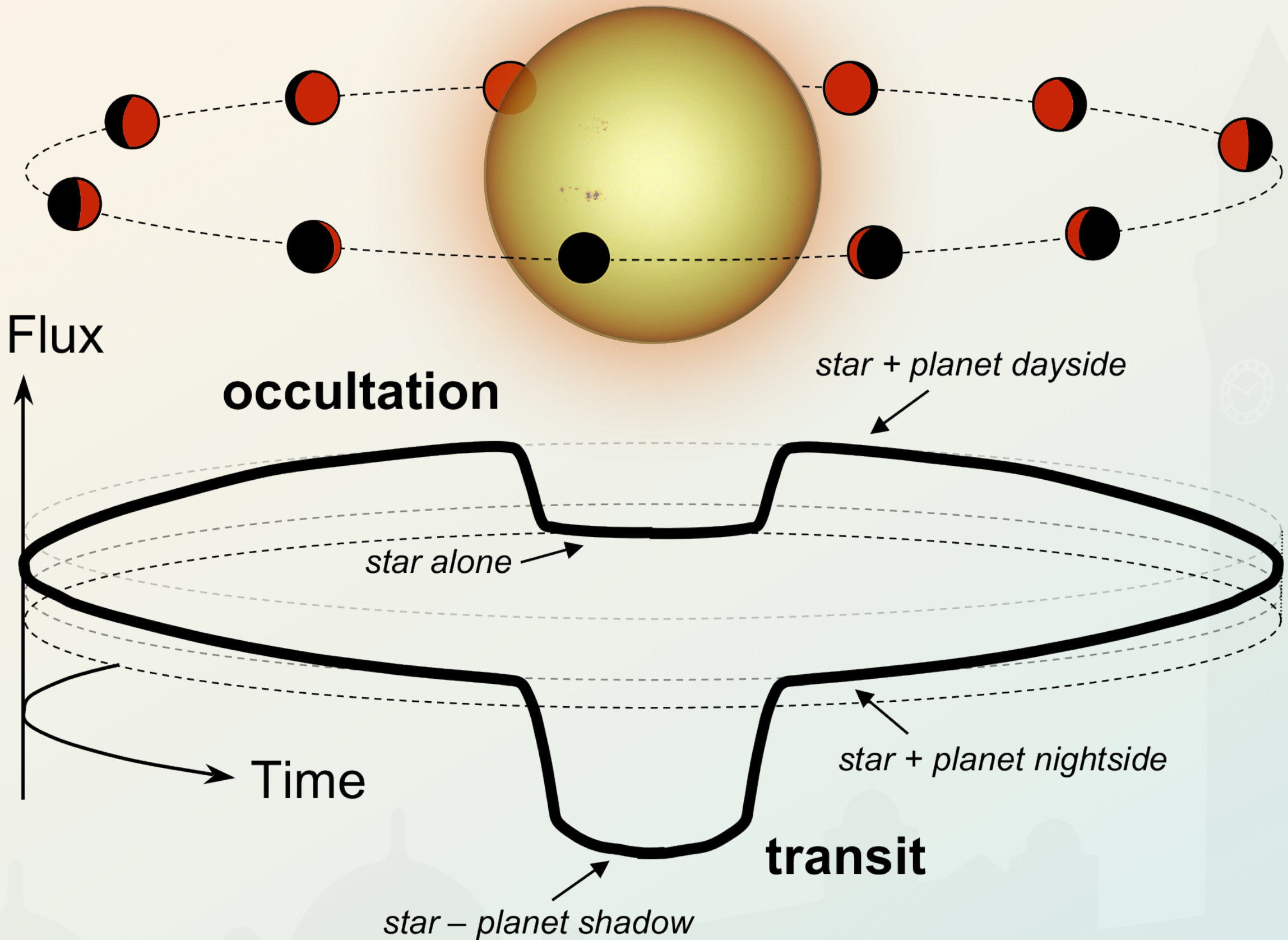
This method is likely the simplest to understand conceptually. There is a star and a planet passes between that star and our telescope. The starlight dims, producing a **transit**.

Although this method is very simple, and could have been used decades before the detection of 51 Peg b in 1995, the first transiting planet, HD 209458b, was only measured in 1999. The planet had first been detected with radial-velocities.

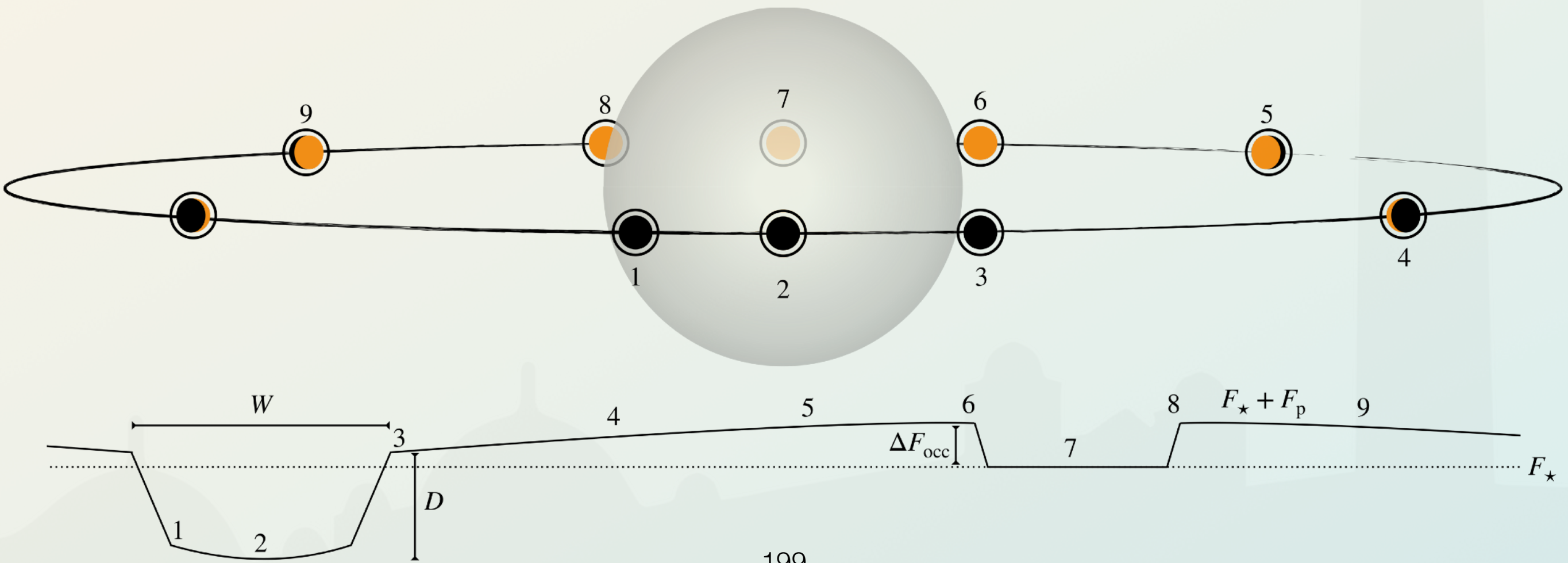
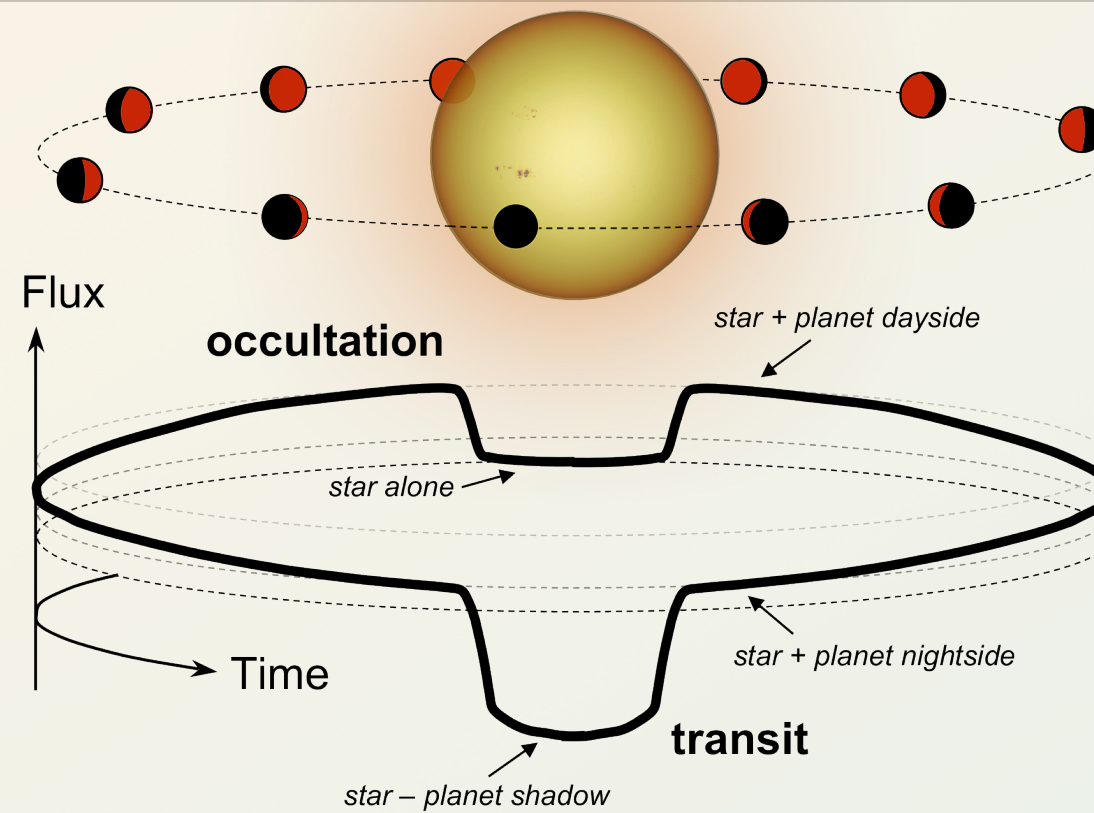
The reason is again, that most people thought gas-giants, the only planets that can practically be detected using ground-based telescopes, were thought to only occupy long orbits, where the probability of transit is vanishingly small.

With the radial-velocity method, there is a signal throughout the orbital phase. For transits, there is only a signal for a tiny fraction of the orbital phase.

THE TRANSIT METHOD



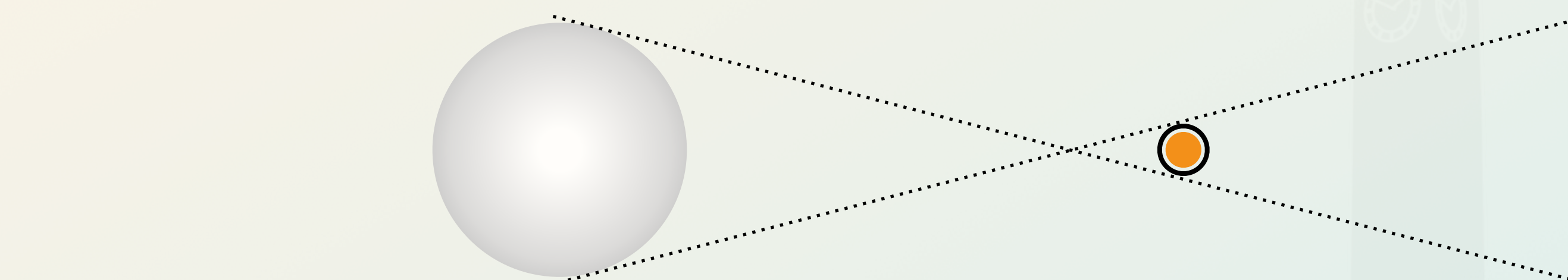
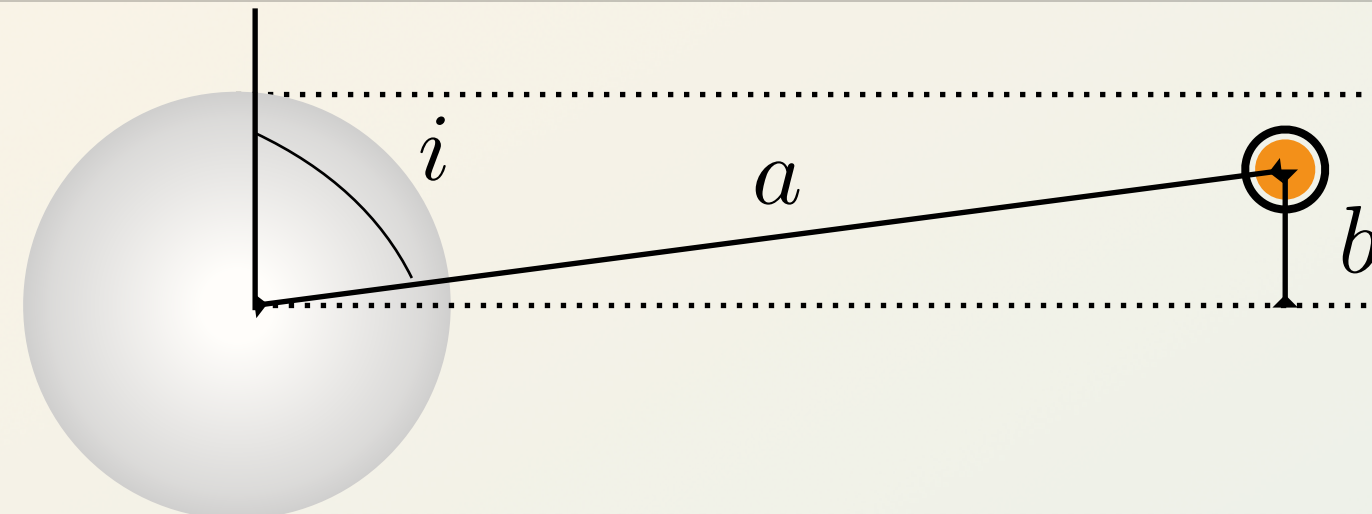
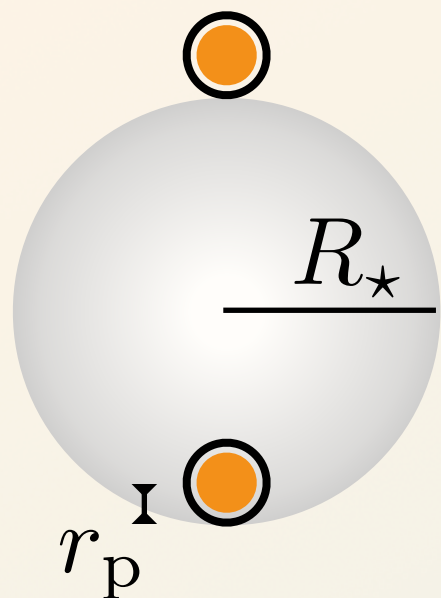
THE TRANSIT METHOD



NOMENCLATURE

transit	a planet passes in front of its host star
eclipse	a star passes in front of another star within the same system
occultation	an object totally disappears behind another one. A planet behind its host star, a far away star behind the Moon etc.
primary [event]	the secondary object passes in front of the primary object
secondary [event]	the primary object passes in front of the secondary object
primary	the more massive, or the brighter of the two objects
superior / inferior conjunction	applies to transiting and non transiting systems

TRANSIT PROBABILITY



Transits happens when:

$$p_{\text{trans}} = \frac{R_\star \pm r_p}{a} \sim \frac{R_\star}{a}$$

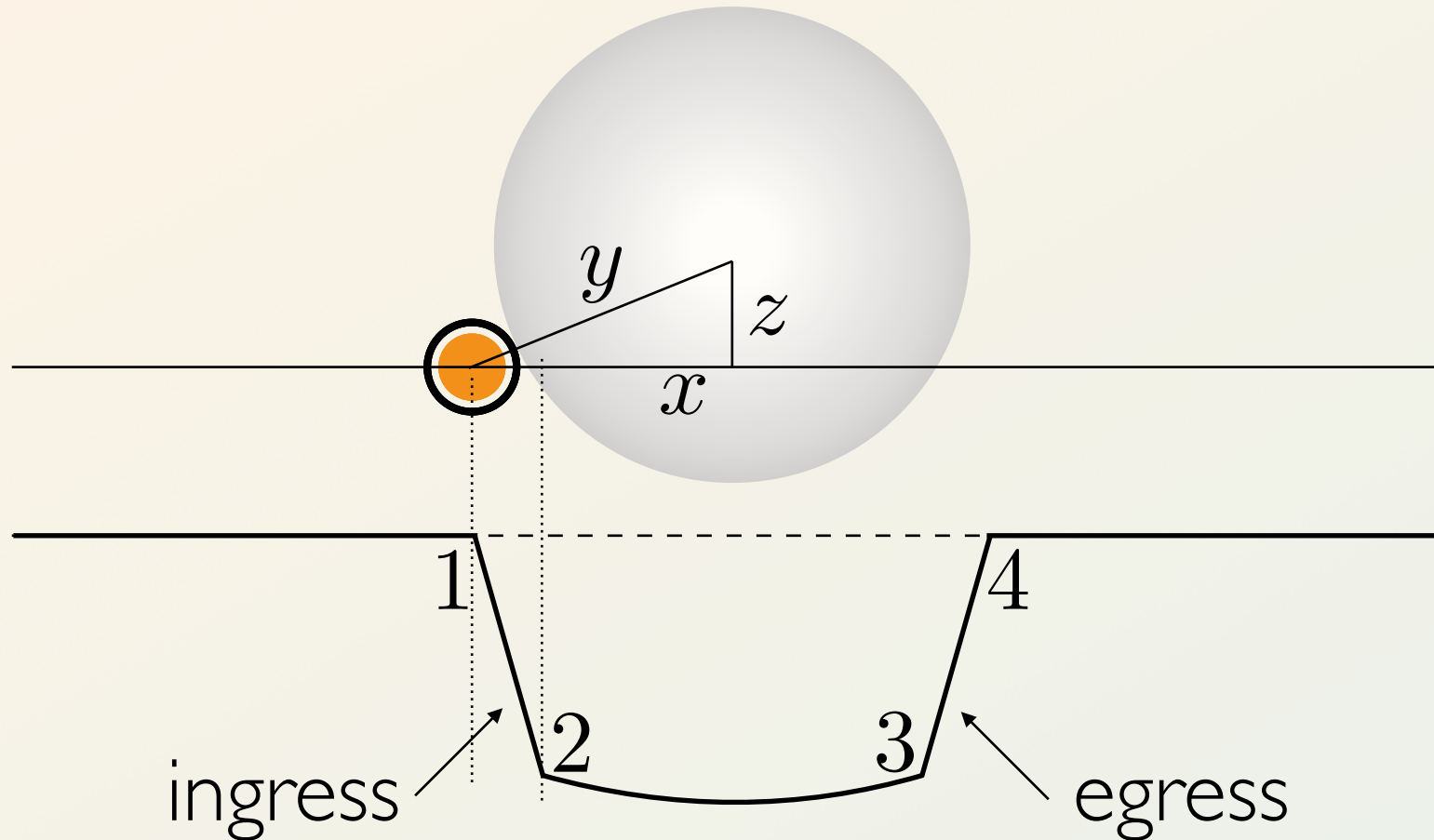
Transits signal depth is

$$D = \frac{F_{\text{out}} - F_{\text{in}}}{F_{\text{out}}} \sim \left(\frac{r_p}{R_\star} \right)^2$$

3.14

3.15

SCALED RADIUS



geometrically, the **scaled radius** is:

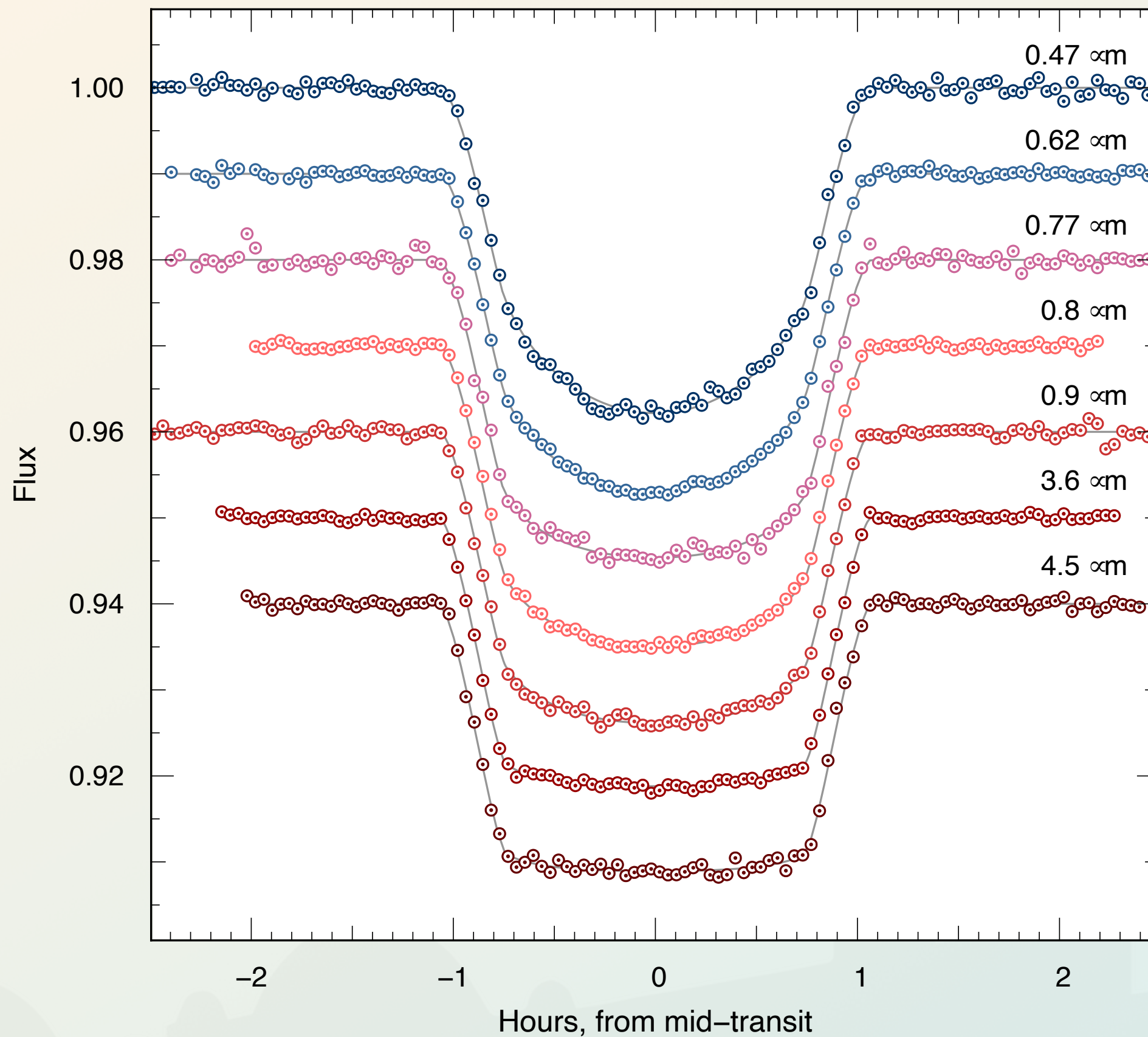
$$\frac{R_\star}{a} = \frac{W}{T} \frac{\pi}{\sqrt{(1 + \sqrt{D})^2 - b^2}} \frac{1 + e \sin \omega}{\sqrt{1 - e^2}}$$

can also get r_p/a

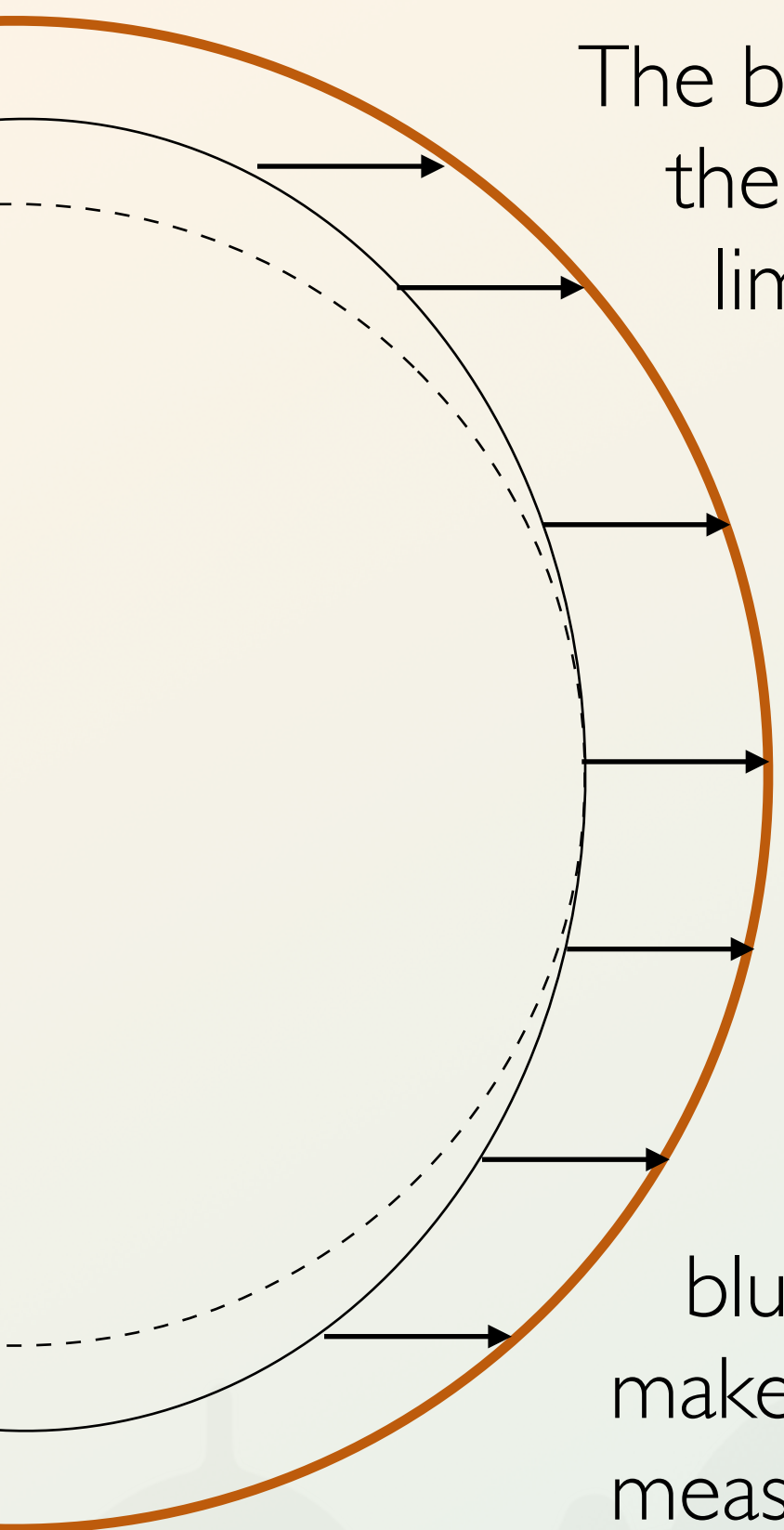
useful for tides!

3.16

TRANSITS IN MULTIPLE WAVELENGTHS



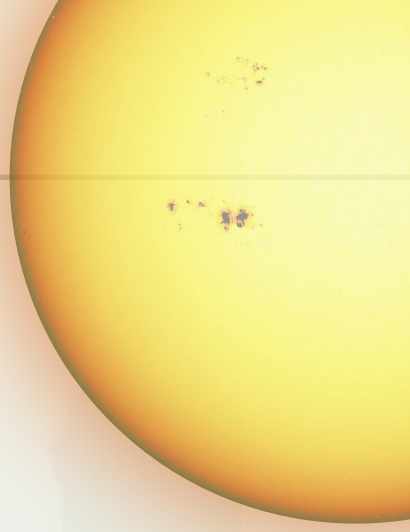
LIMB DARKENING



The brightness of a star is dimmer near the edge compared to the centre. This is limb darkening. This effect is wavelength dependent.

Near the edge of a star, the emerging flux comes from a shallower region of the star. Since temperature is hotter deeper into the star, light from the edge has a colder black body and thus appears darker.

Limb darkening is typically more pronounced in bluer wavelengths. Accounting for limb darkening makes the transit shape rounder, and can refine the measure of b , the impact parameter.



LIMB DARKENING

There are several proposed laws for limb darkening, but the most used is the quadratic limb darkening law.

Each law defines how brightness I changes as a function of μ , the distance from the centre of the stellar disc

$$\mu = \sqrt{1 - (X^2 + Y^2)}$$

3.17

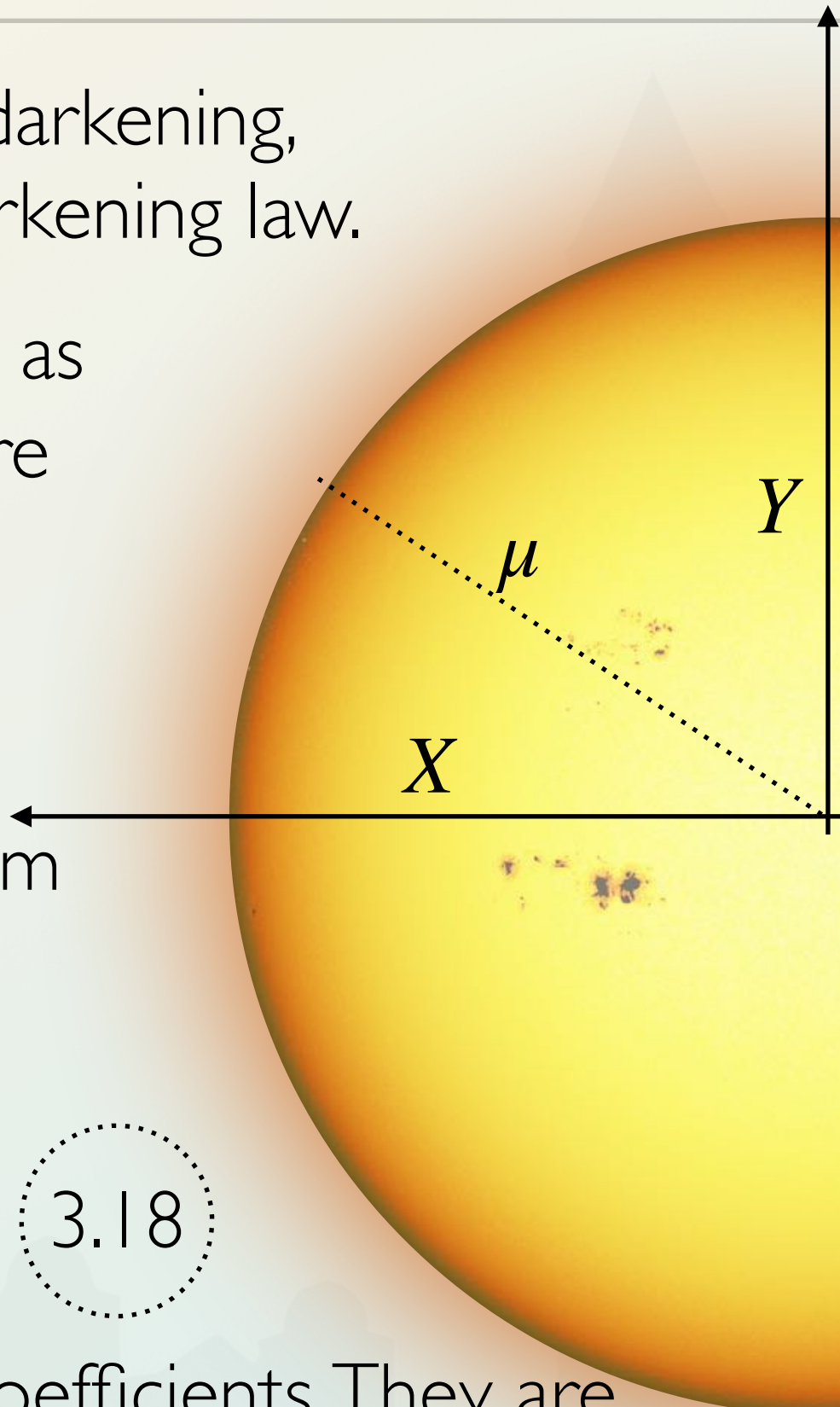
The equation is normalised to the maximum brightness (near the centre of the disc)

The quadratic law:

$$I = 1 - u_a(1 - \mu) - u_b(1 - \mu)^2$$

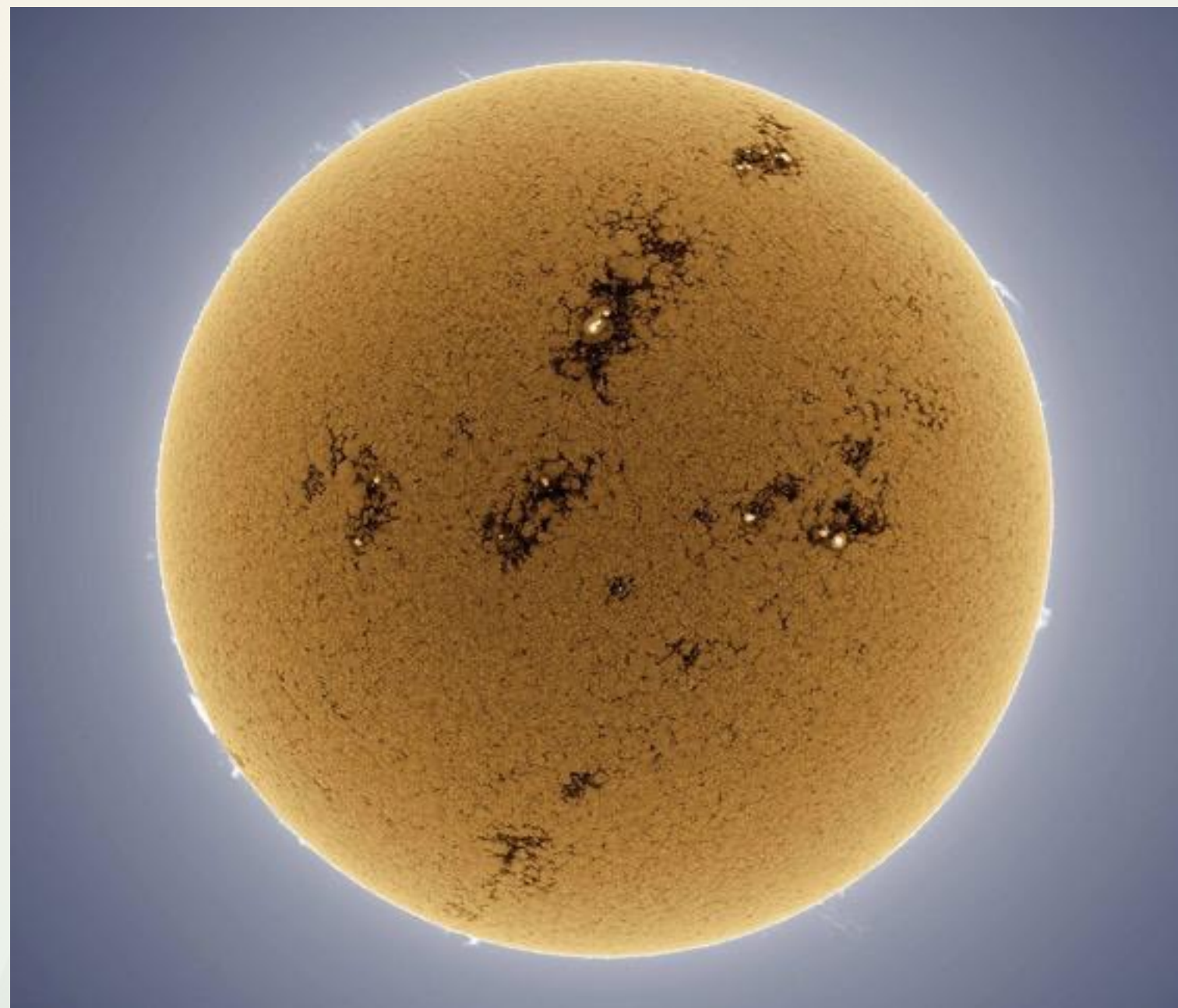
3.18

Where u_a and u_b are the limb darkening coefficients. They are calculated theoretically, and can be fitted to the light curve



LIMB BRIGHTENING

In certain wavelengths, temperature increases with distance from the centre of the star. This will create a limb brightening. Typically this will be in emission lines. For instance Ca H & K, which track chromospheric activity.

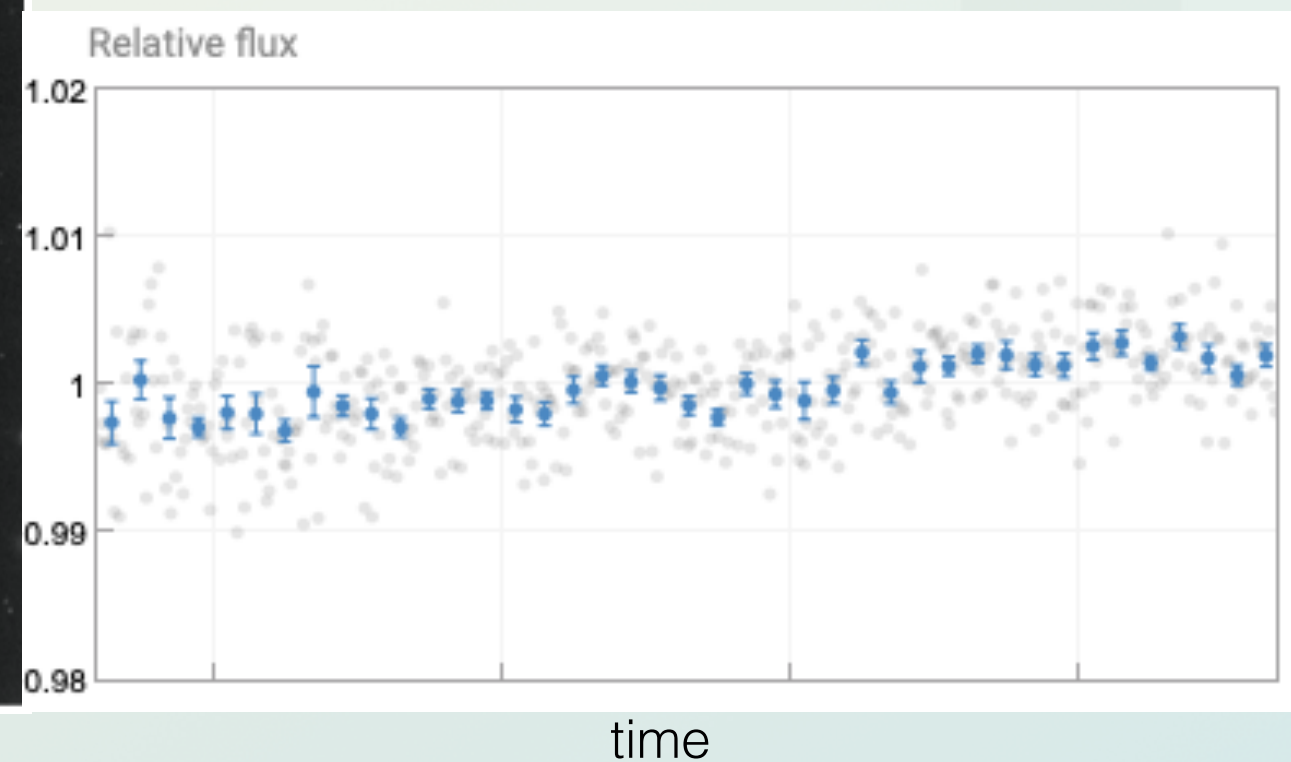


HOW TO DO TRANSIT PHOTOMETRY

The transit method relies on making snapshots of the sky repeatedly. Each star has its brightness measured, and the target star is compared to all others to produce a relative flux light curve.



It is in that light curve that transits are searched for. The observing strategy depends on the instrument the type of planets that are sought.

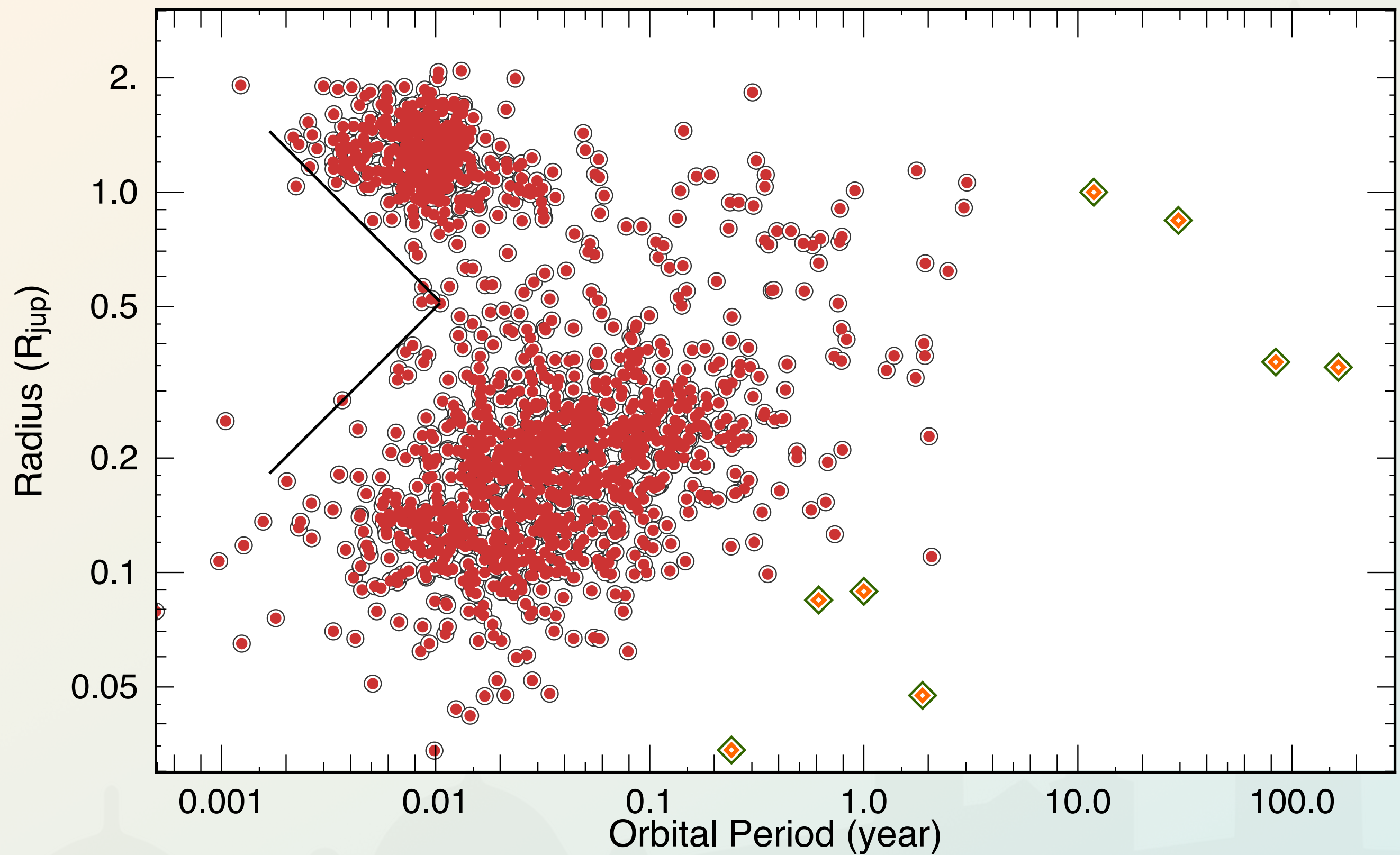


CURRENT & PAST MISSIONS

Typical precisions of ground & space-based photometric surveys for a V=10 magnitude star for one hour.

- WASP: 10cm, 30 million stars surveyed, 1% precision, 200 planets discovered
- Ganymede: 1m, pointed telescope, 120ppm precision
- Kepler: 1m, 200,000 stars observed, 50ppm precision
2500 planets discovered, faint stars mostly
- TESS: 10cm; 2 million stars monitored, 200ppm precision,
500 planets discovered, 6500 candidates.
- CHEOPS: 30cm, pointed telescope, 50ppm precision
- JWST: 6.5m, pointed telescope, 10ppm precision?

RESULTS



Article

A remnant planetary core in the hot-Neptune desert

<https://doi.org/10.1038/s41586-020-2421-7>

Received: 29 October 2019

Accepted: 20 March 2020

Published online: 1 July 2020

A list of authors and their affiliations appears at the end of the paper.

The interiors of giant planets remain poorly understood. Even for the planets in the Solar System, difficulties in observation lead to large uncertainties in the properties of planetary cores. Exoplanets that have undergone rare evolutionary processes provide a route to understanding planetary interiors. Planets found in and near the typically barren hot-Neptune ‘desert’^{1,2} (a region in mass–radius space that contains few planets) have proved to be particularly valuable in this regard. These planets include HD149026b³, which is thought to have an unusually massive core, and recent discoveries such as LTT9779b⁴ and NGTS-4b⁵, on which photoevaporation has removed a substantial part of their outer atmospheres. Here we report observations of the planet TOI-849b, which has a radius smaller than Neptune’s but an anomalously large mass of $39.1^{+2.7}_{-2.6}$ Earth masses and a density of $5.2^{+0.7}_{-0.8}$ grams per cubic centimetre, similar to Earth’s. Interior-structure models suggest that any gaseous envelope of pure hydrogen and helium consists of no more than $3.9^{+0.8}_{-0.9}$ per cent of the total planetary mass. The planet could have been a gas giant before undergoing extreme mass loss via thermal self-disruption or giant planet collisions, or it could have avoided substantial gas accretion, perhaps through gap opening or late formation⁶. Although photoevaporation rates cannot account for the mass loss required to reduce a Jupiter-like gas giant, they can remove a small (a few Earth masses) hydrogen and helium envelope on timescales of several billion years, implying that any remaining atmosphere on TOI-849b is likely to be enriched by water or other volatiles from the planetary interior. We conclude that TOI-849b is the remnant core of a giant planet.

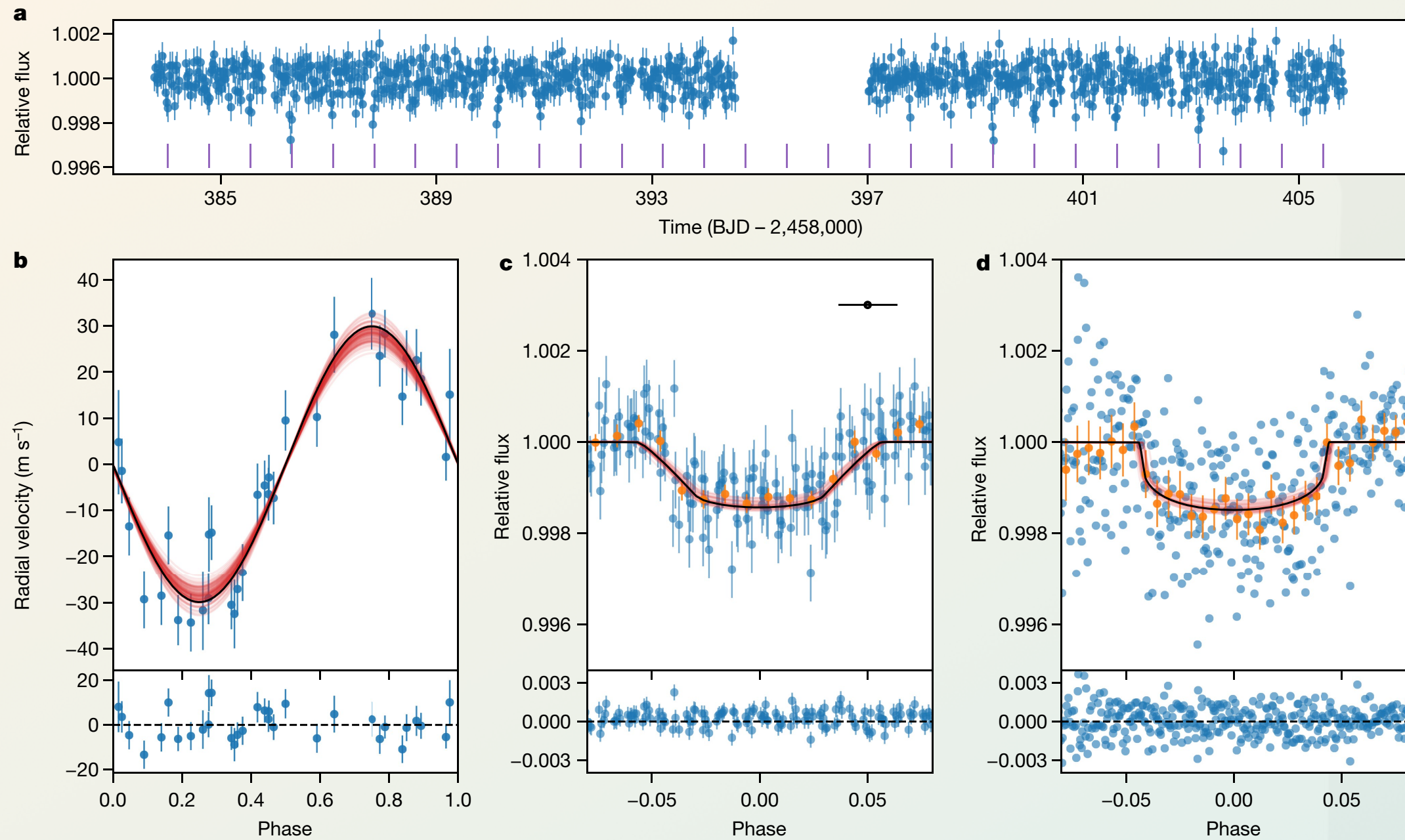
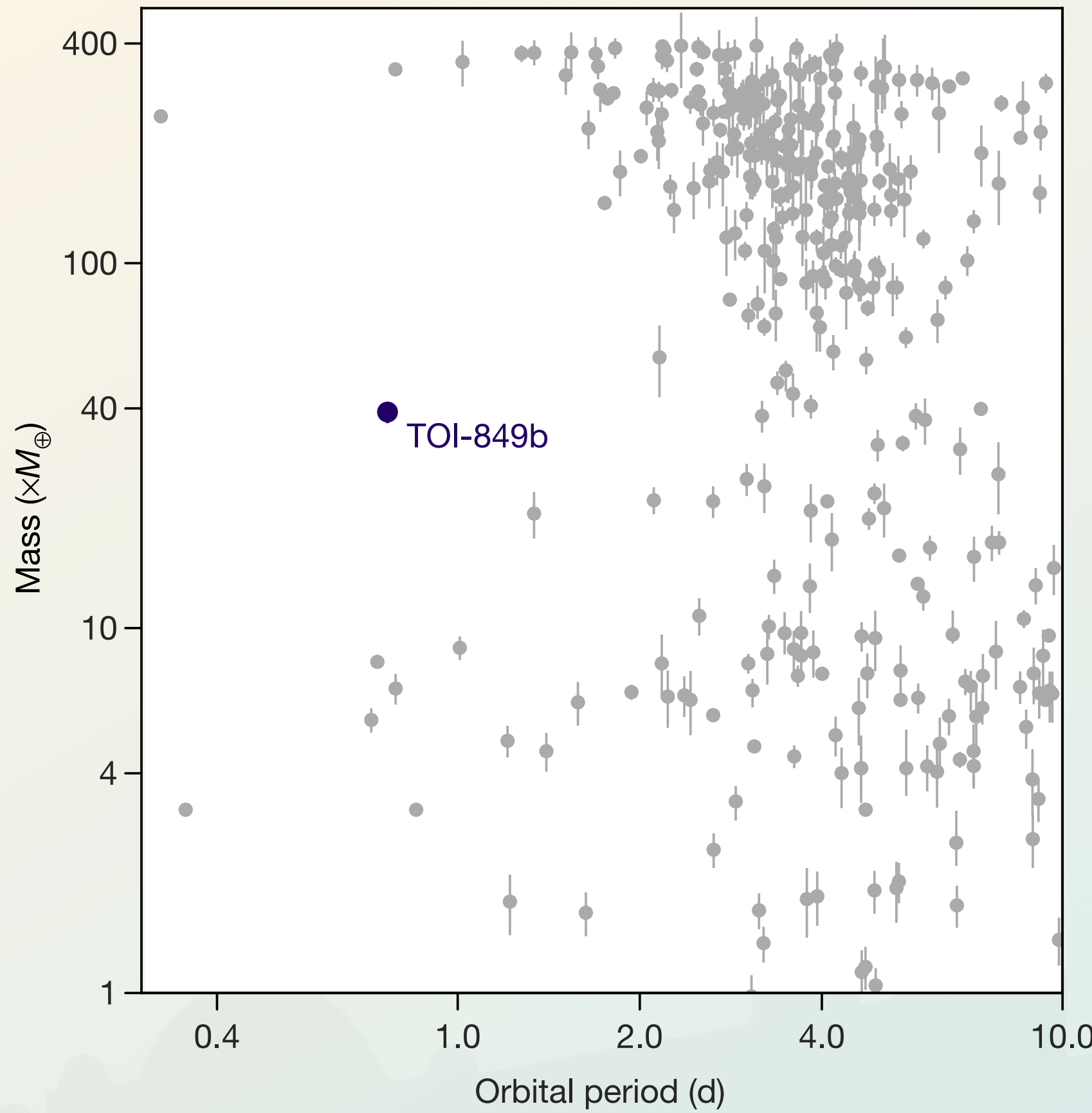


Fig. 1 | Best-fitting model to the TESS, HARPS and NGTS data. **a**, TESS light curve with transit times marked as vertical lines. BJD, barycentric Julian date. **b**, Phase-folded HARPS data (blue symbols) and best-fitting model (black line), with residuals shown in the bottom panel. Several models randomly drawn from the Markov chain Monte Carlo output are shown in red. **c**, Phase-folded TESS 30-min cadence data (blue symbols) and binned to 0.01 in phase (orange symbols, nine individual points per bin), with models as in **b** and residuals shown in the bottom panel. The horizontal error bar shows the TESS cadence. **d**, Phase-folded NGTS data binned to 1 min (blue symbols, 46 individual points

per bin) and to 0.01 in phase (orange symbols, 777 individual points per bin). We plot the binned NGTS data to aid visualization but we fit the models to the full dataset. Models are as in **b**, with residuals in the bottom panel. The cadence is negligible at this scale. Data from Las Cumbres Observatory Global Telescope were also used and are shown in Extended Data Fig. 1. Vertical error bars of individual points show one standard deviation. In the case of binned measurements, points and error bars show the weighted mean and its standard error, respectively.

TOI-849B - ARMSTRONG ET AL. 2020



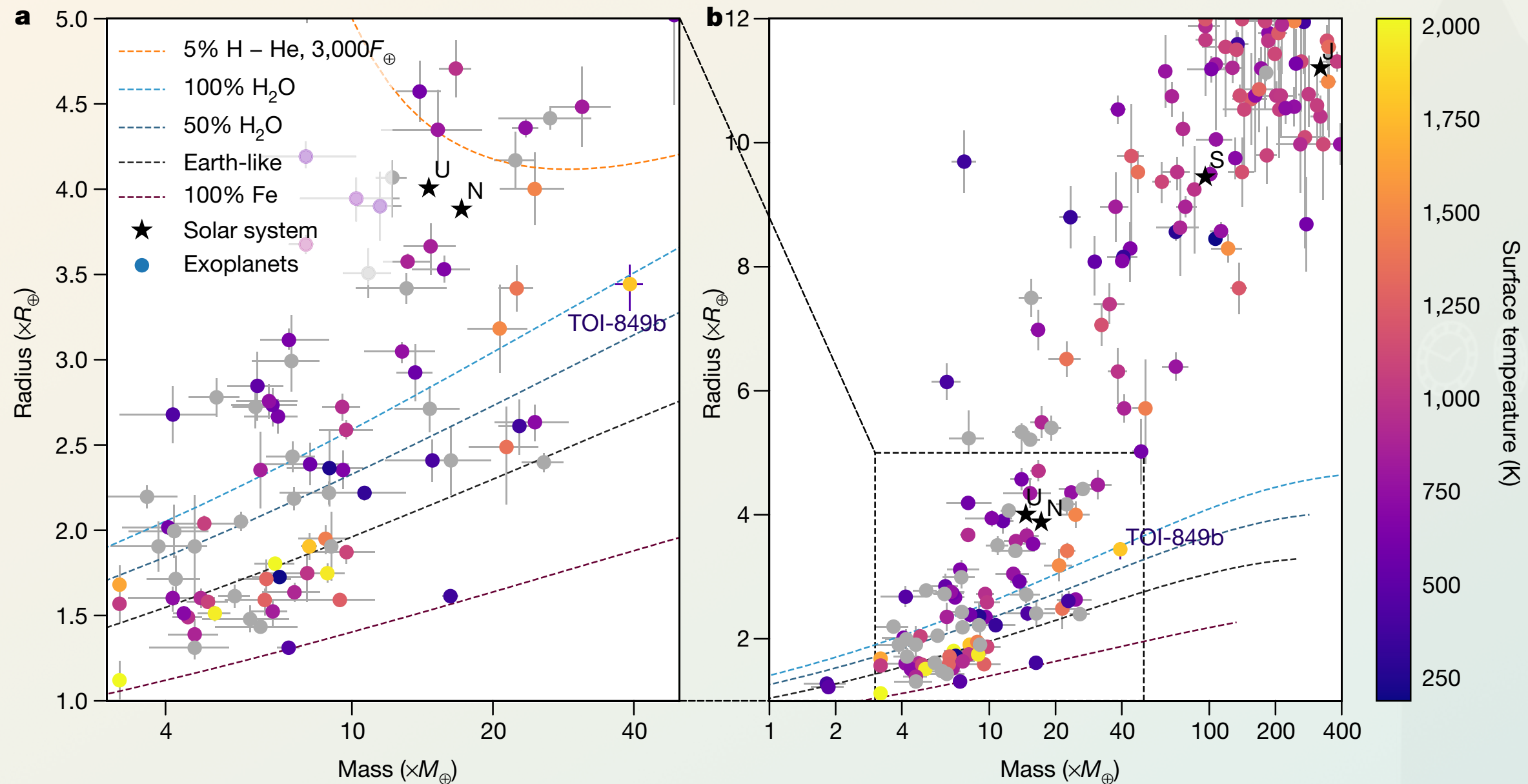
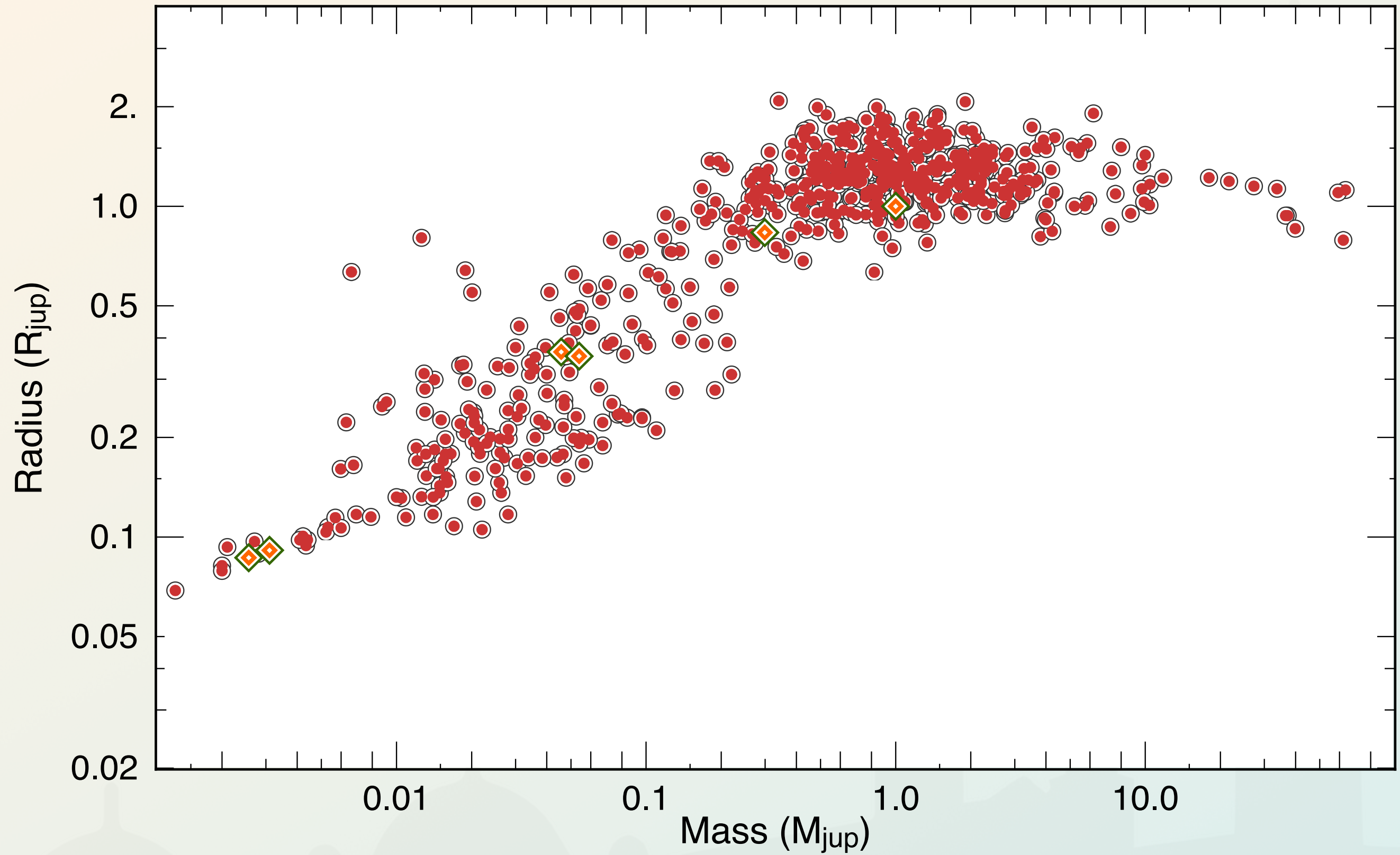


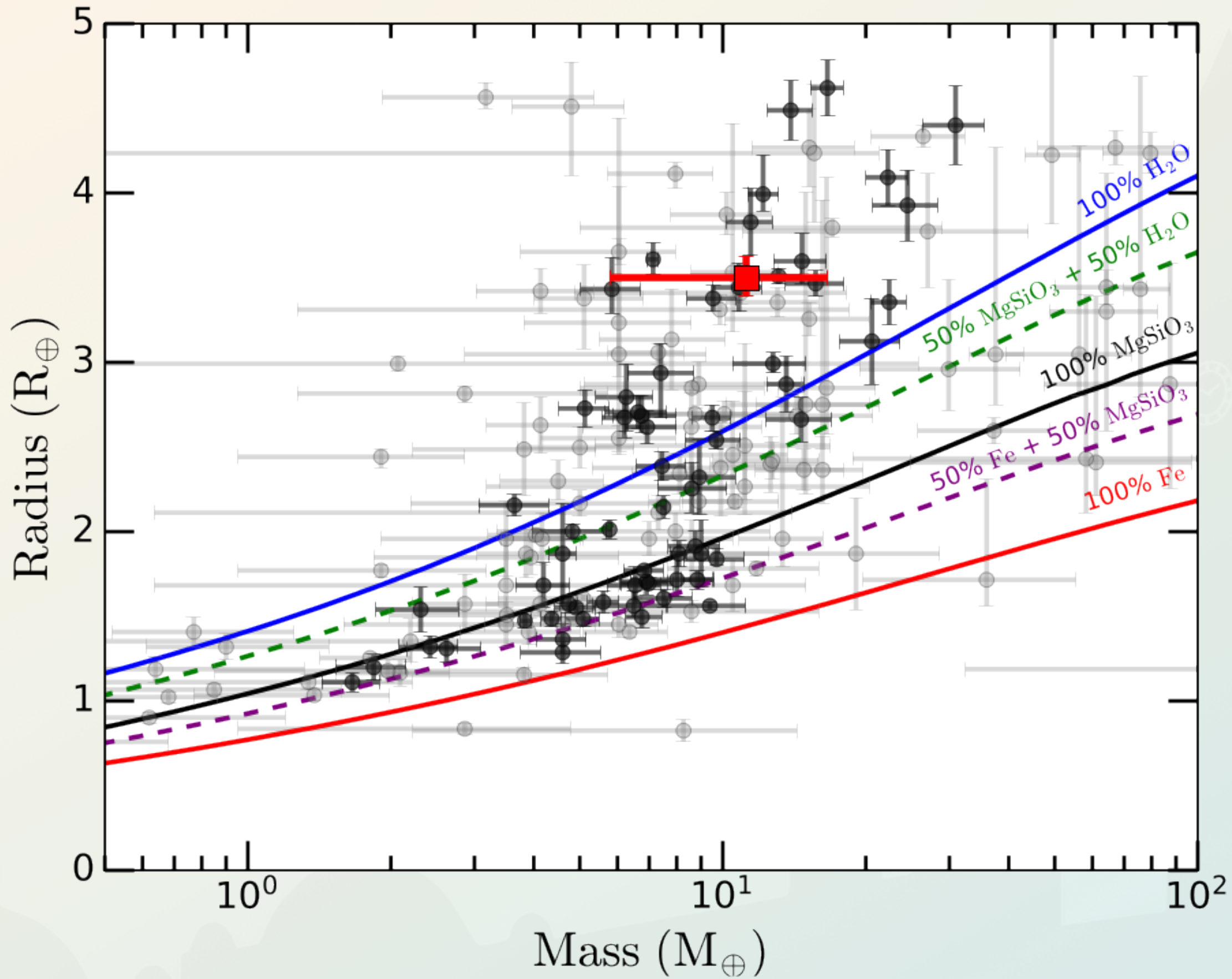
Fig. 2 | Mass–radius diagram of known exoplanets from the NASA exoplanet archive. **a, b**, The archive (<https://exoplanetarchive.ipac.caltech.edu/>) was accessed on 20 January 2020. Planets are coloured according to calculated equilibrium temperature and are grey otherwise. Planets with mass determinations better than 4σ are shown. Planets without a reported mass

determination were excluded³⁰. Composition tracks³¹ are shown as dashed lines, with an additional 5% H–He track at an irradiation level similar to that of TOI-849b. U, N, S and J denote the Solar System planets Uranus, Neptune, Saturn and Jupiter, respectively. F_{\oplus} represents the average solar irradiation received by Earth. **a**, Zoom of **b**. All error bars show one standard deviation.

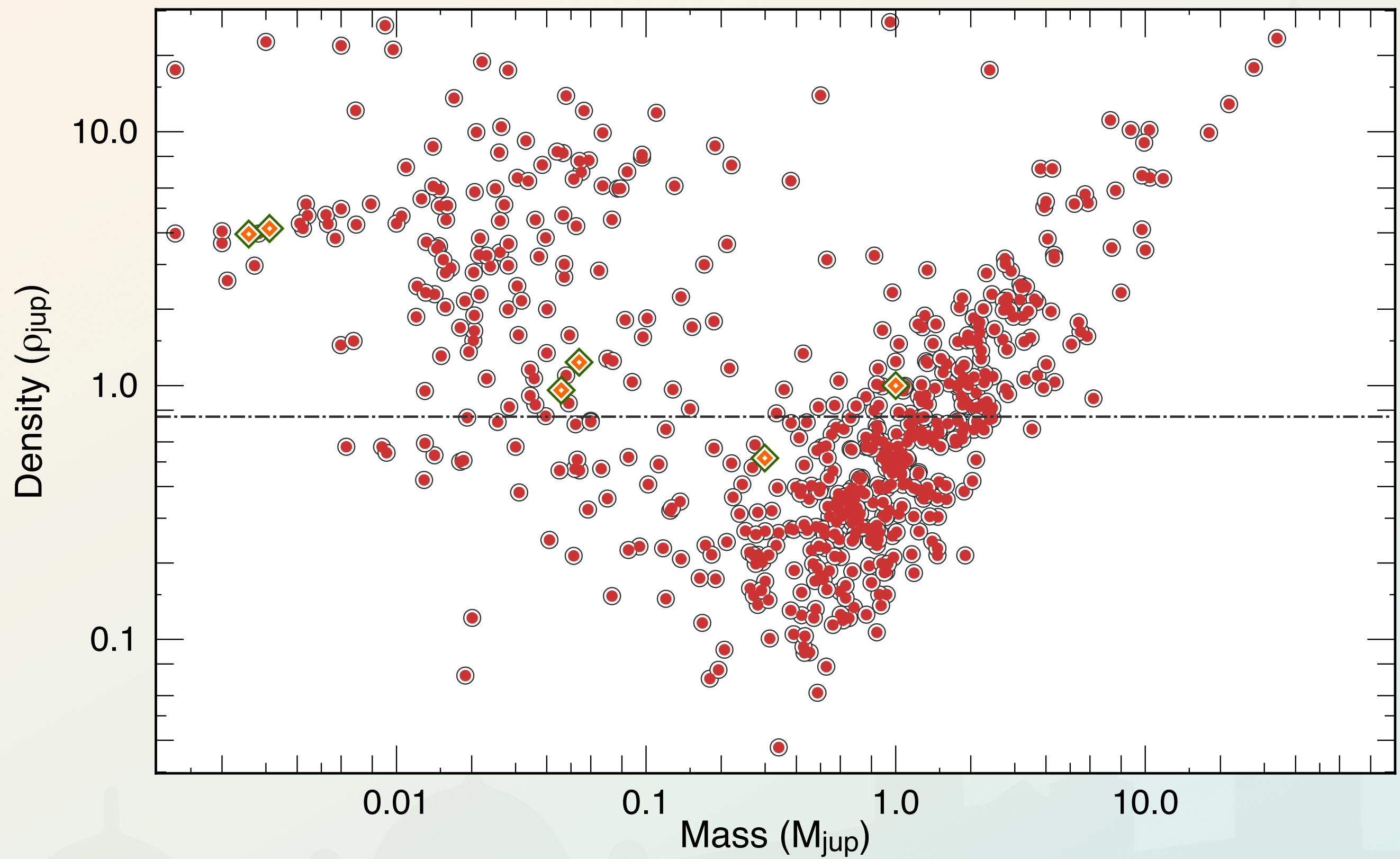
RESULTS



RESULTS

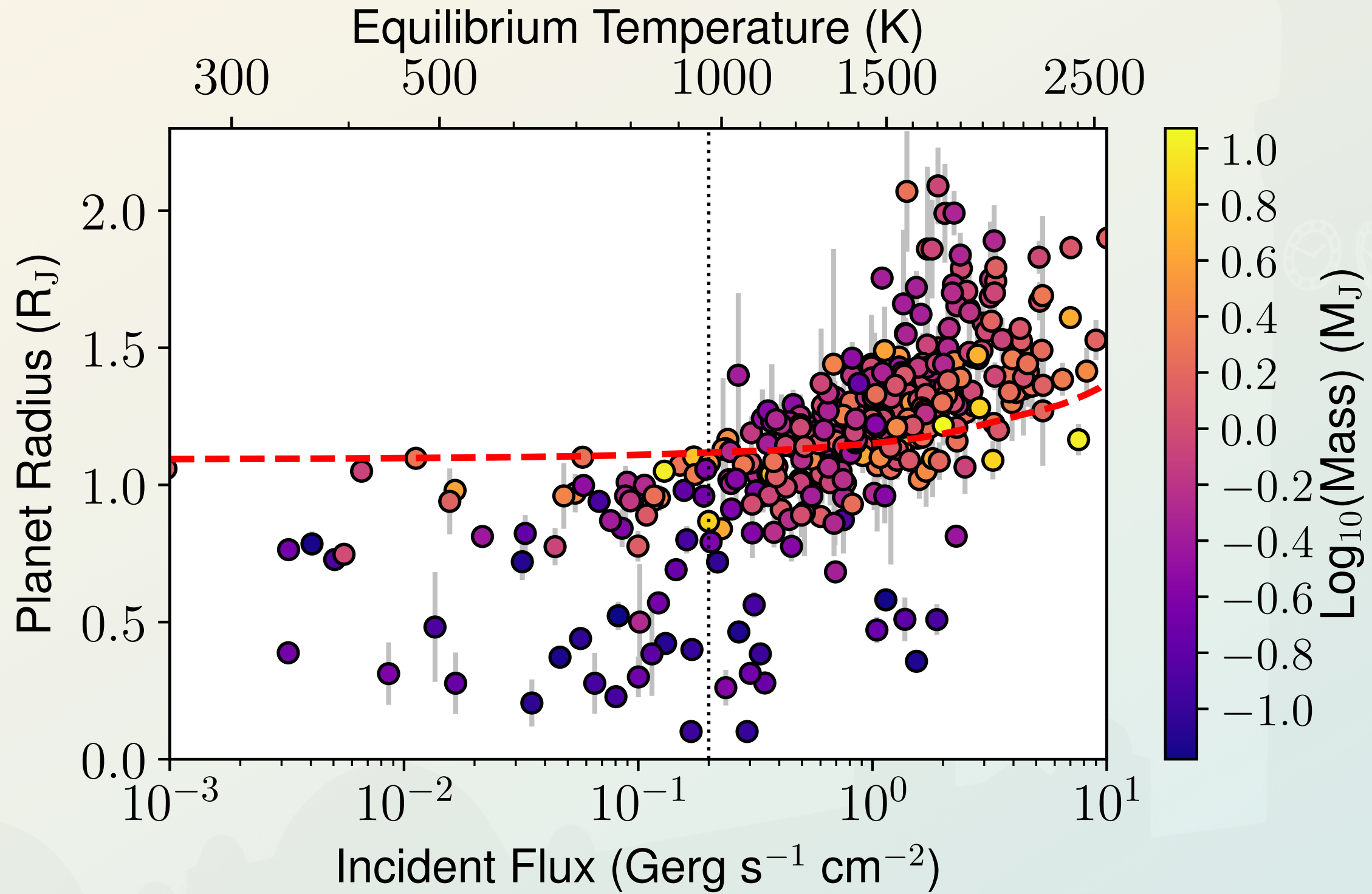


RESULTS



RESULTS: RADIUS INFLATION

Hot Jupiters near their star appear inflated, compared to gas giants at longer distances. Inflation scales with stellar irradiation (incident flux).



MEASURABLE QUANTITIES

Thanks to transits we measure the stellar density

$$\rho_\star \rightarrow \frac{M_\star}{R_\star^3} + \frac{m_p}{R_\star^3} = \left(\frac{a}{R_\star} \right)^3 \frac{4\pi^2}{GP^2}$$

3.19

Now, let's combine with radial velocities:

we measure $\sin i$, leading to **true masses** (assuming M_\star)

Starting from 3.13, we also obtain the planet's gravity (in **absolute**)

$$g = \frac{2\pi}{T} \frac{K_1 \sqrt{1-e^2}}{\sin i} \left(\frac{a}{r_p} \right)^2$$

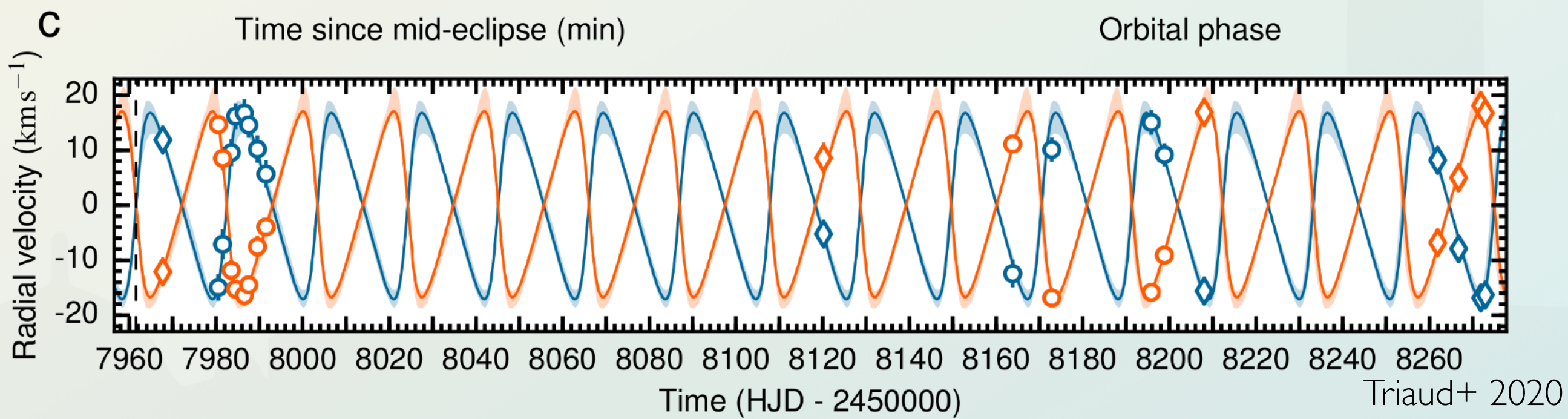
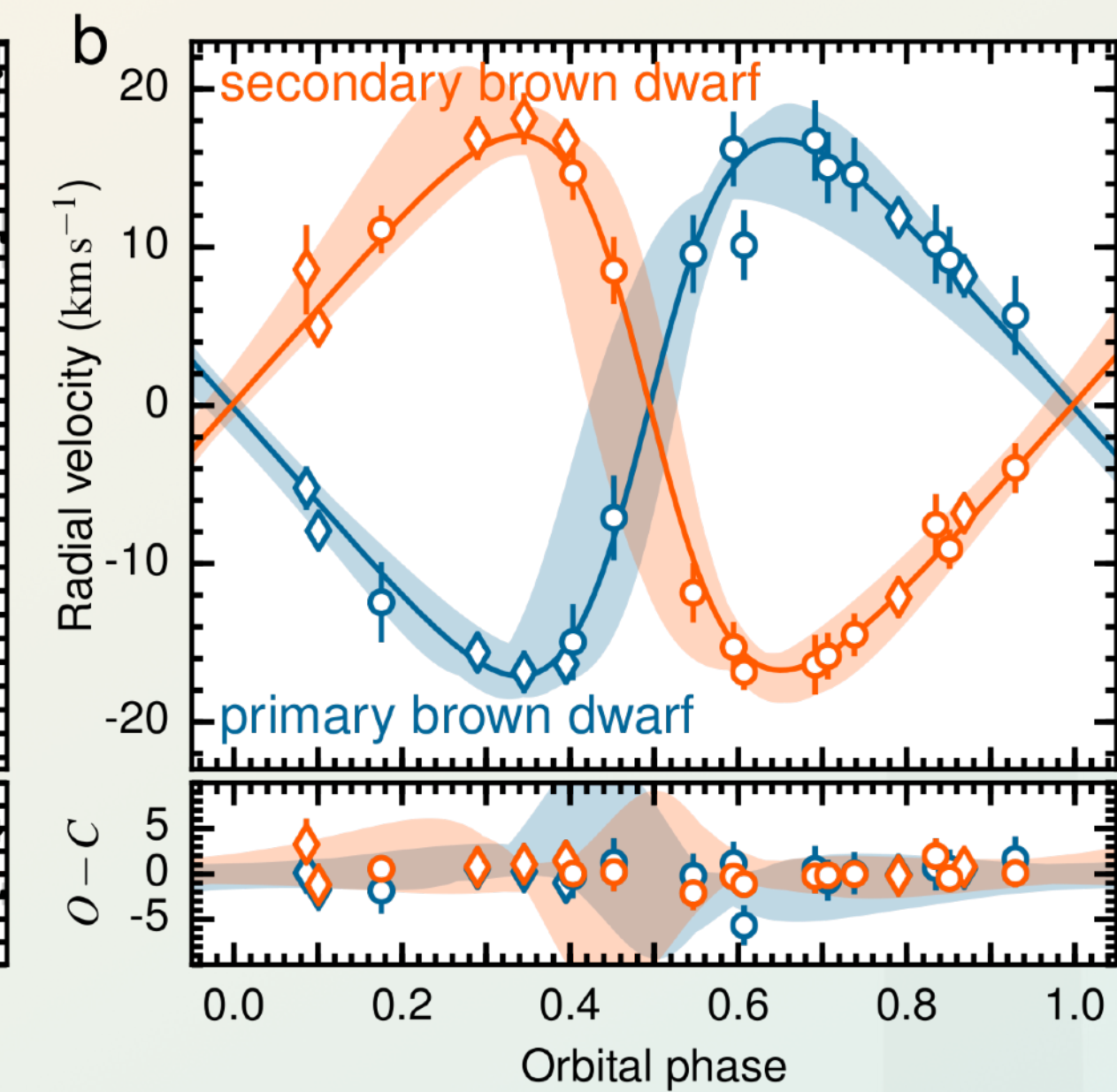
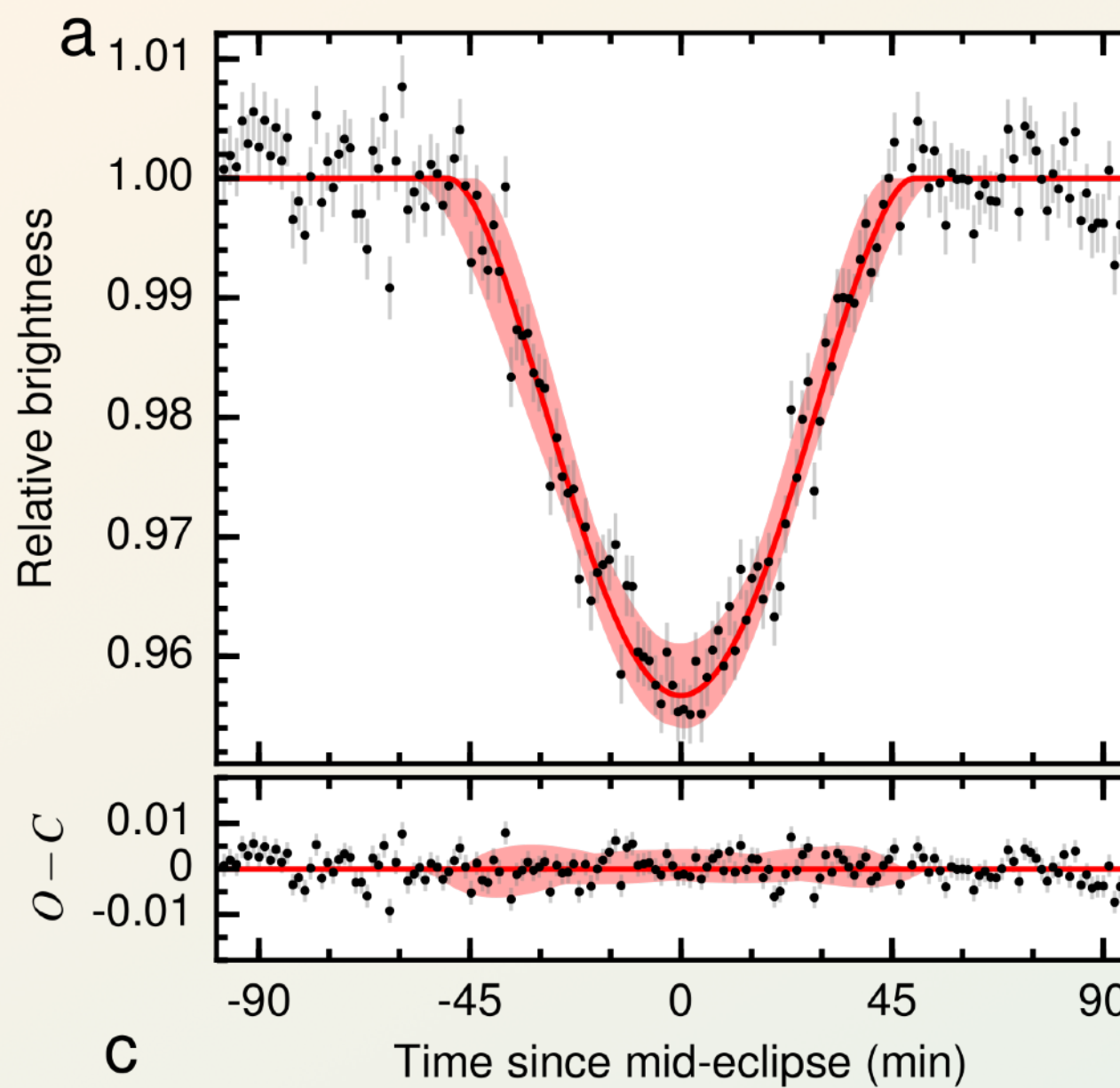
3.20

surface gravity is often expressed as $\log g$, in cgs units.

$$\log g_\oplus \sim 3 \text{ [cgs]} \quad \log g_\odot \sim 4.5 \text{ [cgs]}$$

without M_\star , all other quantities are mass and radius ratios, i.e. they remain relative to the central star's parameters.

ECLIPSING DOUBLE-LINE BINARIES



ABSOLUTE VS RELATIVE PARAMETERS

Contrary to a transit, the eclipse depth of a binary star is not just D since the brightness of the two stars need to be accounted for.

$$D_{\text{pri}} = \frac{(F_1 + F_2) - (\mathcal{A}_{\text{pri}} F_1 + F_2)}{F_1 + F_2} \quad D_{\text{sec}} = \frac{(F_1 + F_2) - (\mathcal{A}_{\text{sec}} F_2 + F_1)}{F_1 + F_2}$$


where \mathcal{A} is the (l- ratio of areas) covered during the eclipse.

Eclipsing binaries for which both eclipses are measured can have their radii measured in **absolute** terms.

If they are also double-lined binaries, then **absolute** masses and radii can be obtained.

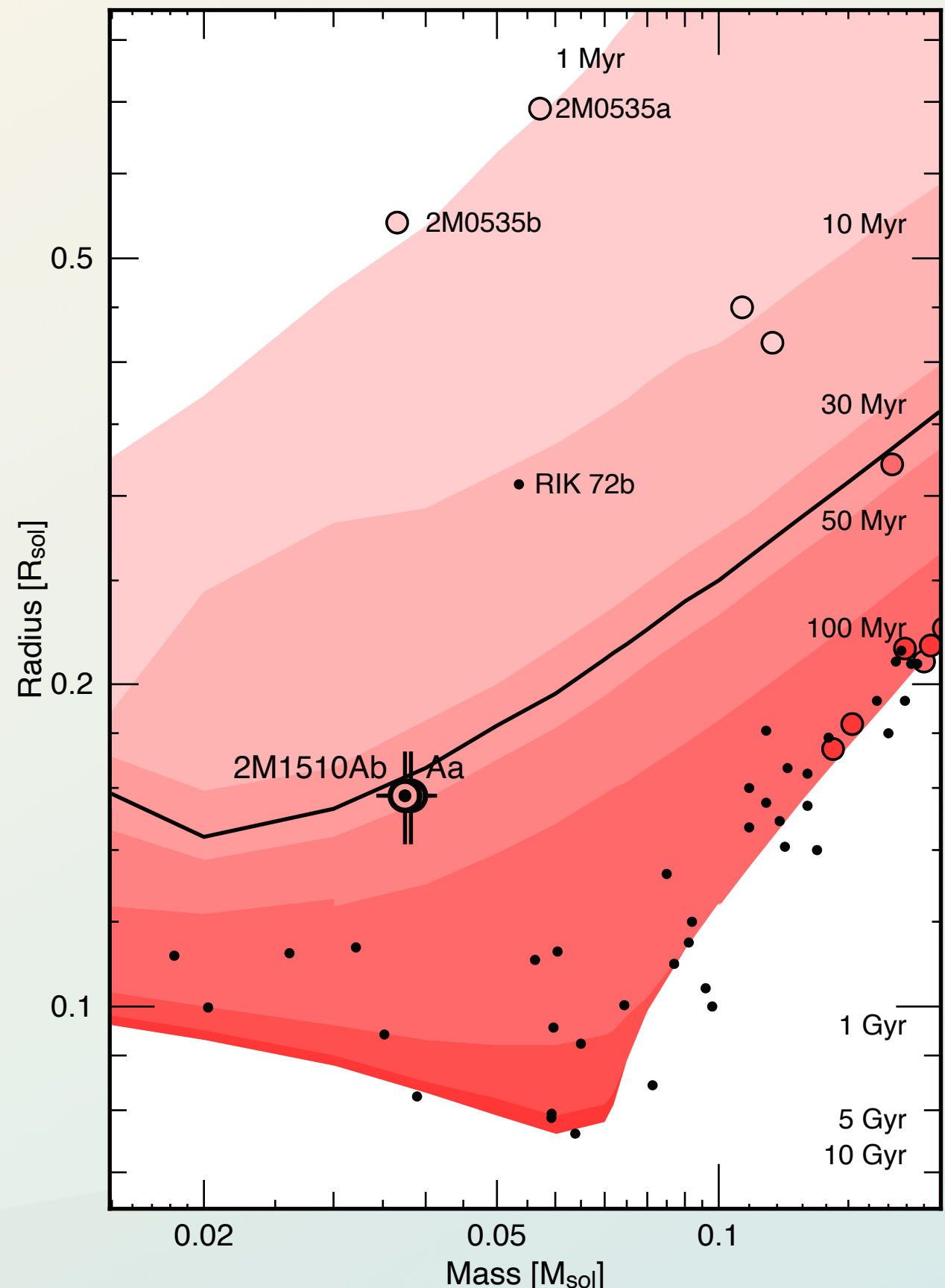
In the vast majority of other situations, only $\log g$ can be estimated in **absolute** (eq. 3.20). Other parameters remain **relative** to the central object's parameters.

ABSOLUTE VS RELATIVE PARAMETERS

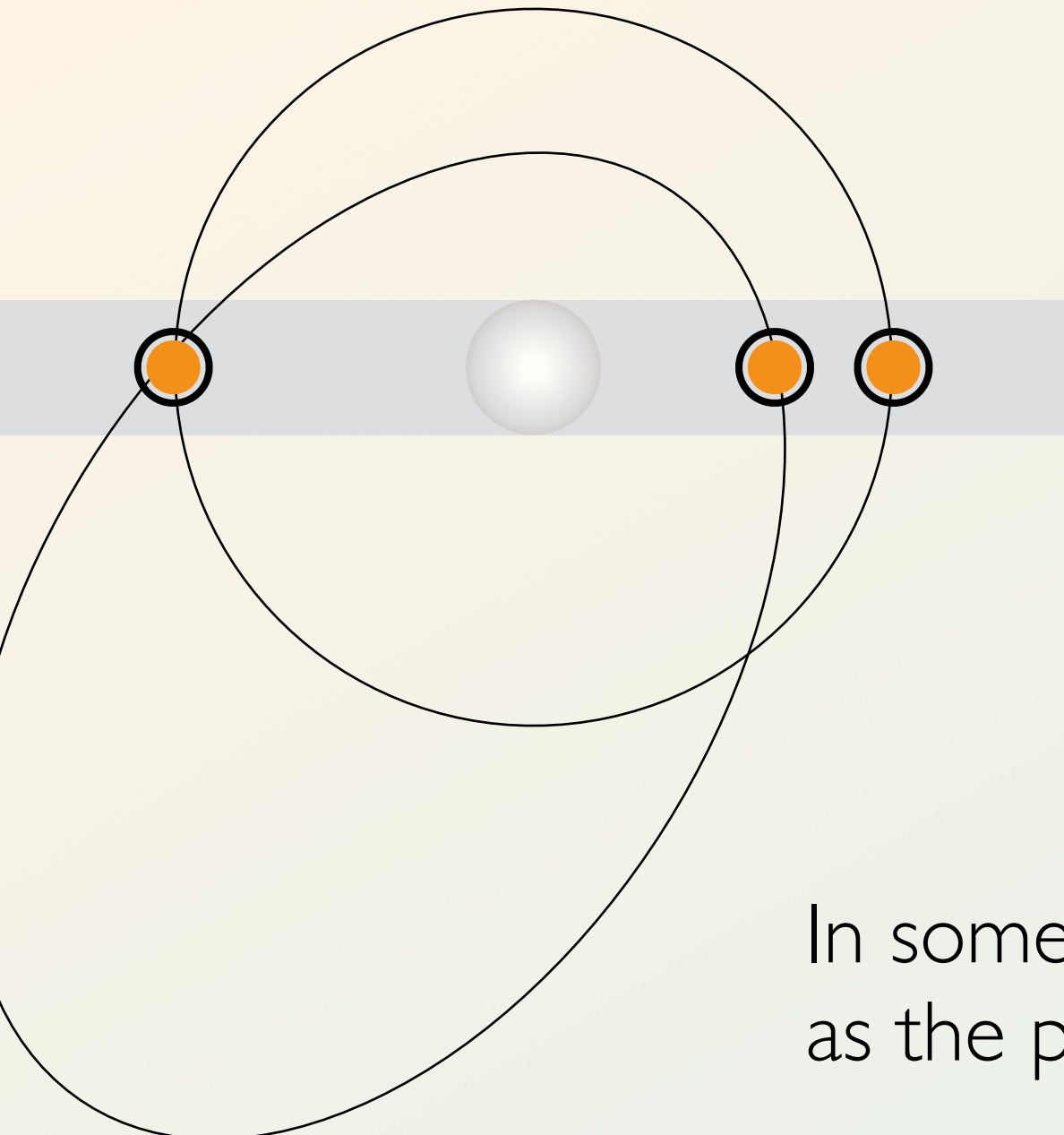
Absolute mass and radius measurements can be compared to stellar/planetary evolution models.

Stars & planets both contract after formation. If an age can be estimated for the system, the models can become calibrated.

Most often, planetary parameters are relative. However there is a small fraction of systems for which absolute parameters can be obtained.



ECCENTRICITY FROM SECONDARY ECLIPSES



The duration of transit encodes the instantaneous orbital velocity (vis-viva equation; 2.16). For eccentric orbits, the occultation and the transit can have different durations

$$\frac{W_{\text{occ}}}{W_{\text{tra}}} \sim \frac{1 + e \sin \omega}{1 - e \sin \omega}$$

3.22

In some cases, the transit shape can be affected, as the planet changes velocity during transit

The time between transit and occultation can measure eccentricity

$$\Delta t \sim \frac{T}{2} \left(1 + \frac{4}{\pi} e \cos \omega \right)$$

3.23

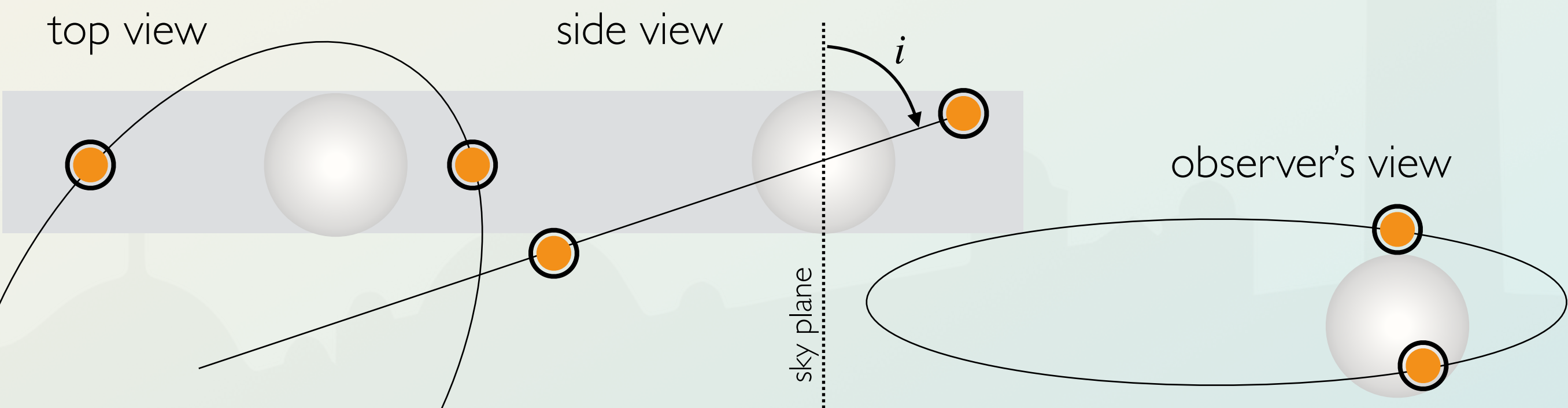
MISSING TRANSITS/ECLIPSES

Sometimes a transit can happen at inferior conjunction, but not at superior conjunction. The opposite is also true. This depends on the orbital inclination i , on the eccentricity e , but importantly, on the angle of periastron ω .

We can define a function of the apparent distance between both objects projected on the plane of the sky, $\delta(f)$ where

$$\delta(f) = \frac{1 - e^2}{1 + e \cos f} \sqrt{1 - \sin^2 i \sin^2(f + \omega)}$$

3.24



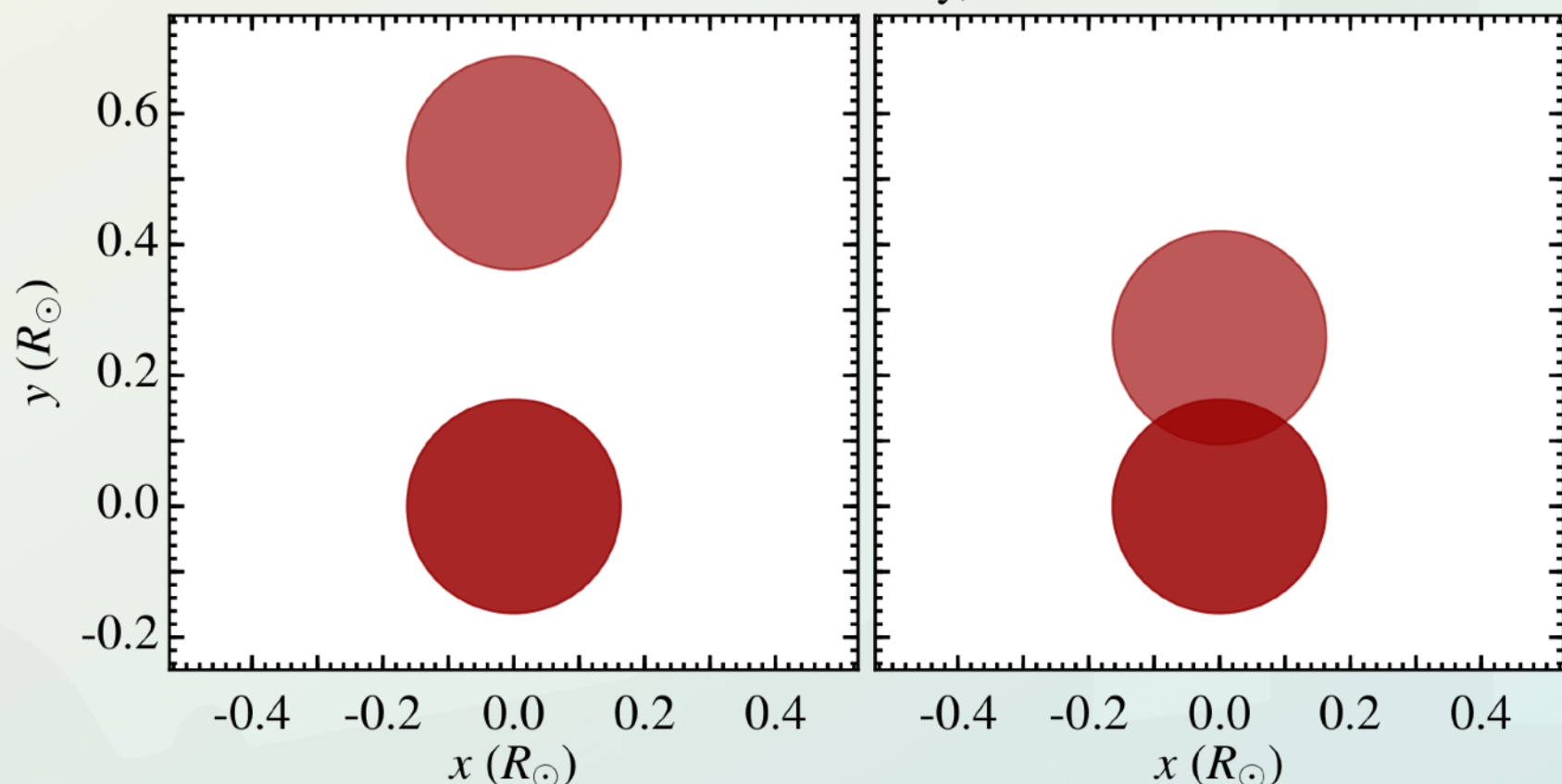
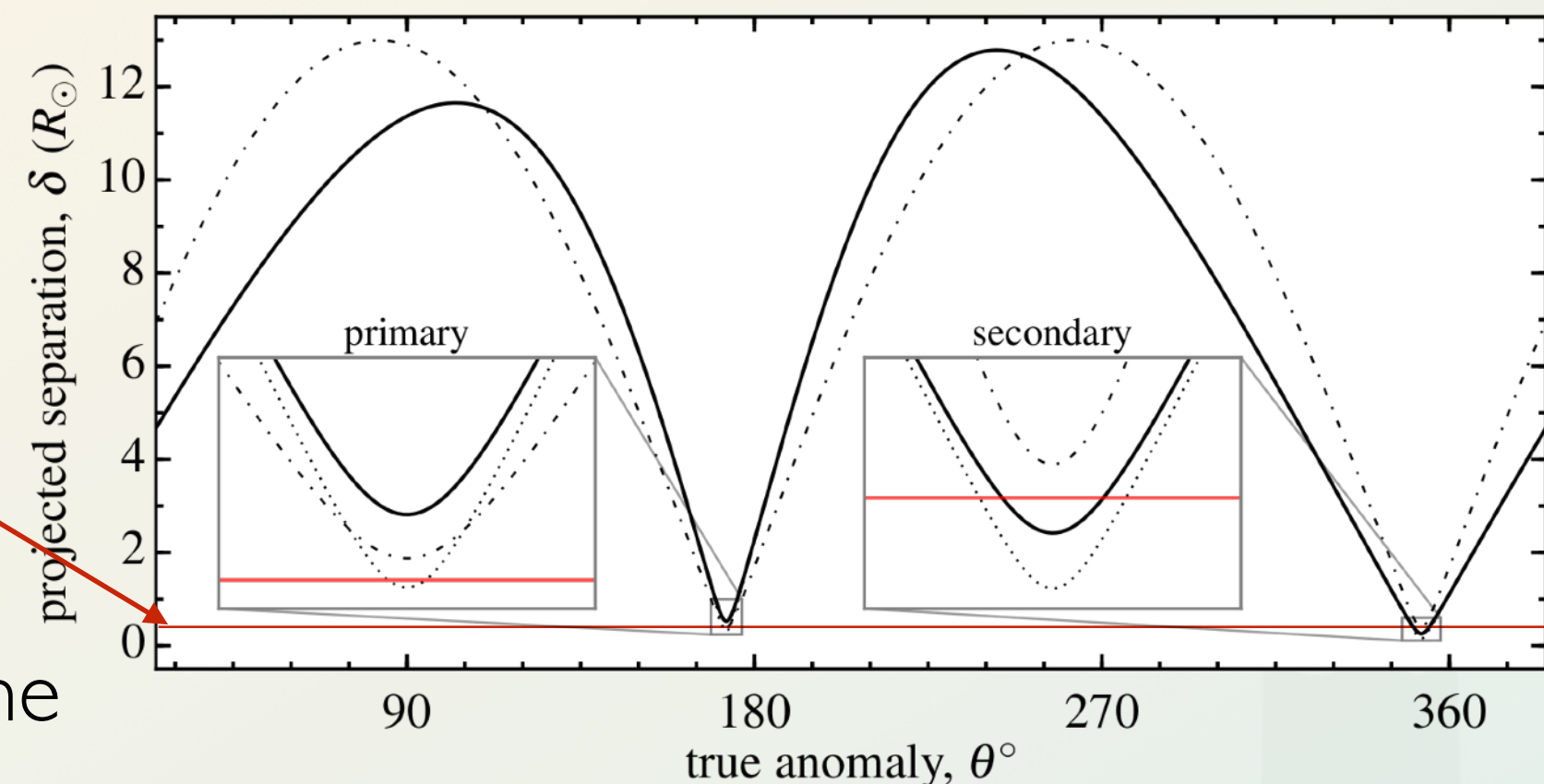
MISSING TRANSITS/ECLIPSES

An eclipsing geometry happens when

$$3.25 \quad \delta(f) < \frac{R_1 + R_2}{a}$$

$\delta = b$ at the middle of the primary eclipse/transit

In this particular case, because M_1 and M_2 are almost equal, we assumed R_1 and R_2 were also equal in order to measure the system's parameters



TRANSIT TIMING/DURATION VARIATIONS

The mid-time of a transit is often written as T_0 , and acts as a reference time. In a series of transits (for instance, like observed by *TESS*, or *Kepler*, a transit time near the middle of the time series is chosen. The next transit are

$$T_n = T_0 + n \times T$$

3.26

which is often referred to as the **transit ephemeris** (ephemerides in the plural)

Because of uncertainty the ephemeris can drift, and predicting a new transit is difficult. Transiting planets need to be observed regularly.

Non-Keplerian effects (caused by other bodies in the system, or orbital precession from general relativity, $\dot{\omega}$) can also change the rate of transit mid-times. These are called Transit Timing Variations (TTVs). Similarly, the duration can vary (TDVs).

ASTROMETRY

Celestial coordinates

Declination (dec): δ

Right Ascension (RA): α

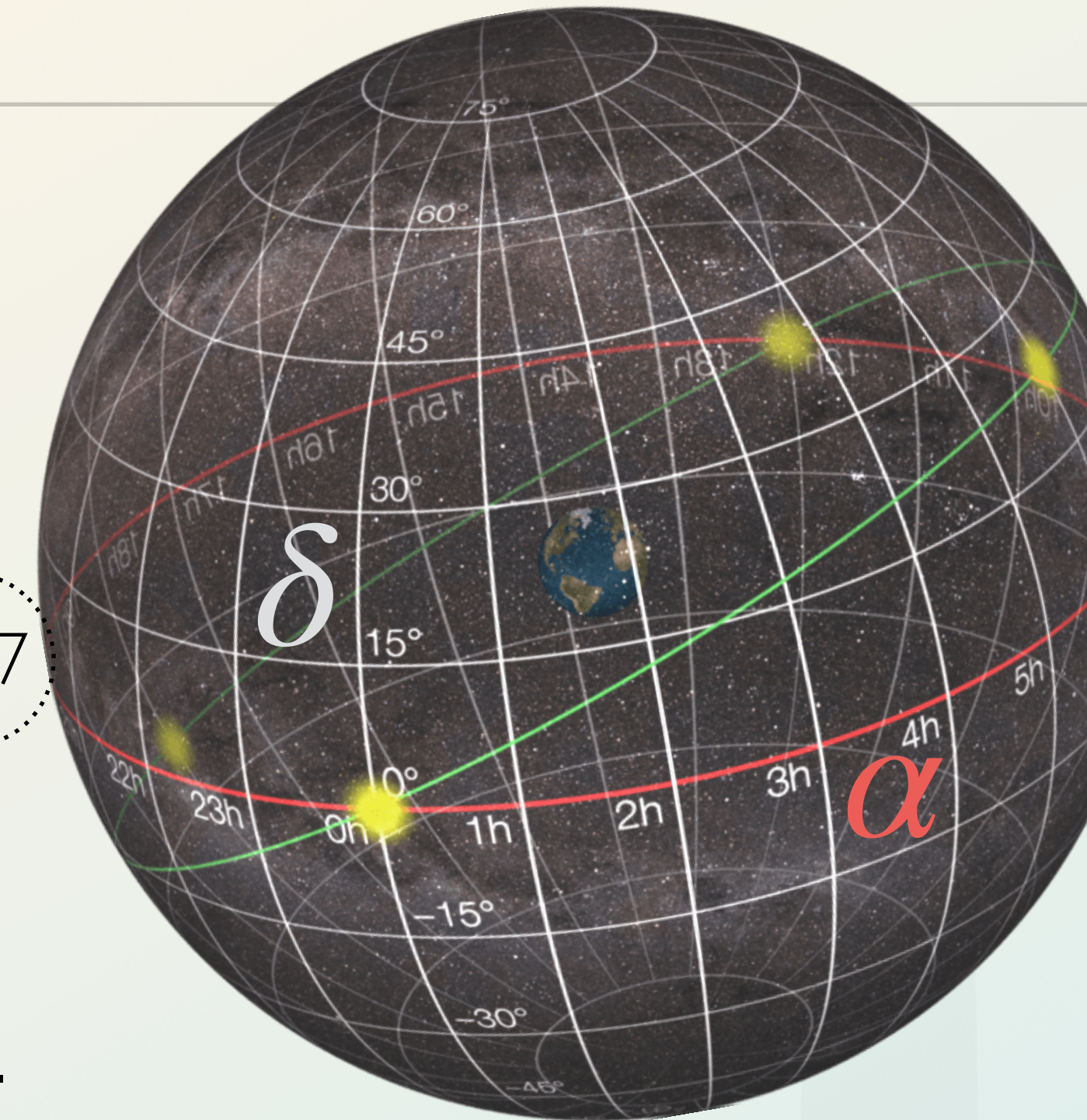
Because of projection on the celestial sphere $\alpha^* = \alpha \cos \delta$

Astrometry is about measuring position in α and δ , but also changes in position, $\Delta\alpha^*$ and $\Delta\delta$.

These changes include parallax, proper motion, and orbital motion

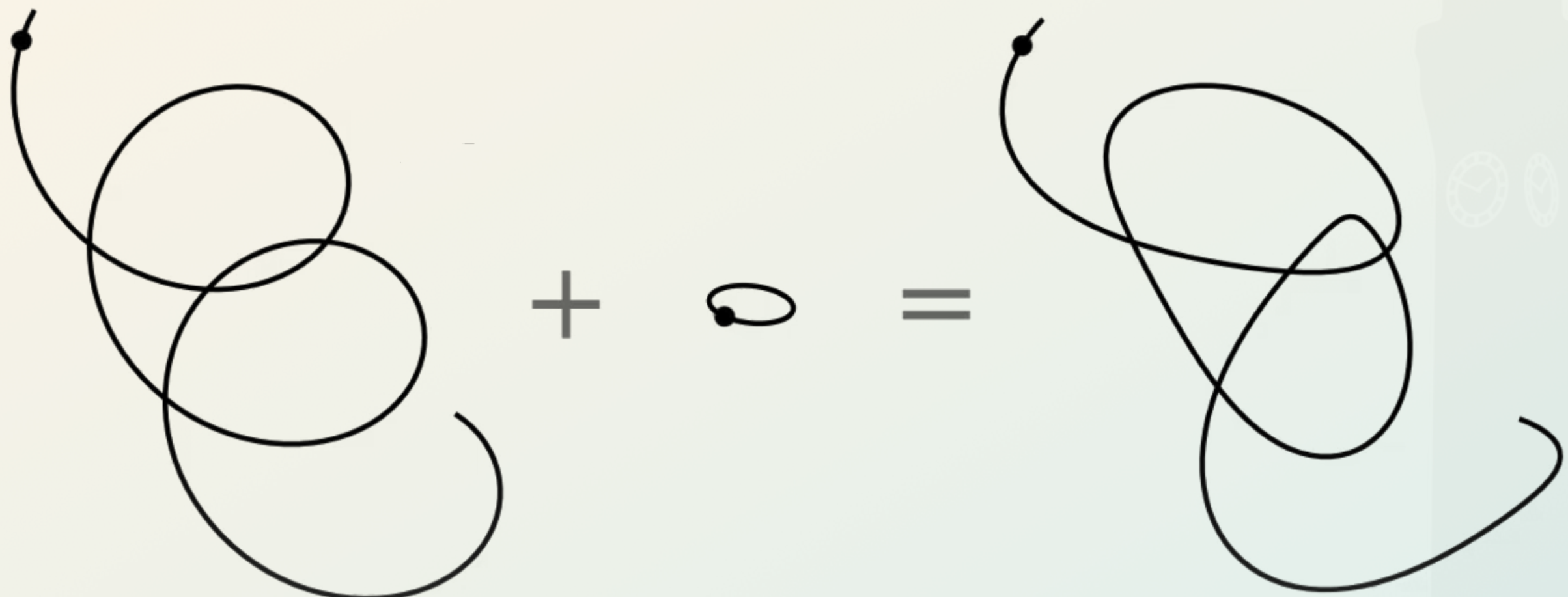
The parallax angle is

$$\varpi = 1'' \left(\frac{1 \text{ pc}}{d} \right)$$

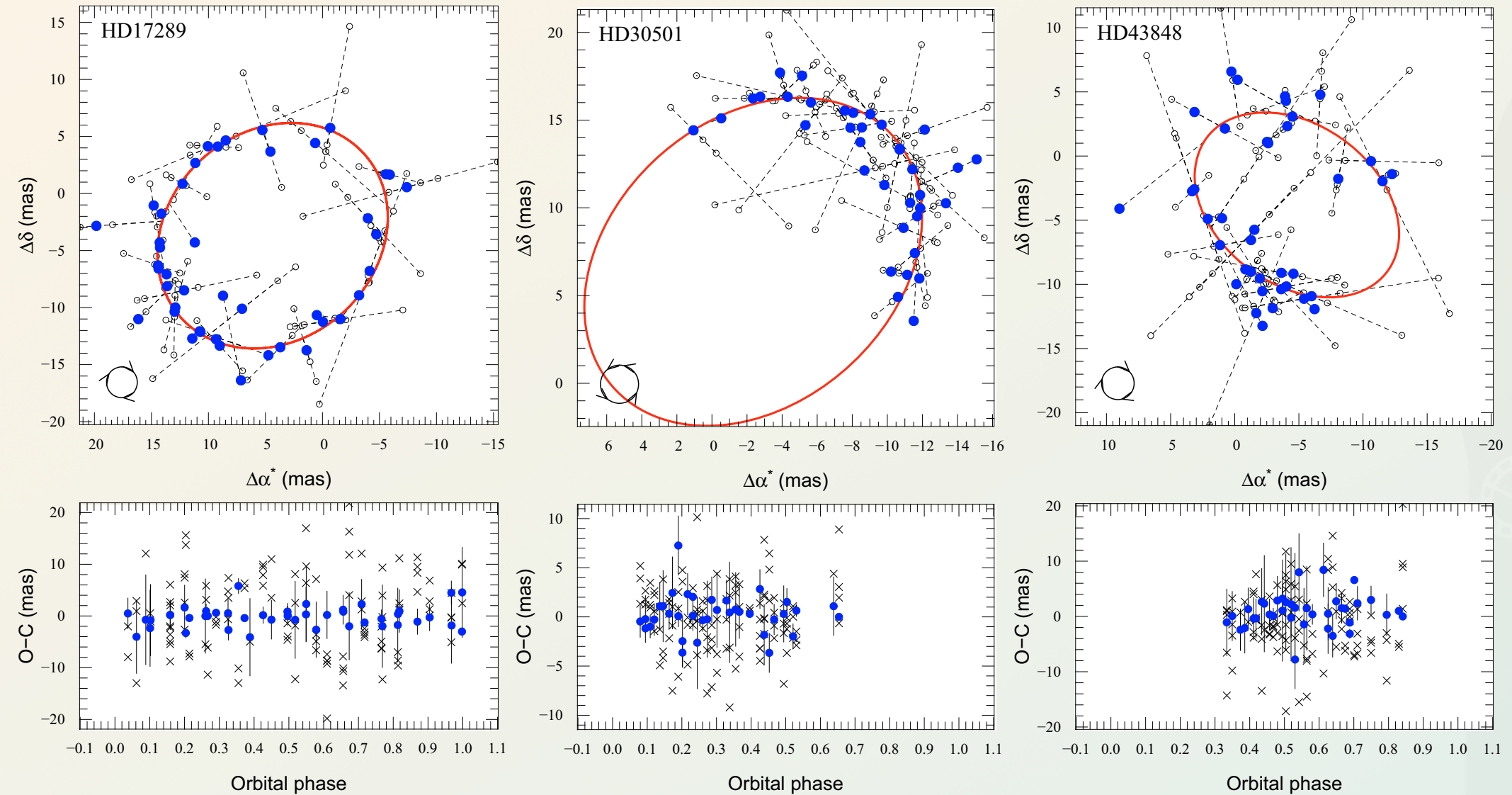


3.28

ASTROMETRY IN PRACTICE



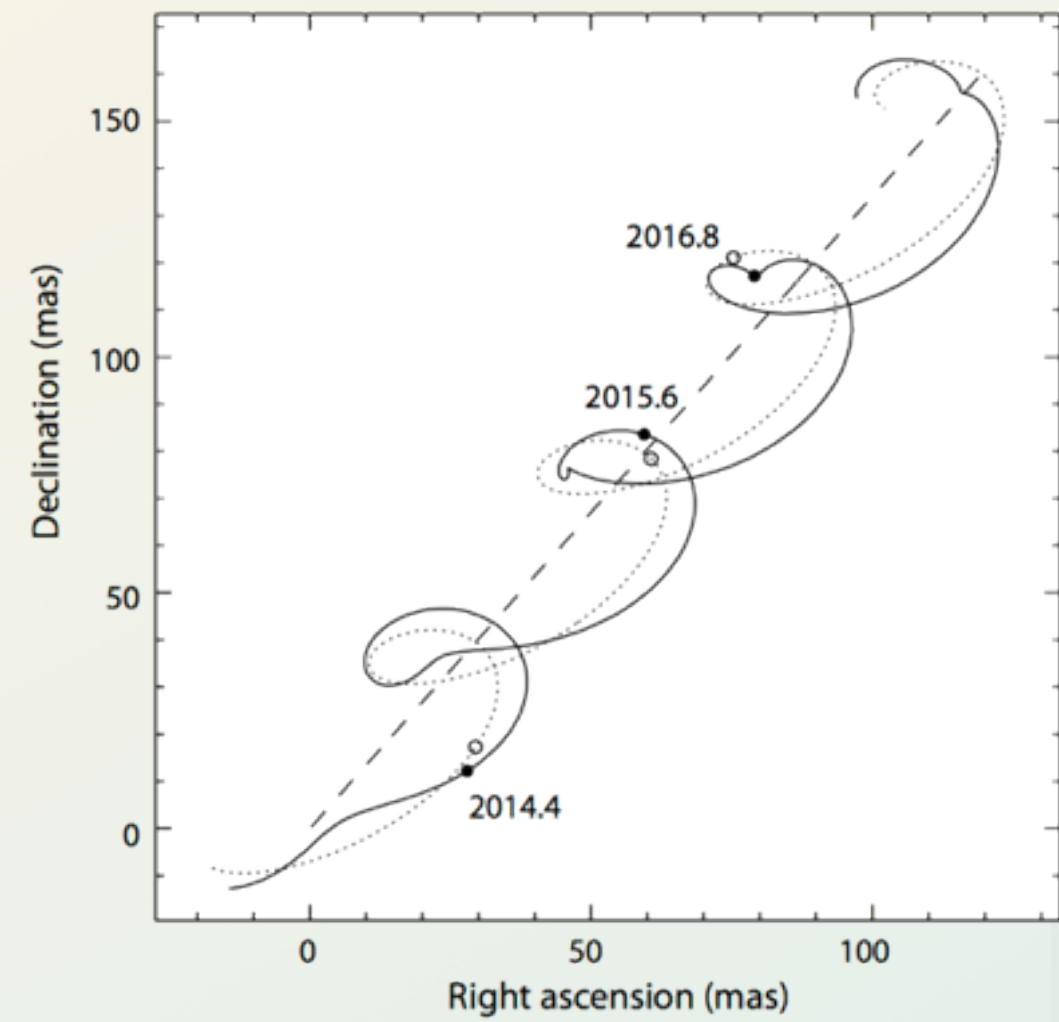
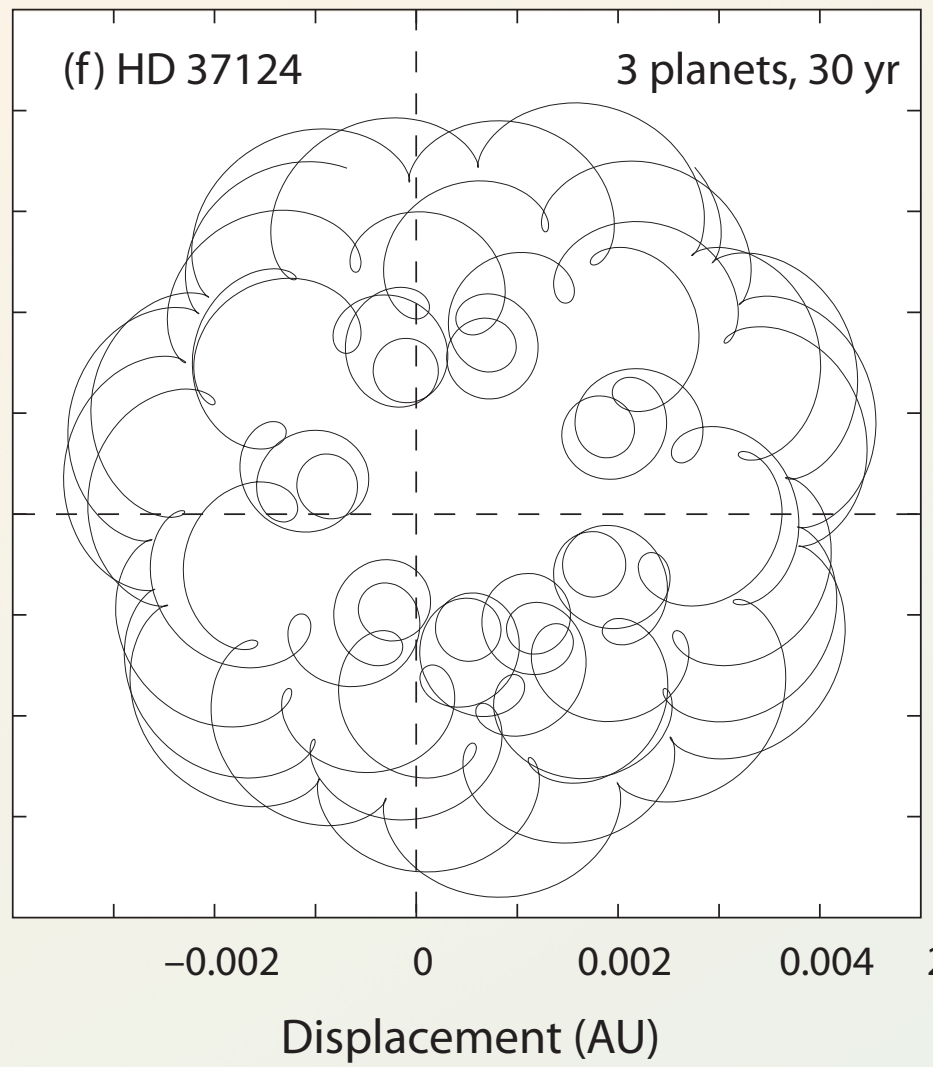
ASTROMETRY



Measure the star wobble with respect to other stars. All orbital elements are needed to fit an astrometric orbit, including Ω .

Inclination i is known, and thus, the **true** m_p as well (but not absolute)

ASTROMETRY

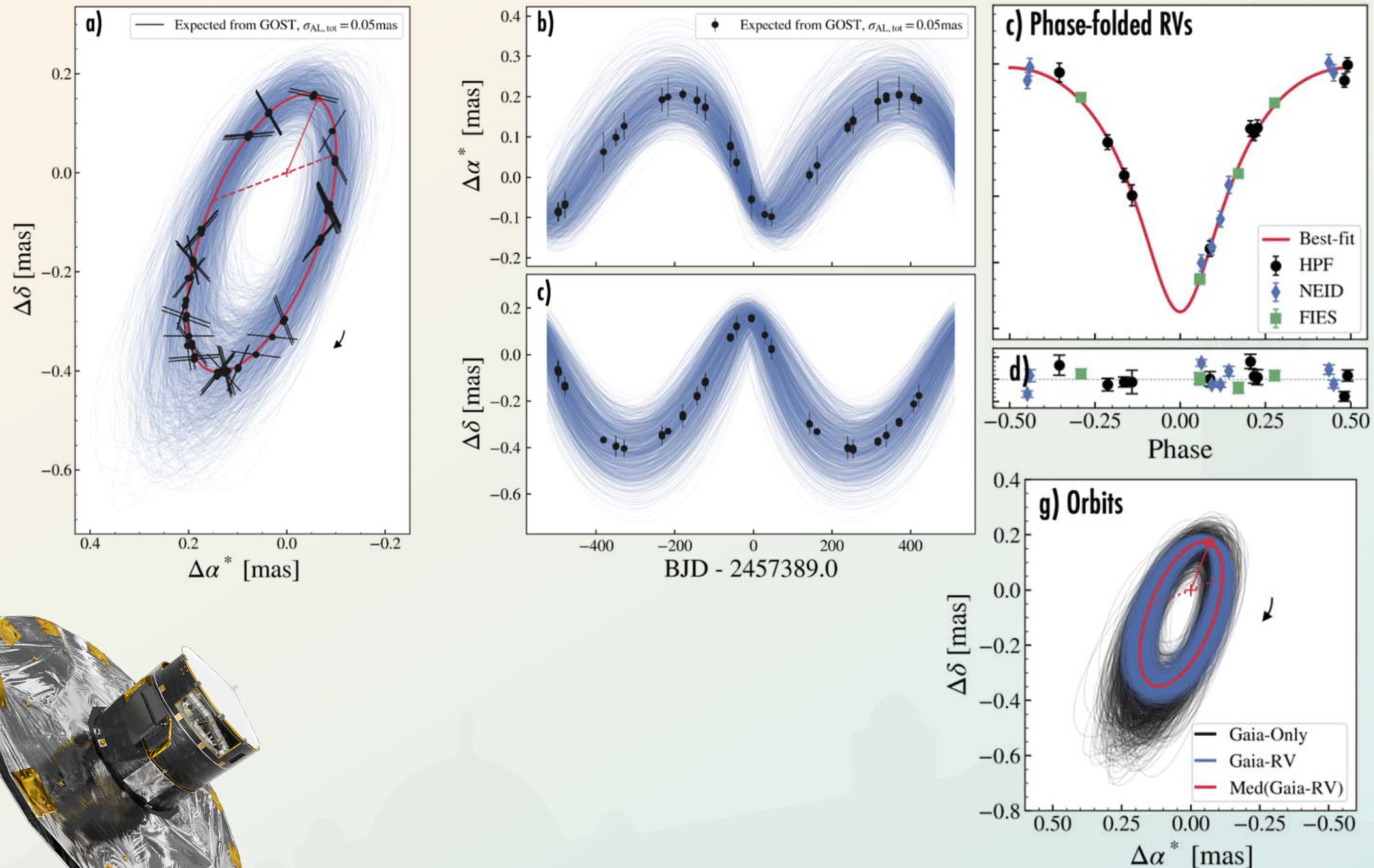


$$\Lambda = 1 \text{ arcsec} \left(\frac{m_p}{M_\star} \right) \left(\frac{a}{1 \text{ AU}} \right) \left(\frac{d}{1 \text{ pc}} \right)^{-1}$$

3.29

Difficult from the ground, easier from space.
Gaia's typical precision is $10 - 20 \mu\text{as}$

GAIA ASTROMETRY & RADIAL VELOCITIES

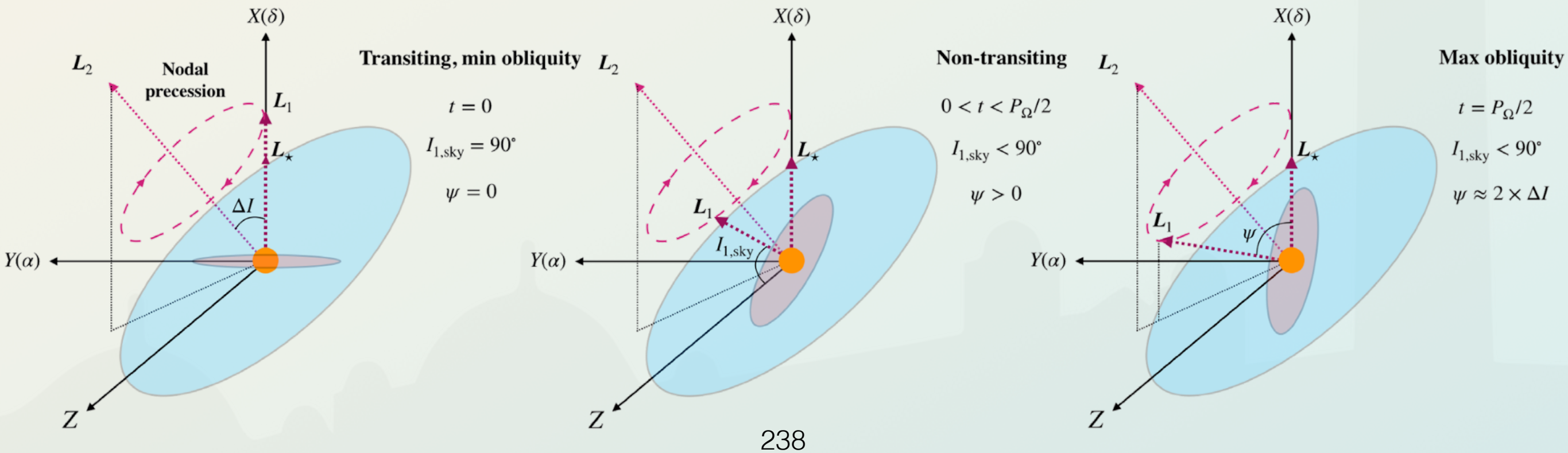


ASTROMETRIC RESULTS

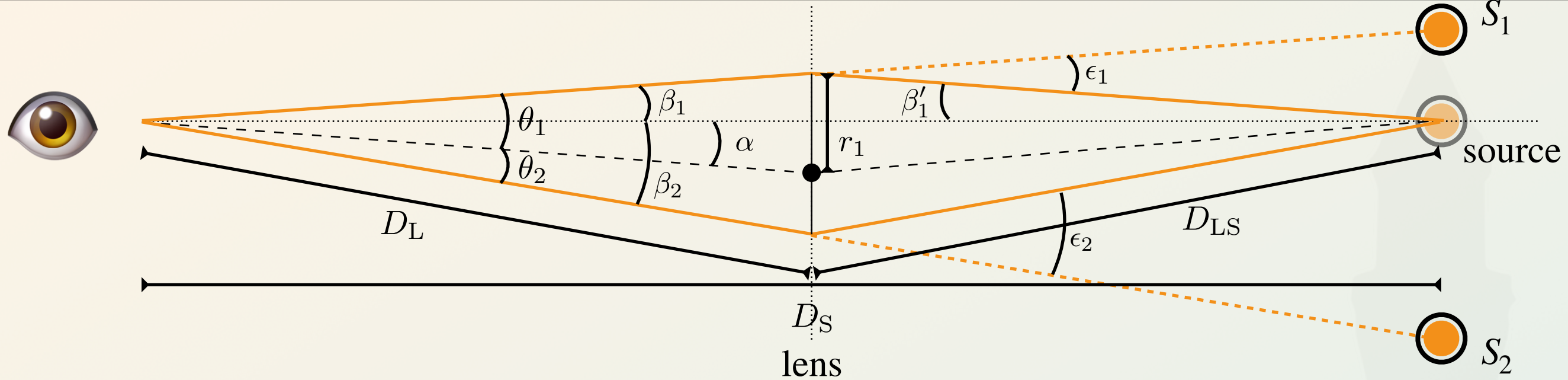
Before orbits were detected with *Gaia*, but had, 1)- scatter of the measurements, and 2) the position of stars now, which can be compared to observation by *Hipparcos*, in the 90s.

Kiefer (2020) showed that HD 114762b, is in fact a $100 \text{ M}_{\text{jup}}$ star, with $i = 62^\circ$, because they find 0.74 milli-arcsecond (mas) of noise.

Xuan & Wyatt (2020) showed that π Men has two planets on different orbital planes.



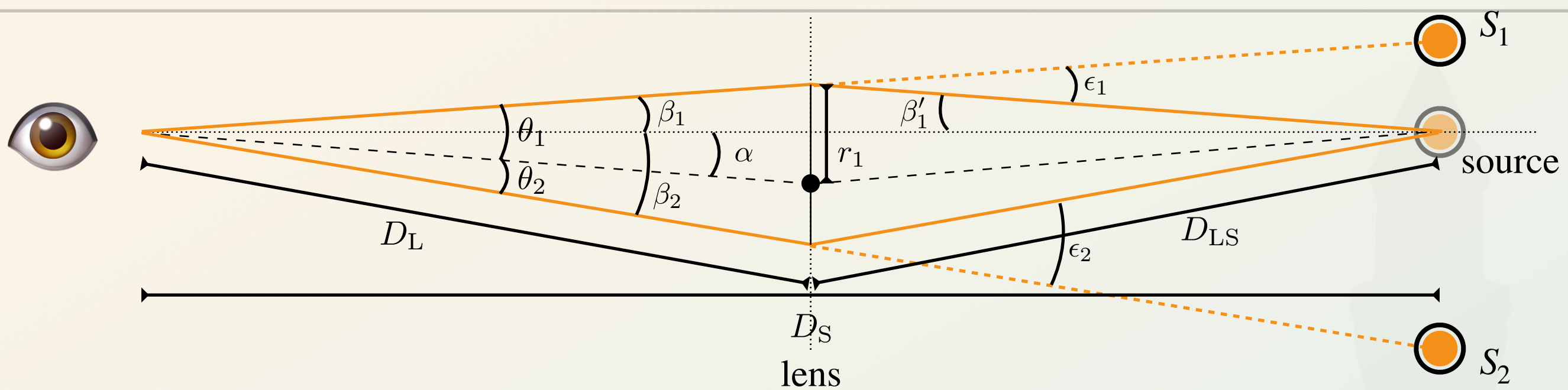
MICROLENSING



Microlensing is the strangest of exoplanet detection methods. It is also an indirect method. The light from a background star is amplified by a **lens star**. If the lens star hosts a planet, the planet too can lens the background star, leading a distinct signal.

Microlensing events are one-off events. The probability of alignment is so remotely small, that they will never be re-observed again. Because of the usual faintness of the lens star and its distance other methods can usually not be deployed.

MICROLENSING



Light deflection angle

$$\epsilon = \frac{4 G M_L}{r c^2}$$

we arrive at the lens equation

$$\theta_1^2 - \alpha \theta_1 - \theta_E^2 = 0$$

with the Einstein angle

$$\text{where } \mu = 1 + \frac{D_L}{D_{LS}}$$

for $\alpha = 0$, we have alignment, and θ_E , draws a ring.

Typically $D_S \sim 8 - 10$ kpc, to the Galactic bulge, or the halo.

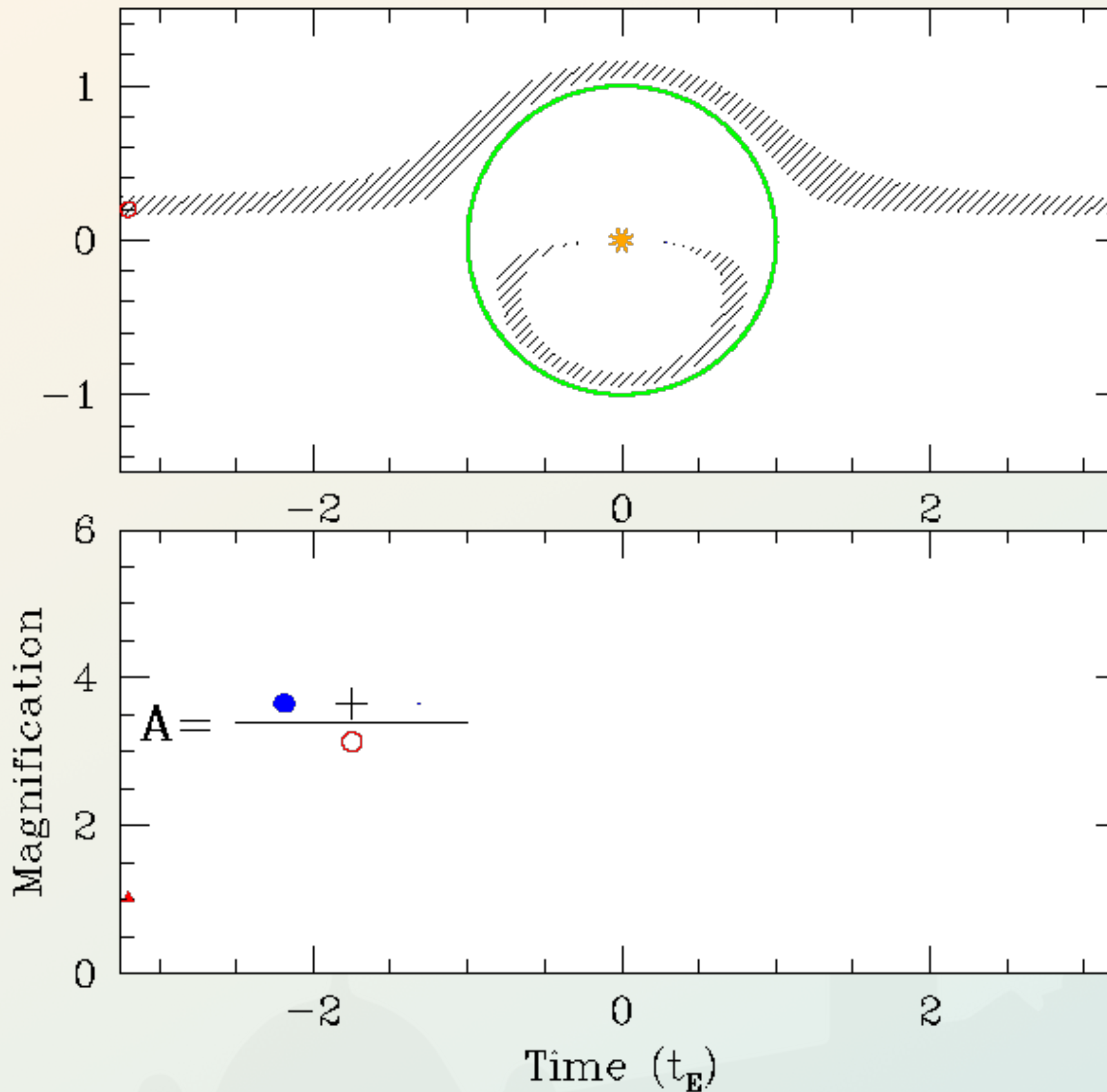
3.30

3.31

3.32

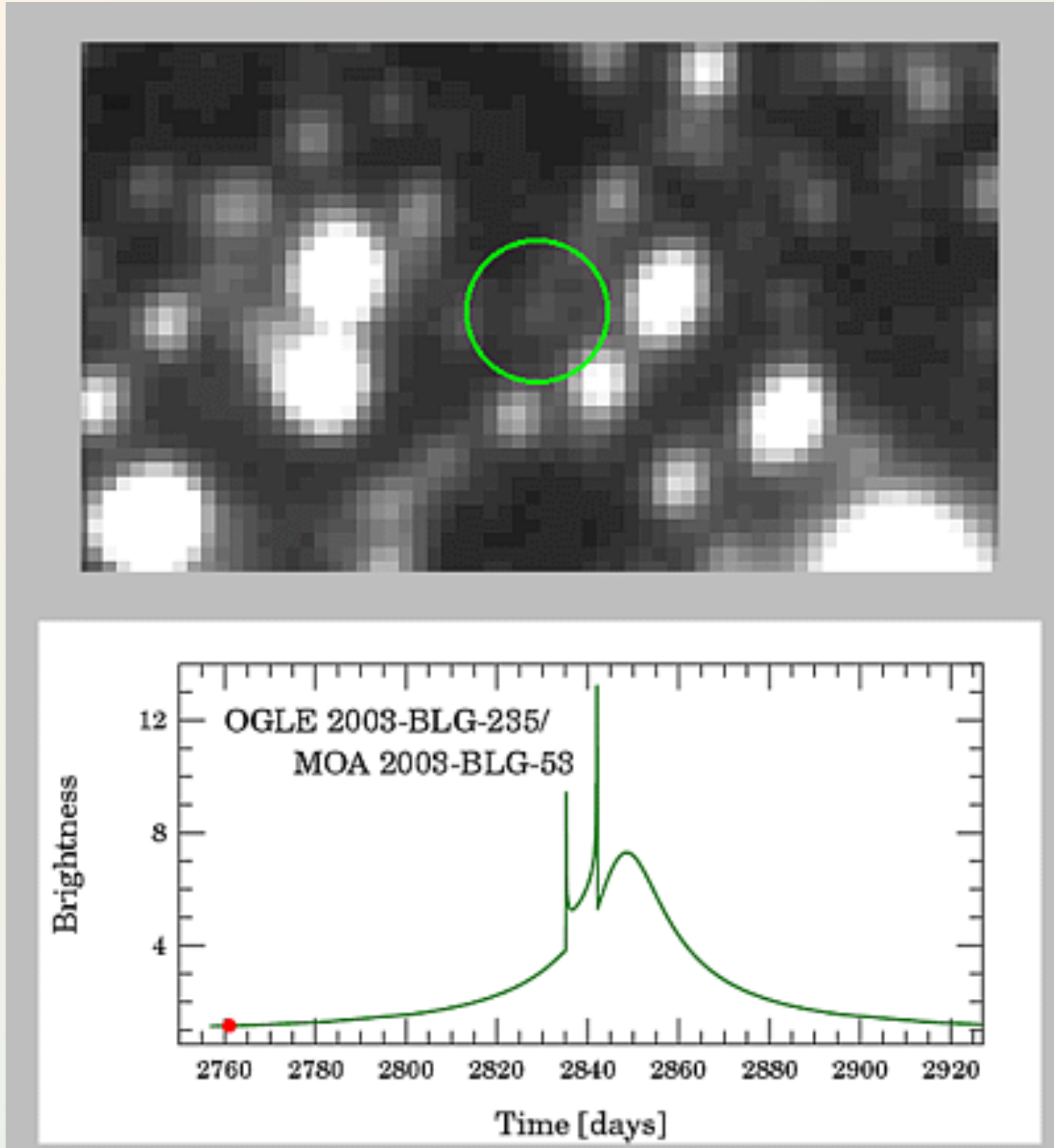
Schwarzschild
radius

MICROLENSING OF A SINGLE OBJECT



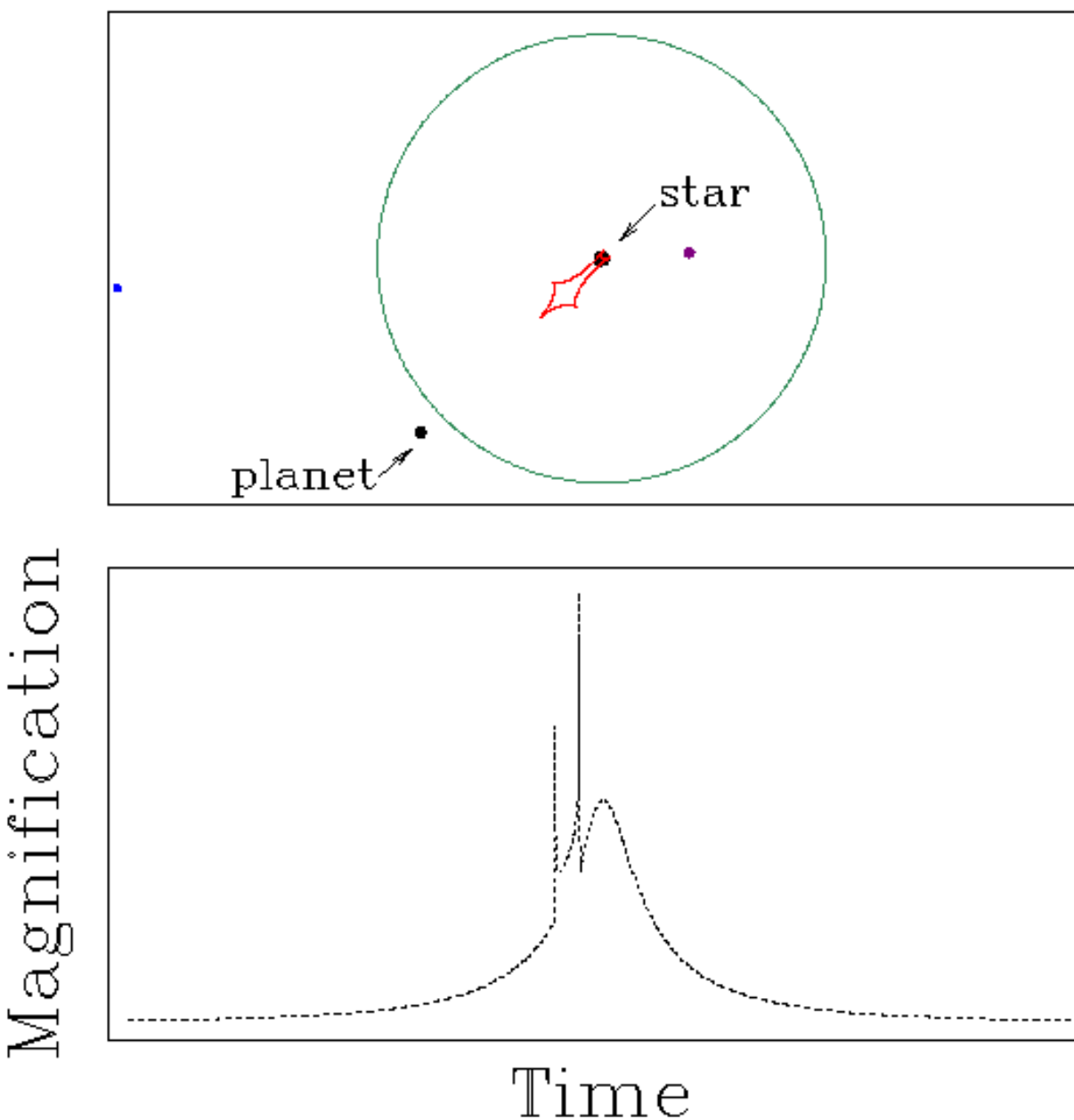
<https://roman.ipac.caltech.edu/movies/yossi2/point.gif>

MICROLENSING OF A STAR & PLANET



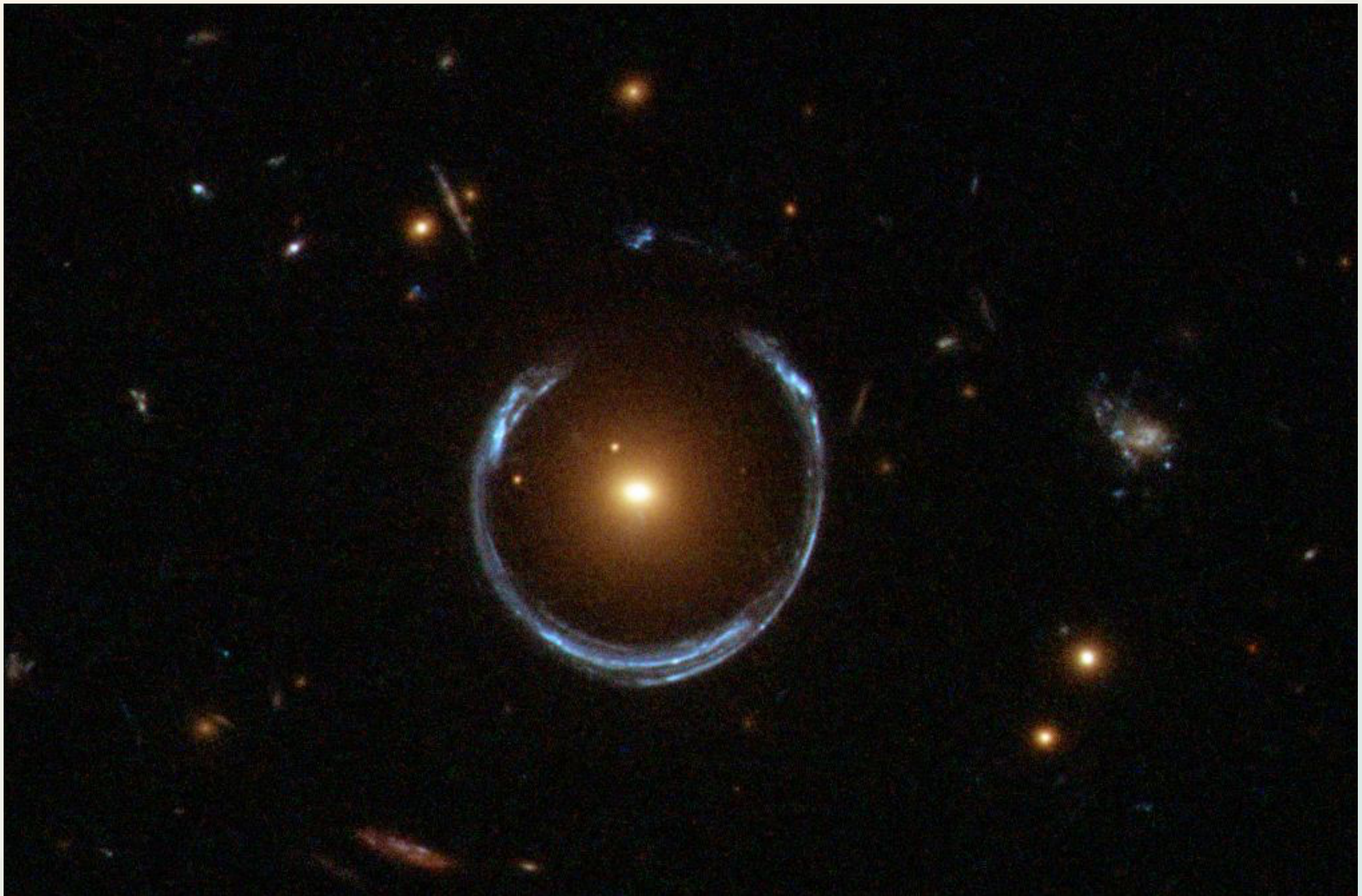
https://roman.ipac.caltech.edu/movies/calen1/ob03235_udalski.gif

MICROLENSING OF A STAR & PLANET

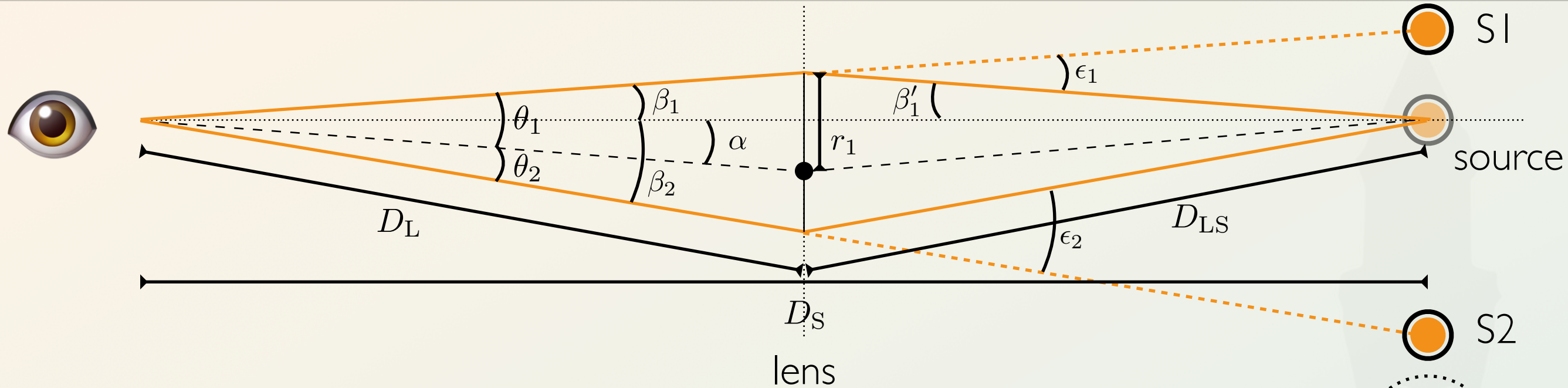


<https://roman.ipac.caltech.edu/movies/yossi1/gaudiplanet4.gif>

GRAVITATIONAL LENSING



MICROLENSING



The physical size of the Einstein radius is $r_E = \theta_E D_L$

thus the Einstein radius is

$$r_E = 2.2 \text{ AU} \left(\frac{M_L}{0.3 M_\odot} \right)^{1/2} \left(\frac{D_S}{8 \text{ kpc}} \right)^{1/2} \left(\frac{x(1-x)}{0.25} \right)^{1/2}$$

solve 3.31 to find:

$$\theta_\pm = \frac{\theta_E}{2} \left(u \pm \sqrt{u^2 + 4} \right)$$

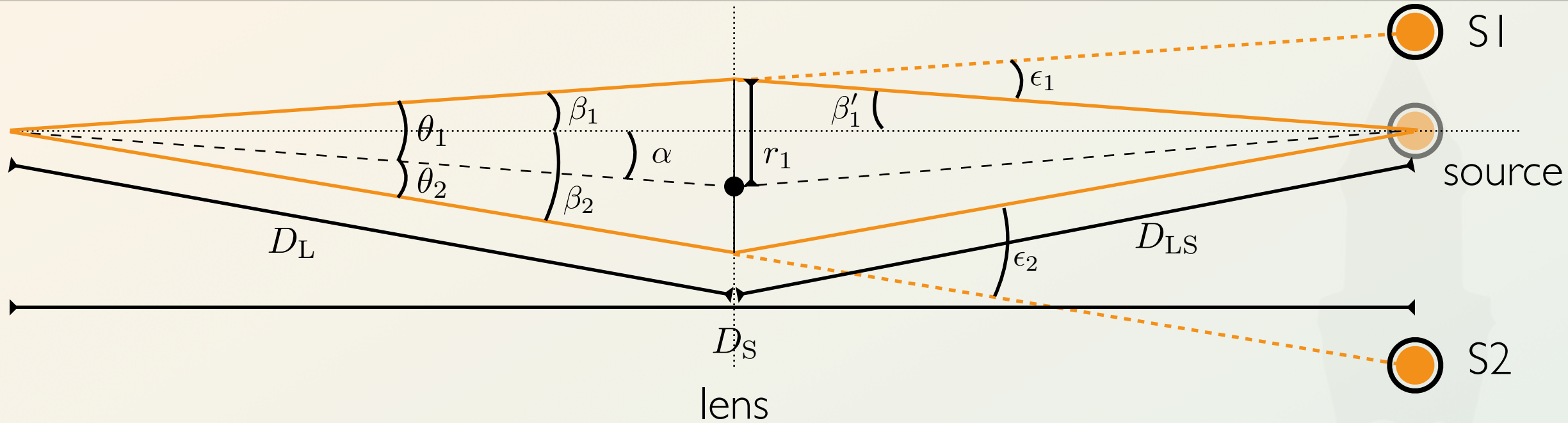
3.33

$$x = \frac{D_L}{D_S}$$

3.34

There are two roots, hence two images, at two different angles

MICROLENSING



The two images (positive and negative) are expressed as

$$\theta_{\pm} = \frac{1}{2}\alpha \pm \left[\left(\frac{1}{2}\alpha \right)^2 + \theta_E^2 \right]^{1/2}$$

3.35

We can now investigate the total magnification, with amplitude A :

$$A_{\pm} = \left| \frac{\theta_{\pm}}{\alpha} \frac{d\theta_{\pm}}{d\alpha} \right|$$

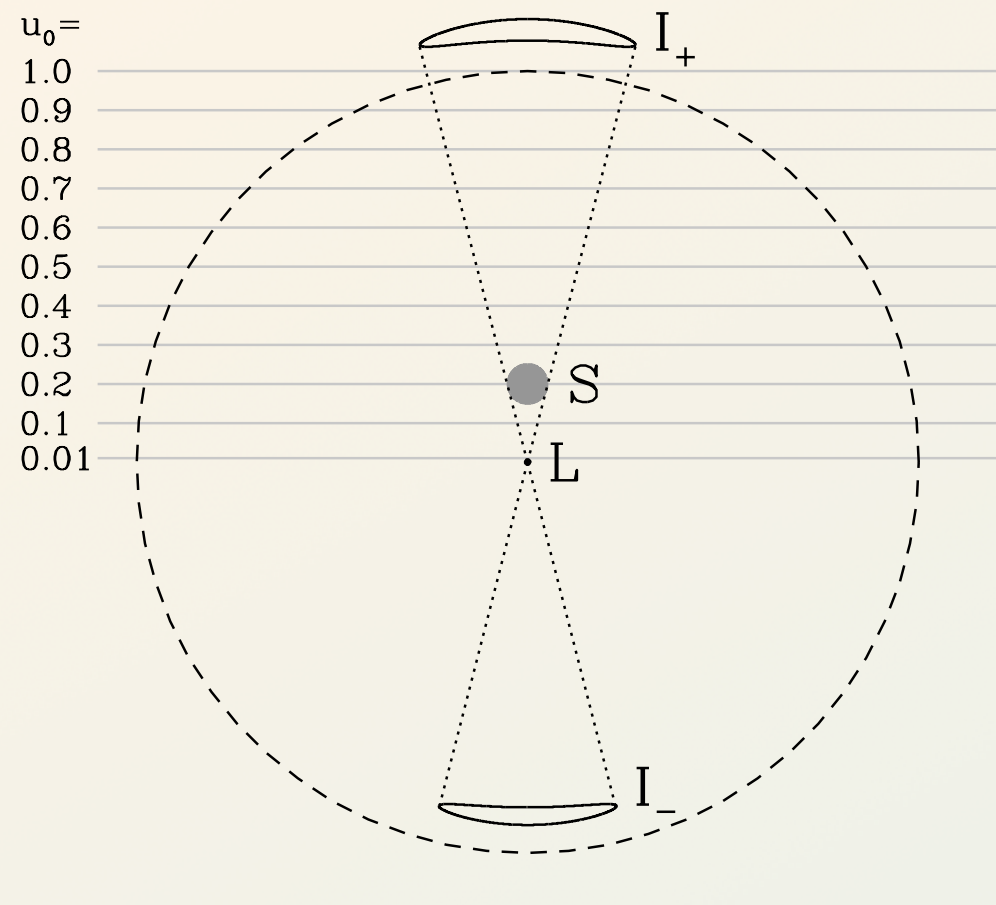
$$= \pm \frac{1}{2} \left(\frac{u^2 + 2}{u\sqrt{u^2 + 4}} \pm 1 \right)$$

3.36

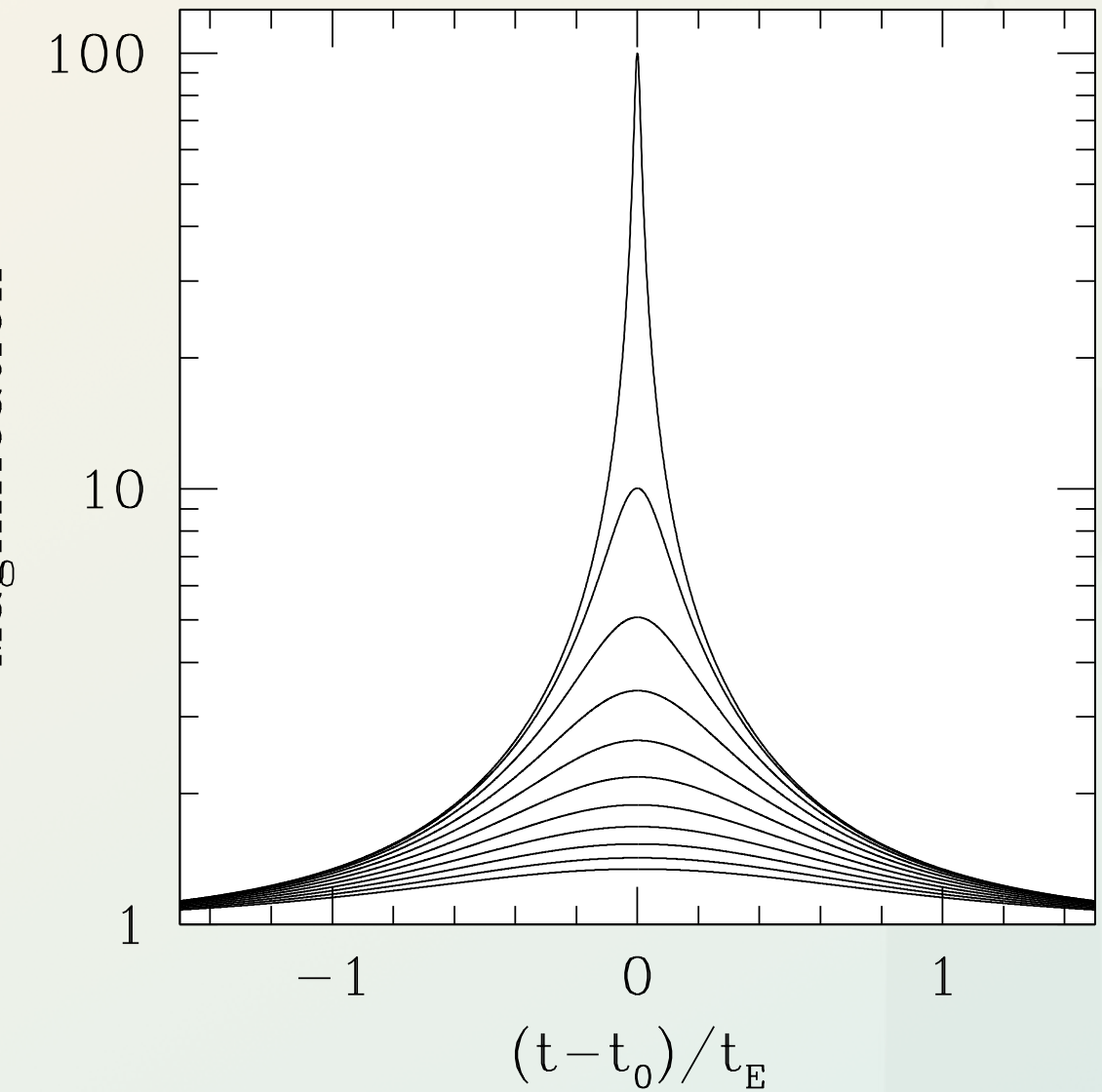
$$A = \frac{u^2 + 2}{u\sqrt{u^2 + 4}}$$

3.37

MICROLENSING



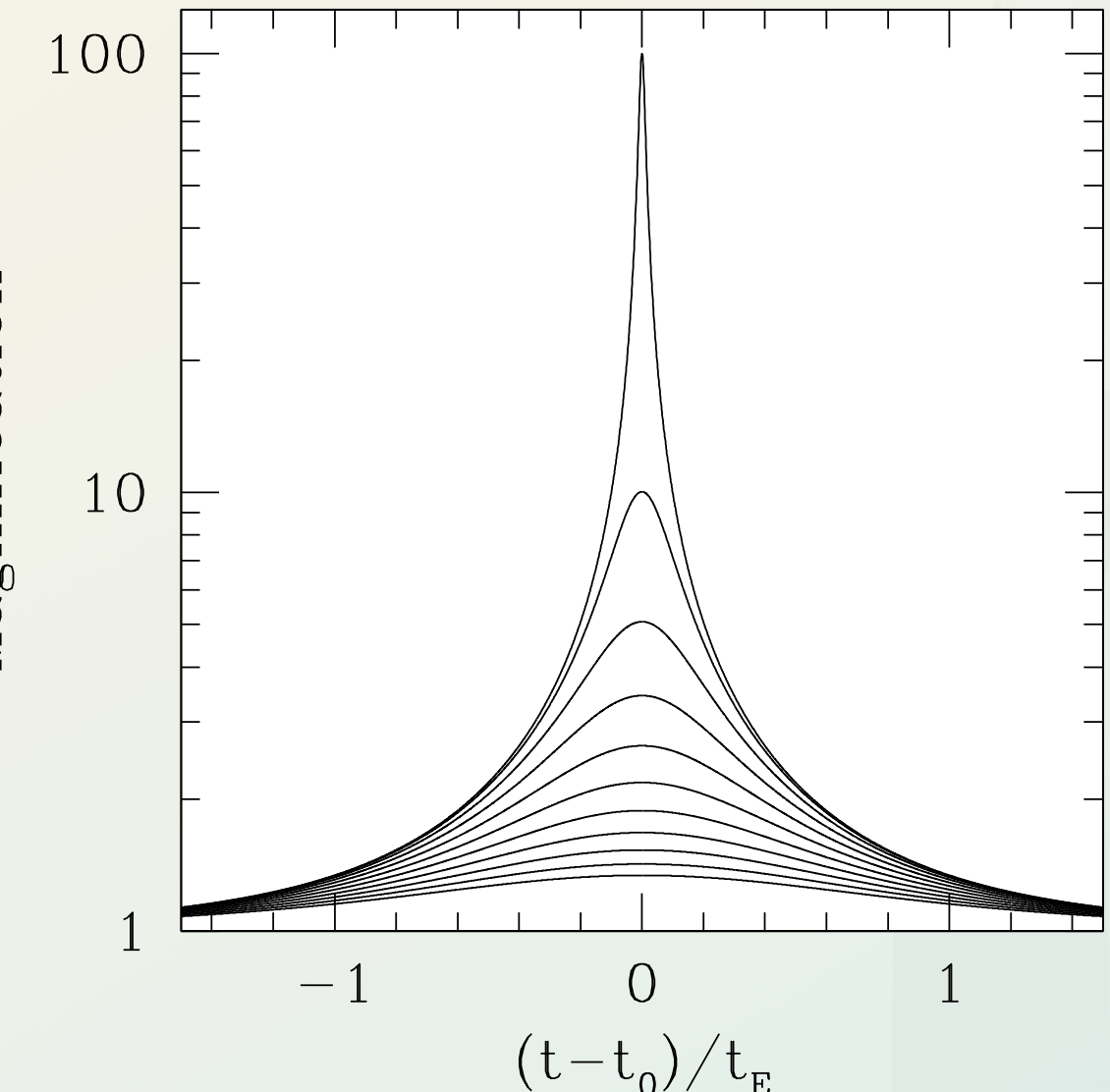
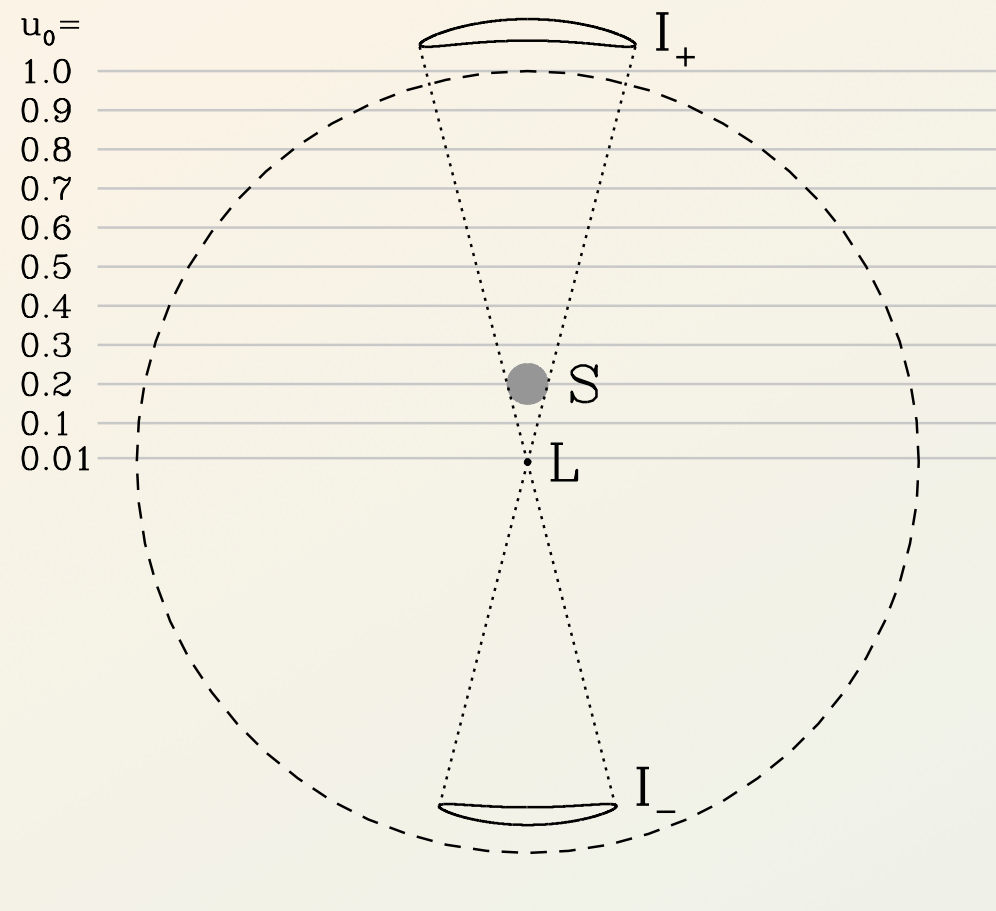
$$\theta_{\pm} = \frac{\theta_E}{2} \left(u \pm \sqrt{u^2 + 4} \right)$$



$$A = \frac{u^2 + 2}{u\sqrt{u^2 + 4}}$$

These are for a point source. A goes to infinity with $u \rightarrow 0$. In practice the physical size of the star/planet limits A .

MICROLENSING



The timescale, t_E of an event depends on the distance and velocity of the lens (and the source to a lower extend)

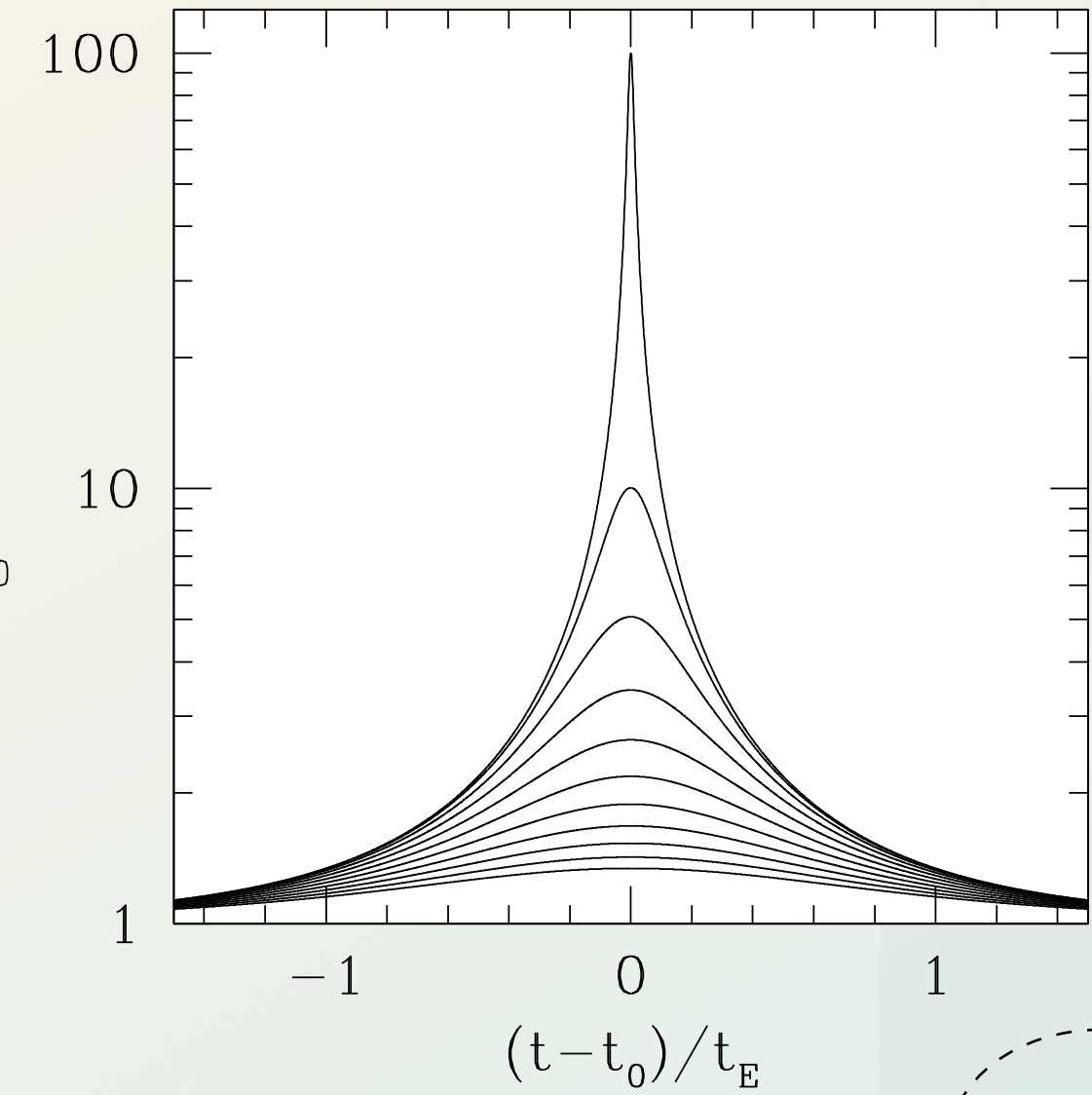
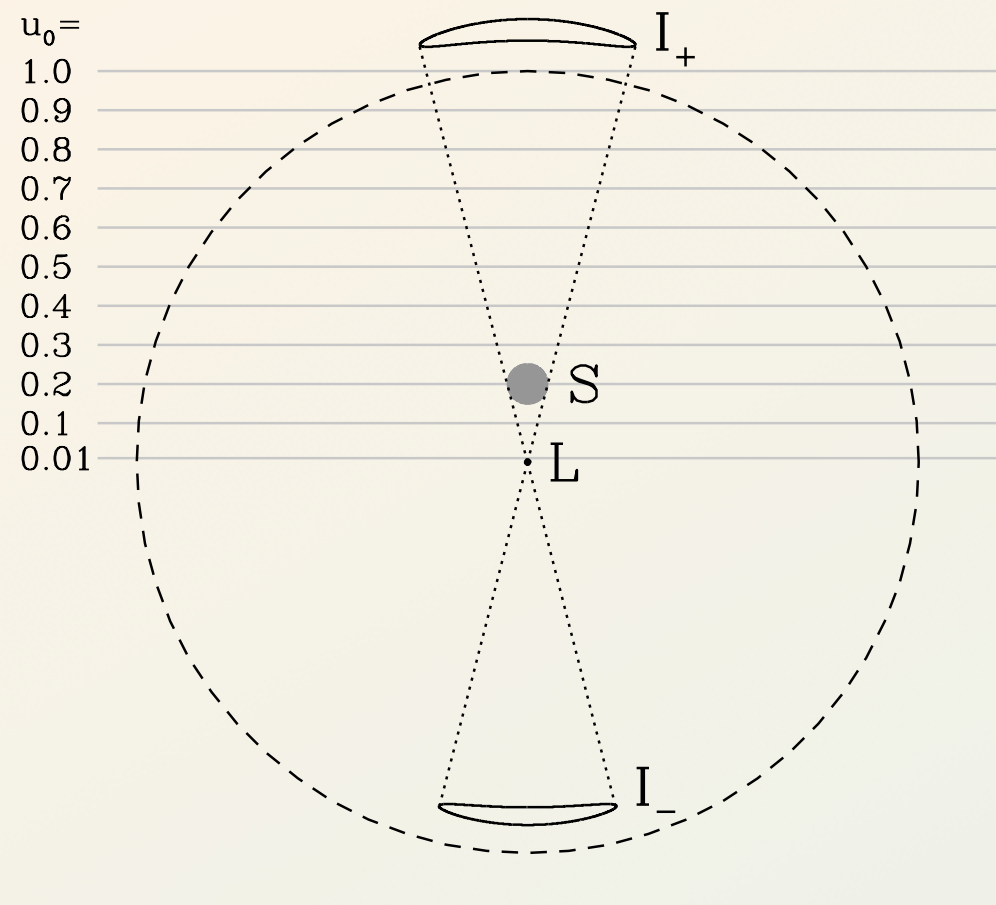
$$t_E = \theta_E / \nu$$

where ν is the relative angular motion, and

100 km s^{-1} @ 4 kpc gives $\nu \sim 1.7 \times 10^{-7} \text{ mas s}^{-1}$

3.38

MICROLENSING

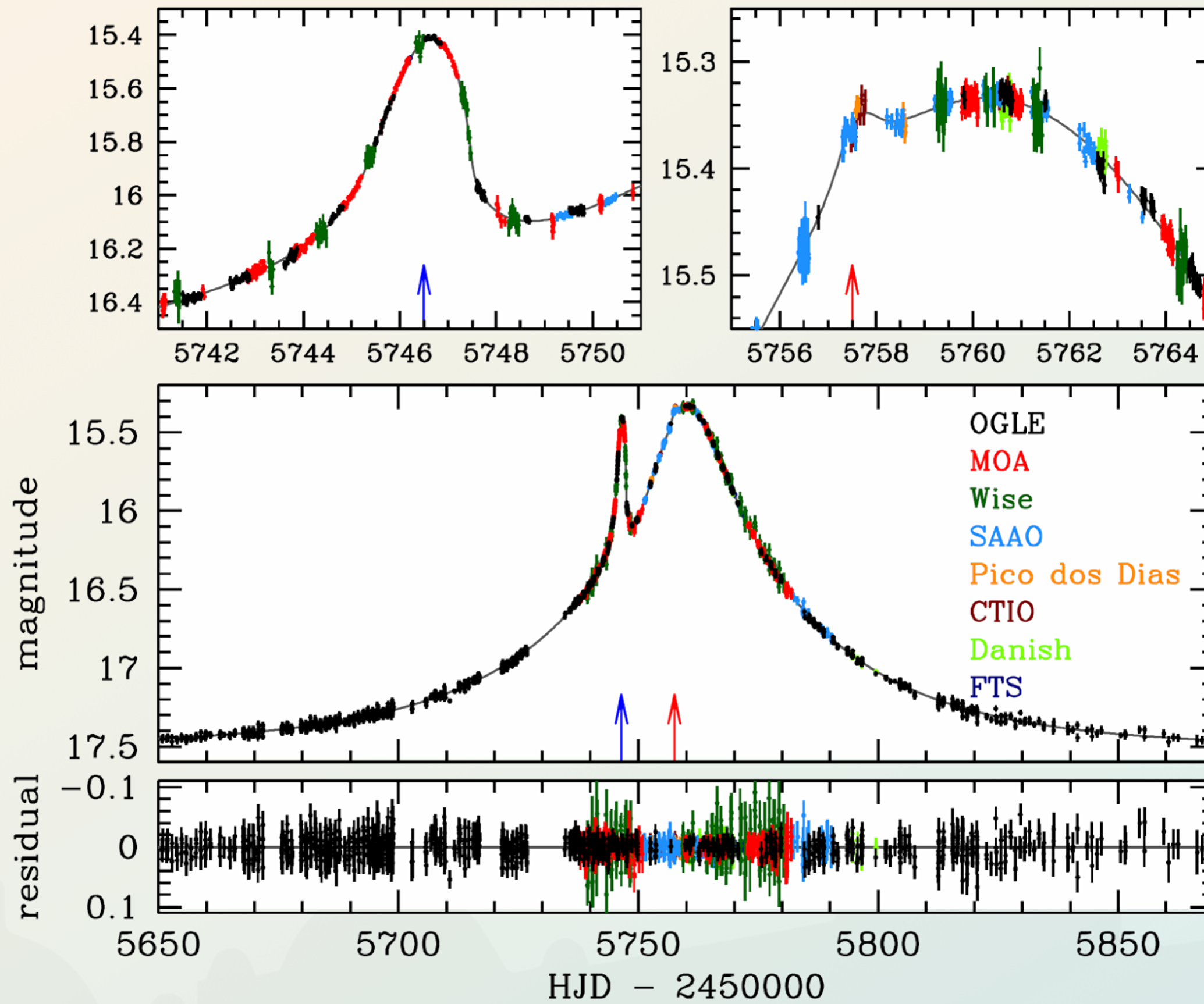


A scaling relation for the timescale can be computed to be:

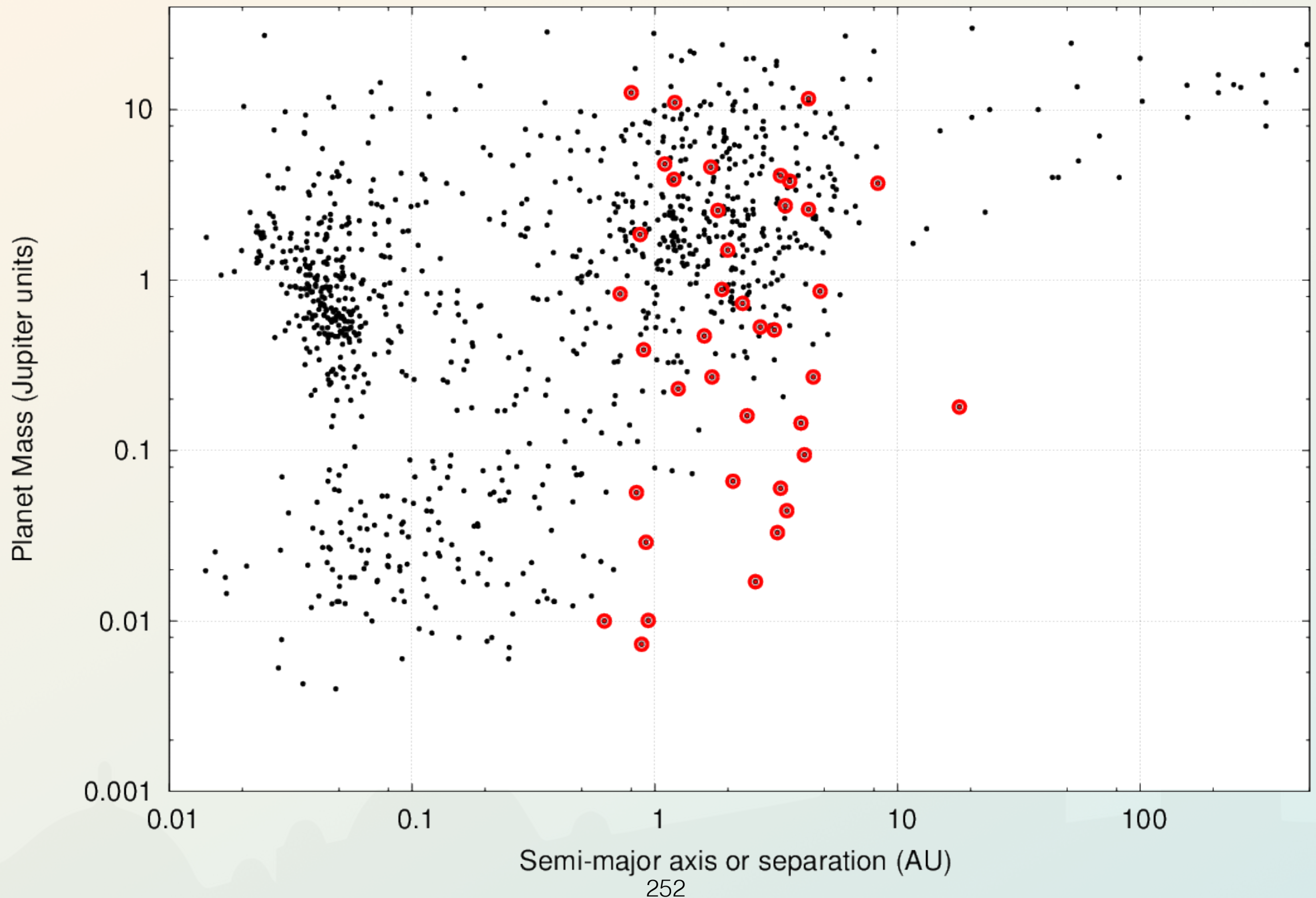
$$t_E \sim 37 \text{ d} \left(\frac{M_L}{0.3 M_\odot} \right)^{1/2} \left(\frac{D_S}{8 \text{ kpc}} \right)^{1/2} \left(\frac{x(1-x)}{0.25} \right)^{1/2} \left(\frac{v_t}{100 \text{ km s}^{-1}} \right)^{-1}$$

and a Jupiter mass planet would therefore be $t_E \sim 2$ days

MICROLENSING RESULTS



MICROLENSING RESULTS

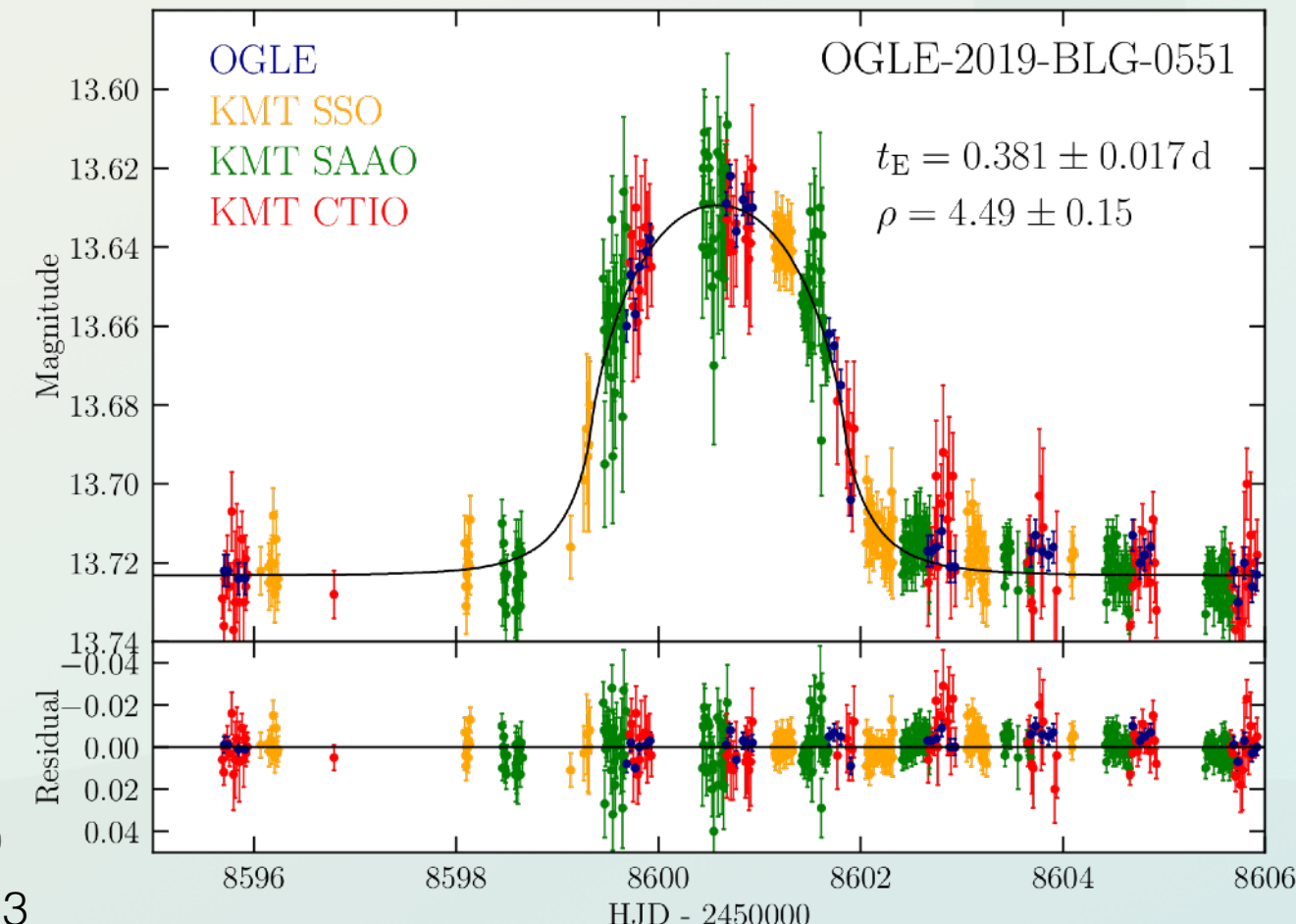
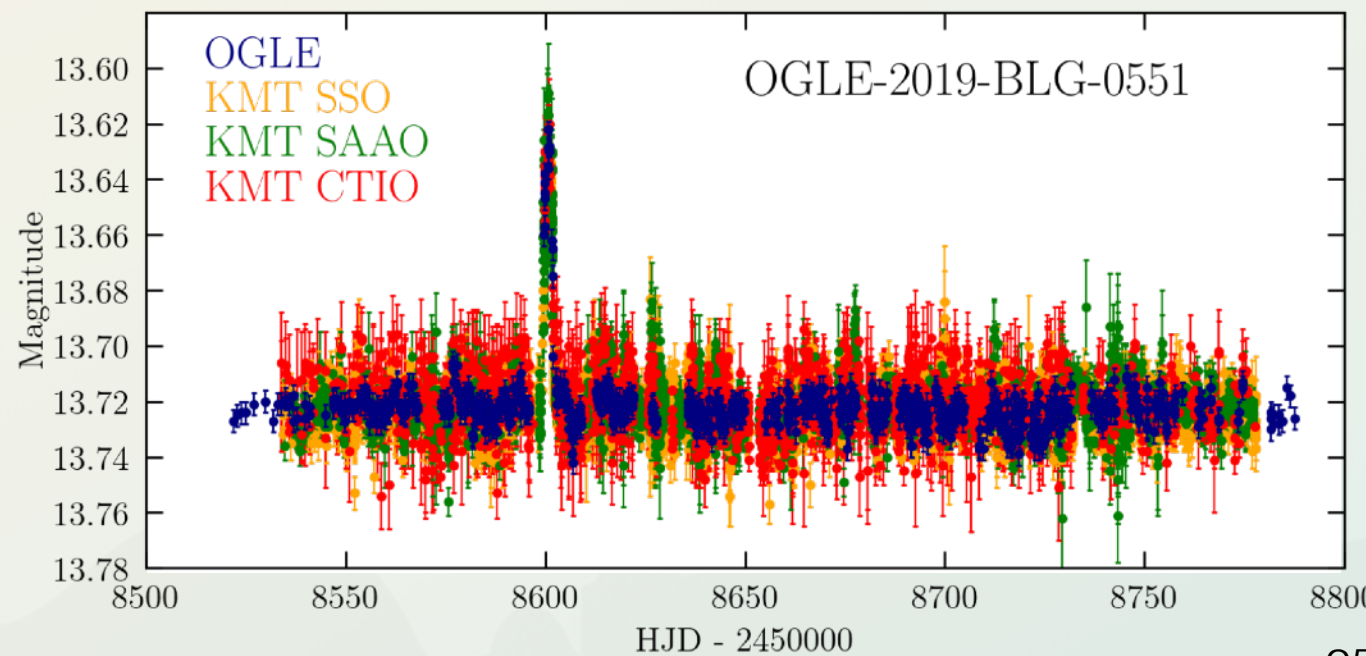


MICROLENSING RESULTS

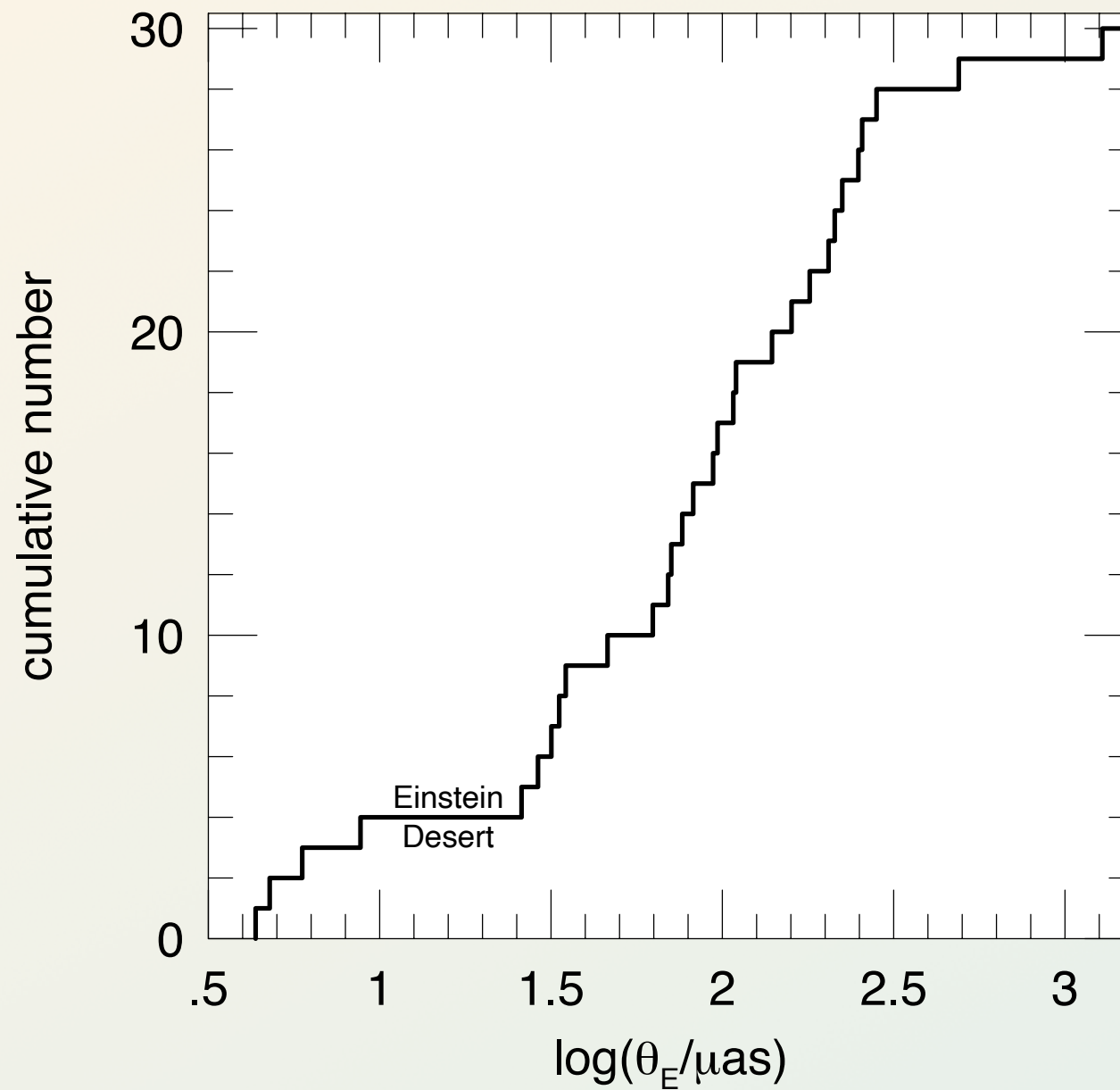
Microlensing is one of only two methods to detection free-floating planets, planets that presumably have been ejected from their planetary system.

The method works in the same way as for the event of a single star. The mass of the planets makes the Einstein ring tiny and the microlensing event is typically very short. There is sometimes a confusion between a free-floating planet, and a planet far from its host star.

Mróz+ 2021: a Saturn mass in the Bulge, or a sub-Neptune in the Disc



MICROLENSING RESULTS



Four short microlensing events detected separated by “Einstein Desert”, meant to be similar to the brown dwarf desert. Fitting these data it would appear there are 130 to 200 M_\oplus of free-floating objects per star in the Galaxy. If true, this is about twice as much as for bound planets.